



UNIVERSITÀ DEGLI STUDI DI PADOVA

DIPARTIMENTO DI INGEGNERIA INDUSTRIALE

TESI DI LAUREA MAGISTRALE
IN INGEGNERIA AEROSPAZIALE

*DEVELOPMENT OF A CONTROL SYSTEM FOR A
TIDAL TURBINE*

*SVILUPPO DI UN SISTEMA DI CONTROLLO PER
UNA TURBINA SOTTOMARINA*

RELATORE:

PROF. ERNESTO BENINI

CORRELATORE:

DR. JOAO AMARAL TEIXEIRA

LAUREANDO: *ILARIO ZANETTI*

MATRICOLA: *1036679*

ANNO ACCADEMICO 2012/2013

SOMMARIO

Il crescente interesse nella produzione di energia evitando l'inquinamento dell'ambiente ha introdotto la necessità di trovare nuovi tipi di risorse rinnovabili. La tecnologia delle turbine sottomarine è stata sviluppata per sfruttare l'energia cinetica presente nelle correnti marine.

Questa tesi presenta lo sviluppo di un sistema di controllo per una turbina sottomarina. Il sistema considerato è il concetto DeltaStream della Tidal Energy Limited. Il dispositivo in questione è costituito da una base a delta che sfrutta l'azione della gravità per rimanere appoggiata sul fondale. Tre turbine da 400kW l'una sono montate ai vertici della base. Lo sviluppo ed il collaudo di un sistema di controllo su una turbina sottomarina sono di fondamentale importanza sia per la produzione di energia che per l'affidabilità del dispositivo.

La presenza di un sistema di controllo permette di migliorare la qualità dell'energia prodotta e di ridurre le forze assiali applicate sulla struttura. Quest'ultimo punto è cruciale, soprattutto per il progetto DeltaStream, dato che il dispositivo è appoggiato al fondale. Poiché i sistemi di controllo per turbine sottomarine non sono spesso analizzati, in questo studio sono esaminati alcuni esempi derivanti dal campo delle turbine eoliche, per capire quale di questi potrebbe essere una scelta appropriata per un sistema sottomarino. Infine è presentata la strategia utilizzata dal dispositivo DeltaStream.

La turbina è stata interamente modellata in MATLAB. Numerose simulazioni sono state effettuate sottoponendo il sistema a diversi campi di moto e i risultati sono stati analizzati e discussi. Le conclusioni principali sono che la strategia di controllo implementata misurando ad ogni istante la velocità del flusso in arrivo, per controllare il voltaggio e quindi la coppia del generatore, è efficace sebbene difficile da applicare. D'altra parte, l'utilizzo di una velocità media incrementa la fattibilità del controllo riducendone però l'accuratezza.

Parole chiave:

DeltaStream, turbina sottomarina, coppia, sistema di controllo, MATLAB

ABSTRACT

The increased interest in producing energy without polluting the environment has led to the necessity of finding different types of renewable resources. Tidal turbine technology has been developed in order to exploit the kinetic energy present in marine currents.

This thesis presents the development of a control system for a tidal turbine. The device considered is the DeltaStream concept of Tidal Energy Limited. DeltaStream is a three turbine delta-shaped gravity-based device with each of the 400kW turbines mounted at every apex of the delta.

The development and testing of a control system on a tidal turbine is of fundamental importance both for the extraction of power and for the reliability of the system.

The presence of a control system permits to improve the power output quality and to reduce the axial loads applied on the structure. The last point is crucial, in particular for the gravity-based DeltaStream project. Because control systems for tidal turbines are not often analysed, some examples from the wind turbine technology are presented and examined in order to understand which of these can be a suitable choice for a tidal energy conversion system. Finally, the DeltaStream strategy is examined.

The complete turbine has been modelled in MATLAB. Simulations have been run using different incoming flow field scenarios, and the results have been analysed and discussed. The main conclusions are that the control strategy implemented measuring the incoming flow velocity at any instant, in order to control the voltage and so the generator torque, is effective although difficult to implement. On the other hand, the use of a mean velocity increases the feasibility of the control but reduces its level of accuracy.

Keywords:

DeltaStream, tidal turbine, generator torque, control system, MATLAB

ACKNOWLEDGEMENTS

This thesis represents the conclusion of a wonderful year spent in Cranfield. I wish to thank all the people that supported me during this experience.

I would like to thank very much my supervisor Dr Joao Amaral Teixeira to have guided me through the project and to have been always available during all the year. I would like to thank Judith Farman, Michael Corsar and Dr James Whidborne to have given me precious advises in order to overcome several obstacles. I wish to thank the Tidal Energy Ltd. to have given me the opportunity to work on this interesting project. I would also like to thank Prof. Ernesto Benini, Dr Roberto Biollo and Domenico Di Cugno, who permitted me to live this great experience.

The greatest thanks goes to my parents, Paolo and Mimina, who have given me the opportunity to come in England. They have supported all my choices and, although the distance, they have always been able to make me feel at home. I want to thank also my sister, Serena, who has given me the strength to overtake difficult periods during the year. A special thanks goes to Olivia, who has always been near me during this adventure. She has given a great contribution to make this year memorable.

Finally, I would like to thank my housemates Fabio, Bris, Saki and Greta for the funny year spent together. I would like to thank Alex to have been a great mate and an even better friend. An important thanks is also reserved to the Handball team and to all my friends who have made the life in Cranfield an incredible experience.

TABLE OF CONTENTS

ABSTRACT	i
ACKNOWLEDGEMENTS.....	v
LIST OF FIGURES.....	ix
LIST OF TABLES	xi
LIST OF EQUATIONS.....	xii
LIST OF ABBREVIATIONS.....	xiv
Nomenclature	xiv
Acronyms	xv
1 Introduction.....	1
1.1 Tidal currents as an attractive resource	2
1.2 Main technical challenges	3
1.3 The DeltaStream project	3
1.4 Control System Rationale	5
1.5 Outline of the thesis	5
2 Literature Review	7
2.1 Control systems for wind turbines	7
2.2 Overview of some tidal turbine projects	13
2.3 The DeltaStream Project.....	19
2.4 Techniques to control the generator torque	21
2.5 DeltaStream Project control system.....	26
2.6 Aim and Objectives of the work	31
3 Methodology.....	33
3.1 Hydrodynamic subsystem.....	33
3.1.1 Validation of the model.....	39
3.2 Gearbox subsystem	42
3.3 Electrical Subsystem.....	43
3.3.1 Working theory	43
3.3.2 Types of Induction Generator.....	45
3.3.3 Dynamic SCIG choice and modelling	45
3.3.4 Validation of the generator model	50
3.4 Controller and Control Strategy	54
3.4.1 PID controller	54
3.4.2 Control strategy	56
3.5 Flow field distributions.....	58
3.6 Complete system	61
4 Results	63
4.1 Instantaneous control.....	63
4.1.1 First case study	63
4.1.2 Second case study	67
4.2 Sensitivity analysis.....	73

4.2.1 First case study	73
4.2.2 Proposed strategy improvement	79
5 Summary	85
5.1 Conclusions	86
5.2 Future work recommendations	87
REFERENCES.....	89

LIST OF FIGURES

Figure 1.1 a) "La Rance" tidal turbine power plant [2] (left), b) DeltaStream tidal turbine [4] (right).....	1
Figure 1.2 Comparison between tidal and wind turbine dimensions - [5]	2
Figure 1.3 The DeltaStream Project - [7].....	4
Figure 2.1 Passive Stall Control - [10].....	8
Figure 2.2 Aerodynamic Spoiler - [10].....	9
Figure 2.3 Dynamic Pitch Control & Active Stall Control - [10]	10
Figure 2.4 Power Output vs. Wind Speed - [10]	11
Figure 2.5 Rotor Thrust vs. Wind Speed - [10]	12
Figure 2.6 SEAFLOW System - [12].....	13
Figure 2.7 SEAFLOW System Sketch - [13].....	14
Figure 2.8 SEAGEN System - [15]	15
Figure 2.9 AK-1000 - [18].....	16
Figure 2.10 Maximum Power Curve - [19].....	17
Figure 2.11 DeltaStream Thrust vs. Tides Speed (Courtesy of Tidal Energy Limited)	20
Figure 2.12 Desired Generator Slip - [24].....	27
Figure 2.13 Desired Slip vs. Actual Slip - [24]	28
Figure 2.14 Complete DeltaStream System Model - [24]	29
Figure 2.15 Large scale turbulence desired and real slip comparison PID torque controller - [24]	30
Figure 2.16 Small scale turbulence desired, slip comparison PID controller - [24]	30
Figure 3.1 Stream tube divided in annular sections - [25]	34
Figure 3.2 Relative Velocity - [25].....	35
Figure 3.3 Local loads - [25].....	36
Figure 3.4 Wind turbine case, C_p comparison - [24].....	40
Figure 3.5 Tidal turbine case, C_p comparison - [24]	41
Figure 3.6 Generalized gearbox system - [37].....	42

Figure 3.7 d-q equivalent circuit of an induction machine - [44].....	47
Figure 3.8 Voltages d-q transformation	50
Figure 3.9 Generator experimental data - [44].....	52
Figure 3.10 Generator simulation data	52
Figure 3.11 Simulation of the generator with a torque applied	53
Figure 3.12 Generator slip using a P control	55
Figure 3.13 Generator slip using a PI control	56
Figure 3.14 Optimum RPM vs. Tides Speed (Courtesy of Tidal Energy Limited)	57
Figure 3.15 First time dependent velocity distributions.....	58
Figure 3.16 Second time dependent velocity distributions	59
Figure 3.17 Third time dependent velocity distributions	59
Figure 3.18 Time-space dependent turbulent flow field - [46].....	60
Figure 3.19 Velocity distribution obtained by the time-space dependent flow field	61
Figure 3.20 Complete system.....	62
Figure 4.1 First case study - Distribution of velocity	64
Figure 4.2 First case study - Generator slip comparison	65
Figure 4.3 First case study - RPM.....	65
Figure 4.4 First case study - Power production	66
Figure 4.5 First case study - Axial force generation	67
Figure 4.6 Second case study - Time-space dependent distribution of velocity - [46].....	68
Figure 4.7 Second case study - Distribution of velocity	69
Figure 4.8 Second case study - Turbine response to generator inertia variation	70
Figure 4.9 Second case study - Generator slip comparison.....	71
Figure 4.10 Second case study - RPM.....	71
Figure 4.11 Second case study - Power production	72
Figure 4.12 Second case study - Axial force generation	72
Figure 4.13 Sensitivity analysis - Real and mean velocity distributions.....	74

Figure 4.14 Sensitivity analysis - Power production comparison.....	75
Figure 4.15 Sensitivity analysis - Velocity and Power output errors	76
Figure 4.16 Sensitivity analysis - Axial force generation comparison	77
Figure 4.17 Sensitivity analysis - Velocity and thrust generation errors	78
Figure 4.18 Sensitivity analysis - Real and new mean velocity distributions	79
Figure 4.19 Sensitivity analysis - New power production comparison	80
Figure 4.20 Sensitivity analysis - New velocity and power output errors	81
Figure 4.21 Sensitivity analysis - New axial force generation comparison	82
Figure 4.22 Sensitivity analysis - New velocity and thrust generation errors	82

LIST OF TABLES

Table 3.1 Nordtank 500/41 Characteristics	39
Table 3.2 SCIG parameters - [44]	51

LIST OF EQUATIONS

(1-1) - Theoretic Wind Power Output.....	2
(1-2) - Corrected Wind Power Output	2
(2-1) - Generator Slip	22
(2-2) - Electrical Rotational Velocity	22
(2-3) - Steady-state Torque-speed Characteristics.....	22
(3-1) - Angle of Attack	35
(3-2) - Profile Lift.....	36
(3-3) - Profile Drag.....	36
(3-4) - Rotor Plane Normal Loading Component.....	37
(3-5) - Rotor Plane Tangential Loading Component.....	37
(3-6) - Turbine Axial Force Calculation.....	37
(3-7) - Turbine Torque Calculation	37
(3-8) - Axial Induction Factor	38
(3-9) - Tangential Induction Factor	38
(3-10) - Solidity of the Blade	38
(3-11) - Corrected Axial Induction Factor	38
(3-12) - Corrected Tangential Induction Factor.....	38
(3-13) - Lentz's Law.....	43
(3-14) - Three-phase to Two-phase Stationary Frame Conversion	46
(3-15) - Two-phase Stationary Frame tod-q Conversion	47
(3-16) - Stator Quadrature Axis Linkage Flux Rate of Change	48
(3-17) - Stator Direct Axis Linkage Flux Rate of Change.....	48
(3-18) - Rotor Quadrature Axis Linkage Flux Rate of Change.....	48
(3-19) - Rotor Direct Axis Linkage Flux Rate of Change	48
(3-20) - Quadrature Axis Magnetizing Flux.....	48
(3-21) - Direct Axis Magnetizing Flux	48
(3-22) - Quadrature Axis Stator Current	48
(3-23) - Direct Axis Stator Current.....	48

(3-24) - Quadrature Axis Rotor Current.....	48
(3-25) - Direct Axis Rotor Current.....	48
(3-26) - Electromagnetic Torque.....	49
(3-27) - Electrical Angular Velocity Rate of Change	49
(3-28) - Stator Quadrature Axis Linkage Flux Rate of Change in the Space State	49
(3-29) - Stator Direct Axis Linkage Flux Rate of Change in the Space State ...	49
(3-30) - Rotor Quadrature Axis Linkage Flux Rate of Change in the Space State	49
(3-31) - Rotor Direct Axis Linkage Flux Rate of Change in the Space State	49
(3-32) - Electrical Angular Velocity Rate of Change in the Space State	49
(3-33) - PID Control Law	54

LIST OF ABBREVIATIONS

Nomenclature

A	Area
a	Induction factor
B	Number of blades
c	Chord
c_d	Drag coefficient
c_l	Lift coefficient
c_p	Power coefficient
D	Drag force
e	Error
F	Prandtl's tip loss factor
f	Frequency
F_{ij}	Flux linkage
i	Current
J	Inertia moment
K	Controller gain
L_{ij}	Leakage inductance
L	Lift force
P	Power
p	Number of poles
R	Resistance
s	Generator slip
T	Torque
U, v	Voltage
V	Flow velocity
x	Leakage reactance
α	Angle of attack
θ	Local pitch angle
ρ	Density
σ	Blade solidity
ϕ	Flow angle
ϕ_b	Magnetic flux
ω	Angular speed

Acronyms

BEM	Blade Element Momentum
CSC	Current source Converter
DFIG	Doubly-Fed Induction Generator
DSE	Desired Slip Estimator
DTC	Direct Torque Control
DVTC	Direct Virtual Torque Control
FOC	Field Oriented Control
MCT	Marine Current Turbines
MPPT	Maximum Power Point Tracking
MPT	Maximum Power Tracking
PMG	Permanent Magnet Generator
PMSG	Permanent Magnet Synchronous Generator
PWM	Pulse Width Modulation
SCIG	Squirrel Cage Induction Generator
TEL	Tidal Energy Ltd
TFEG	Tidal Flow Electricity Generating

1 Introduction

The increasing importance of producing electricity without polluting the environment has led to the necessity of harnessing as much as possible the renewable resources.

Since long time, the ocean has been considered as a vast renewable energy resource. In fact, it is possible to extract power from the tidal and marine currents, from the energy of the waves, from the ocean thermal energy and from salinity gradients; however, due to technology limitation and high costs, the research and development of both thermal energy and salinity gradients technologies is small in comparison with the other two concepts [1].

The kinetic energy of tidal and marine currents can be converted into electricity using principally two types of technology. A first choice is to build a tidal barrage across a bay in order to exploit the potential energy of high tides; the most important example of tidal barrage is the “La Rance” tidal power plant, shown in Figure 1.1a. The second way is to extract the kinetic energy from the free flow of water using the turbine concept, which has already been extensively developed in the wind turbine sector [3]. An example is presented by the DeltaStream Project shown in Figure 1.1b.



Figure 1.1 a) "La Rance" tidal turbine power plant [2] (left), b) DeltaStream tidal turbine [4] (right)

Although both these cases are interesting, the thesis will focus only on the second concept. The next paragraphs contain the reasons that make tidal

currents an attractive renewable resource, the main technical challenges of this technology and a presentation of the DeltaStream project.

1.1 Tidal currents as an attractive resource

The energy of tidal currents is attractive mainly for three reasons. Firstly, the density of the water is more or less 800 times higher than the density of the air; hence, it is possible to extract the same amount of power with slower flow velocity and with a smaller rotor than the wind turbine technology. In fact, as for the wind turbine, the relation giving the power output is:

$$P = \frac{1}{2} \rho A V^3 \quad (1-1)$$

Where P is the power extracted, ρ is the density of the fluid, A is the rotor area and V is the velocity of the flow. Obviously, there are some losses in the process which must be taken into account and so the formula becomes:

$$P = \frac{1}{2} \rho A V^3 C_p \quad (1-2)$$

Where C_p is named power coefficient and it is considered to be about 0.35-0.5. Figure 1.2 shows the comparison between a wind turbine and a tidal turbine both producing 1MW of power. [3,5]



Figure 1.2 Comparison between tidal and wind turbine dimensions - [5]

Secondly, the tidal current energy is not affected by the weather to the same degree of other renewable resources. For example, solar or wind energies are affected by clouds, rain, wind and fog. Thirdly, and maybe the best advantage, because of the astronomic nature of the phenomena which cause currents and tides, the amount of power that can be produced exploiting this resource can be predicted with extremely high precision and accuracy for a long period of time [3]. Moreover, tides have been predicted for long time and different mathematical models used to predict the tides have been implemented and are available in the literature. [6]

1.2 Main technical challenges

The technical challenges related to the tidal turbine technology are due mainly to the working fluid. As it has been noted before, water is 832 times denser than air. This peculiarity implies that the turbine rotor is exposed to high loads due to the interaction of the water with the blades. Hence, the blades must be shorter and thicker than those used in wind turbine in order to stand the bending moments produced by the interaction with the flow. There is also a technical issue related to the instantaneous variation of intensity and direction of the water flow due to flow turbulence. Because these variations are severe the design of the structure of a tidal turbine is one of the greatest challenges.

Due to the presence of water around all the components, the watertight integrity of the structure is of fundamental importance, in order to exclude water from the internal parts, as generator or nacelle housings. Another challenge is given by the notoriously chemically aggressive marine environment. This problem implies the use of particular materials able to withstand the corrosive effect of salt water, as for example composites [5].

1.3 The DeltaStream project

The DeltaStream device is a tidal energy conversion unit developed by Tidal Energy Ltd (TEL). Its objective is to produce electrical energy harnessing the enormous potential given by tidal currents around the UK and avoiding the generation of greenhouse gases.

It is a triangular based - gravity founded, three stream turbine tidal machine. Rock feet are embedded in the triangular steel base. The turbine rotor is three-bladed and it could have a diameter of 12m or 15 m. Each turbine is rated for a power of 400 kWe. Because the structure is just resting on the seabed, the control of the axial force applied on the structure plays a fundamental rule for the reliability and safety of the device.

An identical induction generator is mounted on each tower. The rotor and the generator are linked through a gearbox with a gear ratio around 72:1. The device is also equipped with an hydraulic yaw system with the purpose of rotating the turbines to face both incoming and ebbing tides to maximise the power output. Moreover, it is possible to park and lock the turbine perpendicularly to the flow. The raw energy generated is sent to the grid through submarine cables at 6.6 kV [7,8]. Figure 1.3 represents a sketch of the complete system.

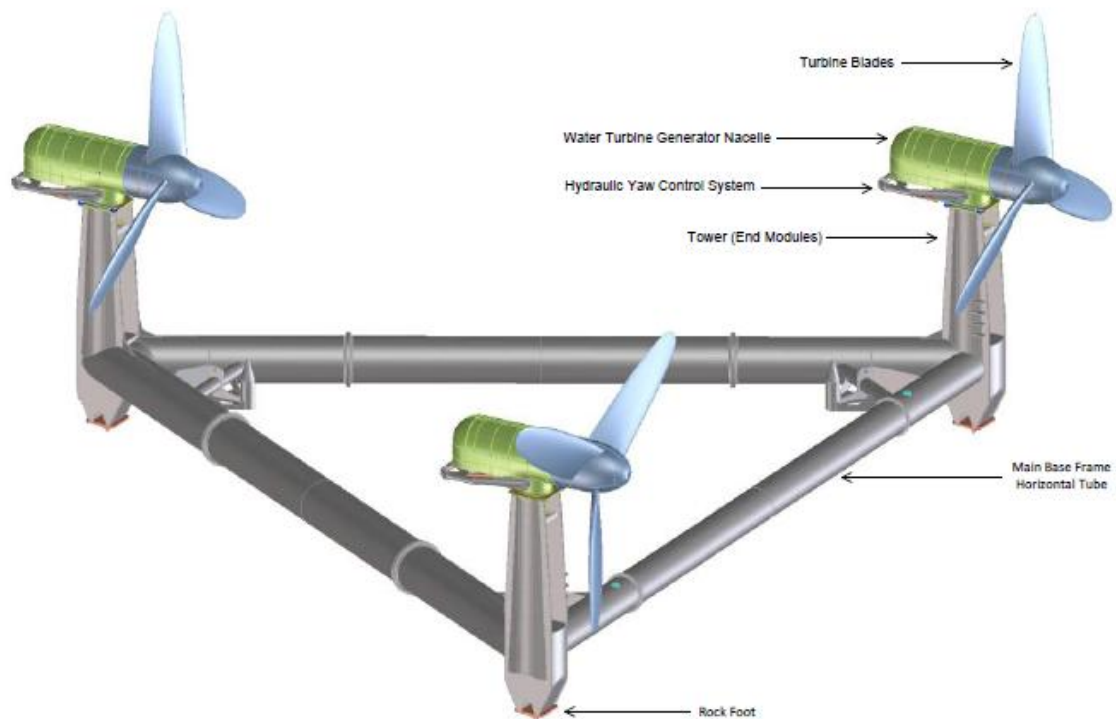


Figure 1.3 The DeltaStream Project - [7]

1.4 Control System Rationale

As mentioned before, there are two main reasons to install a control system on a tidal turbine or on a wind turbine.

Firstly, because the flow that drives the turbine is not constant, a control system is required in order to improve the quality of the electrical power output if the turbine has to be integrated on a grid. Moreover, it is needed to increase the efficiency of the whole device.

Secondly, the control system should work with the aim of reducing the load applied on the structure. The second application becomes even more important in the case of the DeltaStream project. In fact, the structure has a gravity-based foundation and a too high axial load could move the entire structure damaging the connection to the grid or the device itself. Hence, it is the role of the control system to prevent these events.

The thesis objective is then the modelling of a control system aimed to improve the electrical power output of the turbine and to reduce the loads applied on the structure, when it is affected by a flow field variable in time and space.

1.5 Outline of the thesis

The thesis will follow the following pattern. In Chapter 2, a literature review of the available control systems for wind turbines is presented. Some tidal turbine projects will be described in order to understand which control strategy can be applied to this particular energy conversion system. Finally, the adopted strategy will be analysed and illustrated.

Chapter 3 focuses on the modelling of the turbine. The procedures implemented to develop the different subsystems are explained and details of the components are given. Once each part has been developed properly, the complete model has been assembled in order to simulate the behaviour of the whole system.

Chapter 4 shows the results obtained by the different simulations. The data acquired are reported and discussed.

Finally, Chapter 5 contains the most important conclusions achieved and recommendation for the future development of this work are given.

2 Literature Review

The introduction has given an overview of the principal characteristics and advantages of a tidal turbine system. Due to the quite recent development of tidal turbine technology, up to now not many studies have been reported in the open literature regarding the control system. Because of the similarity between wind and tidal turbines, it is sensible to use the control strategies developed for a wind turbine as a starting point for the creation of a tidal turbine control system. The following literature review will present a global view of the control strategies applied to wind turbines. They will be analysed in order to find out which could be appropriate for a tidal turbine system. To conclude, the chosen strategy will be described and explored.

2.1 Control systems for wind turbines

The objectives of a control system, both for wind turbine and tidal turbine, are principally linked to the quality of the electrical power output and to the reduction of the high loads applied to the structure due to the interaction between wind or water and the turbine. In addition, the control system has to limit the tip speed of the rotor in order to reduce the noise generation [9].

It is important to mitigate the loads applied on the structure in order to ensure safe operation condition and to increase the life of the device. Regarding the power regulation, depending on the fact that the power is below or above the value at which the turbine is rated, there are two different objectives. If the power is below the rated limit it is important to maximise the power extraction; in the case that the power produced is above the rated value, it is important to limit the generation of power to the maximum rated value, in order to not overload the turbine [9].

During the last century, different types of control strategies have been developed in order to fulfil the goals of the control. They can be divided basically in two categories: passive control and active control systems. The main differences between these two configurations are described in the following paragraphs.

The principal characteristic of a passive control system is the absence of additional components that can increase the vulnerability of the entire device. Because they are less effective than the active control systems often they have to be at least combined in order to obtain satisfactory results. An example of passive control strategy is the "passive stall control". In this case, the flow around the blade stalls once the velocity of the wind exceeds a certain value, as it is possible to see in Figure 2.1. Thanks to this effect the loads applied on the rotor decrease; however, also the power generated decreases. Moreover, some aerodynamic brakes are required in order to prevent the overspeed of the rotor, in case of a loss of the generator torque. There are different types of spoiler which can be released by exploiting the high centrifugal force due to the high rotational velocity of the rotor [10]. An example is given in Figure 2.2.

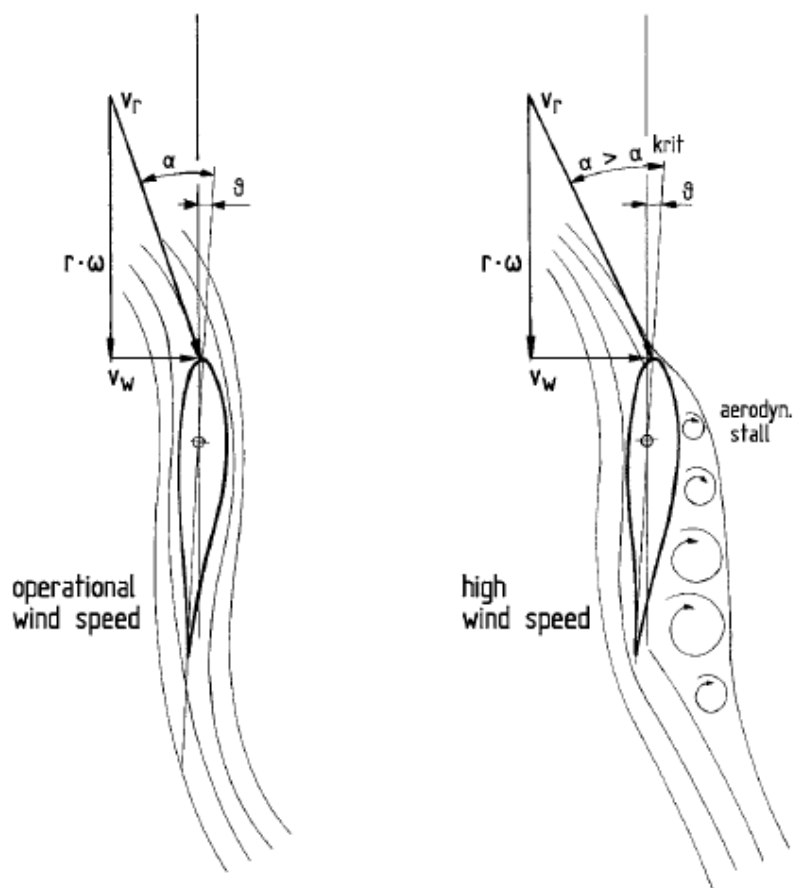


Figure 2.1 Passive Stall Control - [10]

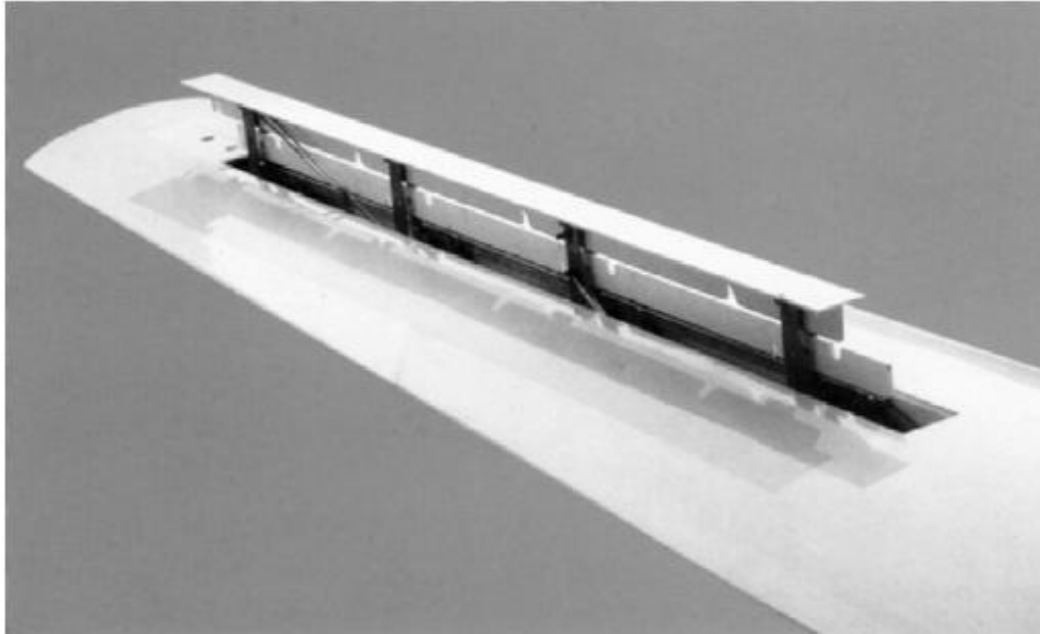


Figure 2.2 Aerodynamic Spoiler - [10]

The active control strategy involves the use of additional devices, as mechanical actuators and electric converters, which increase the accuracy and effectiveness of the turbine giving more degrees of freedom to the designer who can implement a better controller. However, the presence of supplementary devices represents a possible weakness and this reduces the reliability of the whole structure. An example of active control is given by the "pitch control strategy". With this technique the pitch angle of the blade is constantly modified in order to obtain at any instant the required power output. Another control on the blade pitch angle is the "active stall control", which consists in leading the rotor blade to a particular angle of attack called "critical aerodynamic angle of attack". In this situation the flow separates from the blade surface limiting the aerodynamic loads [10]. The above exposed principles of action are shown in Figure 2.3.

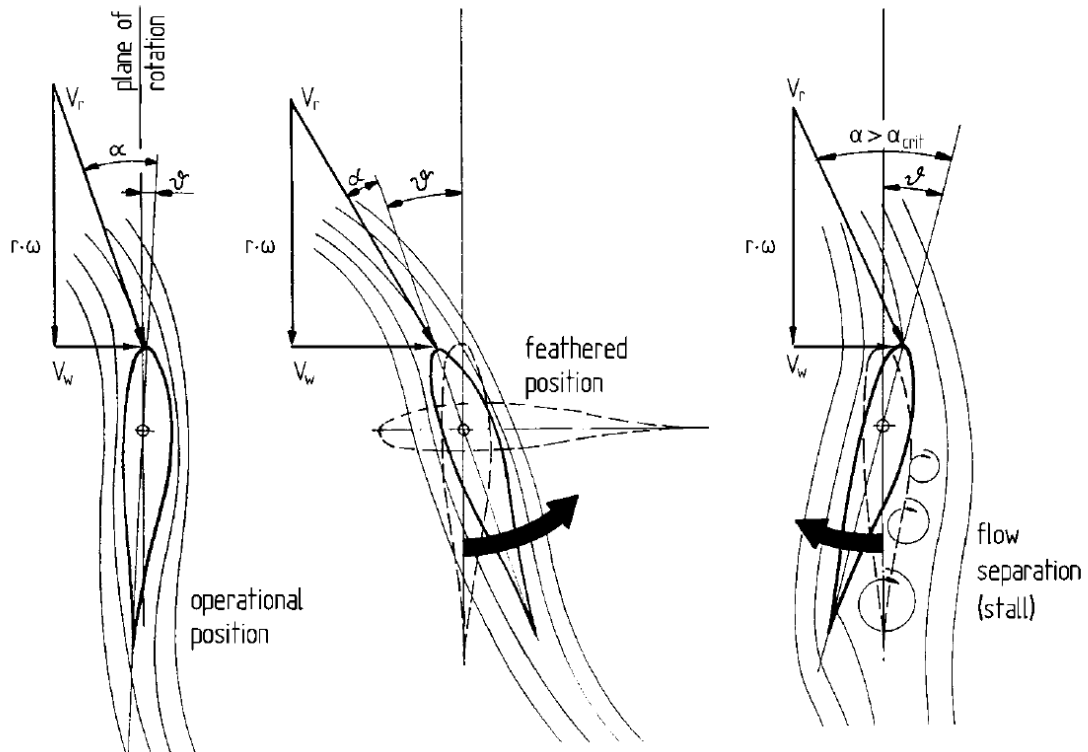


Figure 2.3 Dynamic Pitch Control & Active Stall Control - [10]

Another way of controlling the power and the loads applied on the structure is given by the use of static converters. This strategy permits variable-speed operation which increase both the quality of the power output and the life of the structure of the turbine.

As mentioned before, the active control approach is more effective than the passive control. This behaviour is illustrated Figure 2.4 and Figure 2.5.

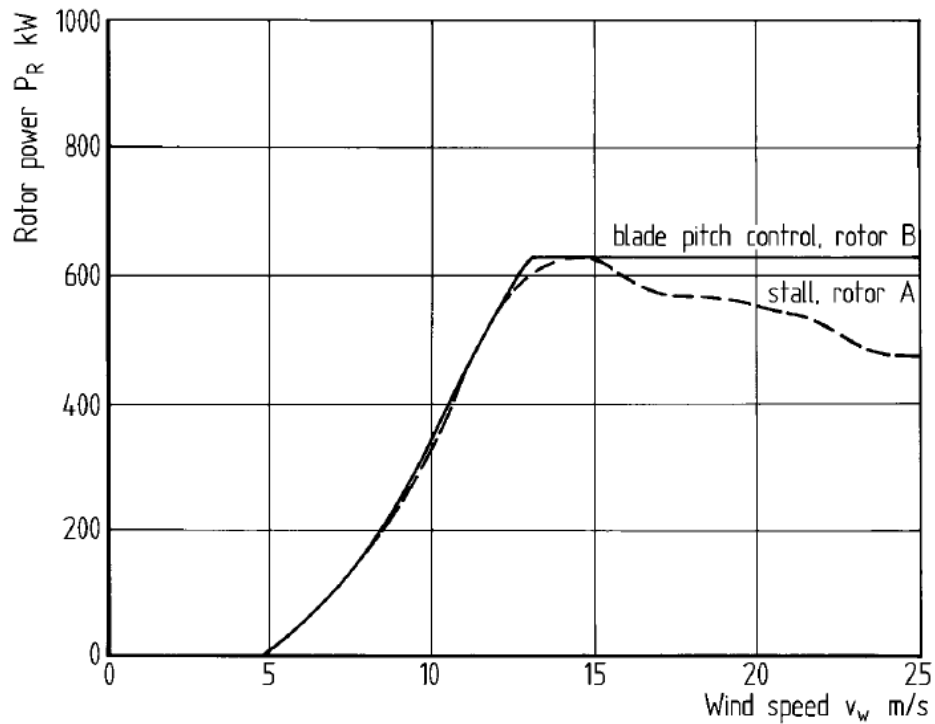


Figure 2.4 Power Output vs. Wind Speed - [10]

Both Figure 2.4 and Figure 2.5 show a comparison between a turbine controlled with a "blade pitch strategy" and a "stall strategy". In Figure 2.4, the power output against the wind speed is presented. As it is possible to see, the pitch control permits to maintain a constant value of power output once that the wind speed exceeds a certain value. On the other hand, the stall control, keeps the value of the power generated under the maximum value but, due to aerodynamic losses linked to the stall, it is not able to achieve the goal of constant power output [10].

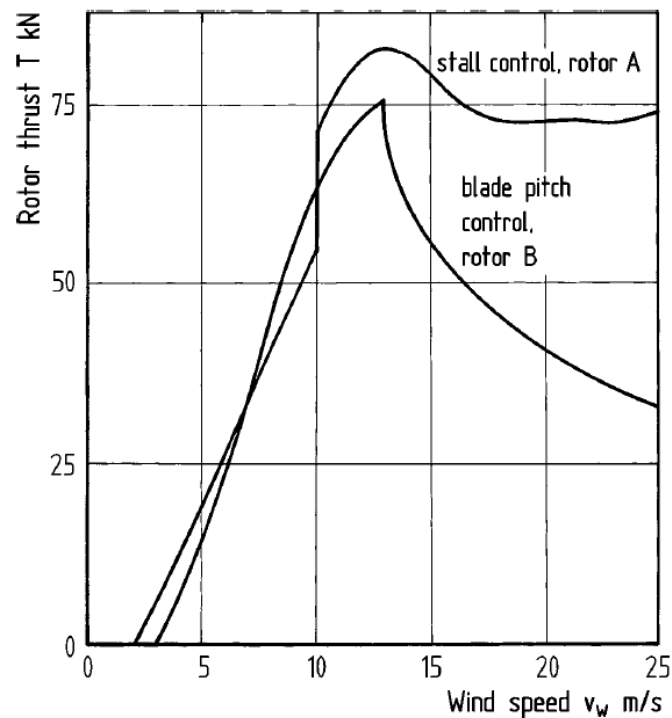


Figure 2.5 Rotor Thrust vs. Wind Speed - [10]

Figure 2.5 shows the behaviour of another important parameter for the turbine, the axial force. It is worth noting that the pitch control permits to strongly reduce the load applied on the structure when the wind speed goes above a determinate value. On the other hand, the stall control prevents the axial force to exceed the set maximum value; however, because the stall phenomena cannot be controlled entirely, this strategy is not able to reduce axial force as much as the pitch strategy [10].

All the considerations made up to now can be extended to the tidal turbine technology. However, due to additional difficulties some of these strategies cannot be implemented.

2.2 Overview of some tidal turbine projects

As it has been described previously, the components and the working theory of wind turbines and tidal turbines are similar. Hence, all the considerations made up to now can be extended to the tidal turbine technology. However, there are some additional issues which must be taken into account. Because of the presence of the water all around the device, the sealing of the machine is of fundamental importance in order to not allow the water to penetrate the components and damage the mechanical and electrical subsystems. This constraint has consequences on the choice of the control strategy. For example, a variable pitch angle turbine means the existence of moving interfaces which could be a threat for the insulation of the structure. On the other side, if it has been decided to use a passive control strategy, it is important to keep in mind the higher stresses, caused by the higher density of the working fluid, which the structure should support.

As for wind turbines, also for tidal turbines the variable speed operation gives several advantages. In fact, a variable speed turbine can adapt to the velocity of the incoming flow maximising the power output. Moreover, this operation strategy reduces the loads applied on the structure [11].

In 2003 the British company Marine Current Turbines (MCT) developed the SEAFLOW project, shown in Figure 2.6.

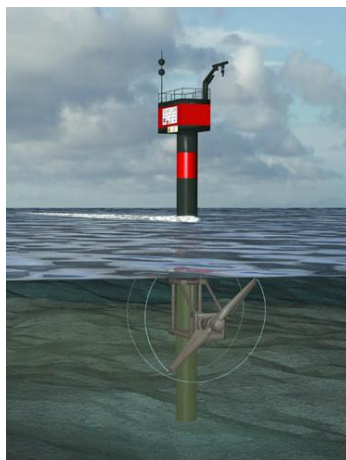


Figure 2.6 SEAFLOW System - [12]

This machine is a prototype of a variable speed tidal turbine with variable blade pitch angle, rated for a power of 300 kW. As Mattarolo et al. (2006) explain, the development and realisation of the new energy generator concept had to face some challenges, as the lack of knowledge concerning the load characteristics, the working environment and the behaviour of the resource used. Hence, using the blade element theory and a model representing the marine currents flow field, different simulations have been run in order to reach a first evaluation of the performance and of the loads. The control strategy of the SEAFLOW project consists of a pitch control and of a speed control. The pitch modulation permits to limit the power generation in case of extremely high current velocity and allow to start and stop the turbine. The speed modification gives the opportunity of increasing the power output and reducing the applied loads. The sketch of the system is shown in Figure 2.7 [13].

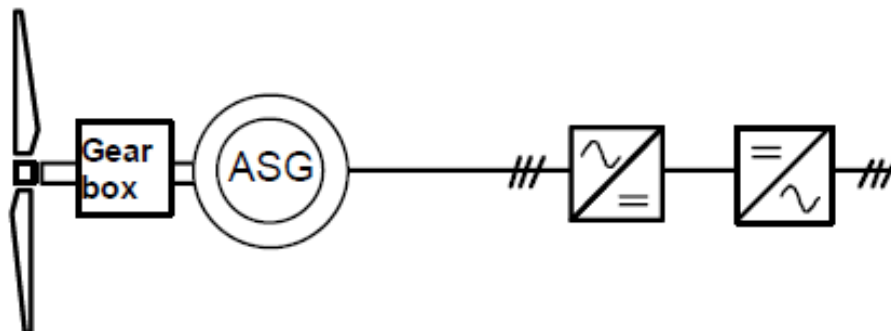


Figure 2.7 SEAFLOW System Sketch - [13]

After the simulations, the system has been accurately tested with positive results. In fact, the machine managed to reach the planned performance.

The SEAFLOW project was the first phase of a bigger project. The second phase, called SEAGEN project, has started in 2005. The system has been modified in order to reduce the costs, achieve higher power extraction and enable a better bi-directional operation [13]. To fulfil the objectives it has been chosen a twin-rotor design, as shown in Figure 2.8. Due to this configuration

new loads resulting from the interaction between the two rotors must be taken into account. Both the turbines are rated at a power of 600 kW so that the total amount of energy which can be extracted is 1.2 MW. On the structure it is installed an induction generator and a multi-stage gearbox. The control system is much more complicated than the previous one, and it consists of a full-span dynamic pitch control. [14]



Figure 2.8 SEAGEN System - [15]

Another project is the AK-1000 turbine, developed by the Atlantis Resource Corporation and illustrated in Figure 2.9. It is the largest tidal current turbine in the world with a rotor diameter of 18 meters and it is rated at a power of 1 MW at a flow velocity of 2.6 m/s. It is characterized by two contra rotating rotors, with fixed pitch blades; a direct drive permanent magnet generator is installed on the structure. The system has been tested in 2011 with positive results, even if at least other two year of testing were required to evaluate the project. [16.17]



Figure 2.9 AK-1000 - [18]

Ben Elghali et al.(2010) analysed the model of a 7.5 kW variable speed tidal turbine coupled with a doubly-fed induction generator (DFIG). The use of a DFIG offers some advantages as variable speed operation, lower converter costs and lower power losses. The proposed strategy is a Maximum Power Point Tracking (MPPT) control; the main objective of this approach is to maximise the power generation whatever the speed of the tidal current. The results have shown that using a first order model to predict the tidal speed it is possible to create a reference for the MPPT control system and obtain up to 95% of the power in all the circumstances. Moreover, thanks to the predictability of the resource it is possible to implement a control even without flow speed sensor [19].

Luo et al. (2002) introduced the development of an integrated control system for a tidal flow electricity generating (TFEG) ship. This system is quite different from a usual tidal turbine. The rotor drives a constant flux pump which pumps the hydraulic oil to the changeable flux motor which drives the generator in order to

produce the electrical power. The main functions of the controller are to stabilise the output voltage and frequency, integrate the system with other power network, protect the generator and control the turbine. The simulations have given promising results [20].

Another project designed to exploit the kinetic energy of tidal current is the C-Plane. This innovative device consists of variable pitch and torque rotors, a wing to produce the lift, mooring cable and control surfaces. The structure will be composed of two 30m diameter rotors and is rated at a power of 1.5MW when the device is exposed to a steady flow velocity of 1.5 m/s [21]. Although the project is interesting, due to the high number of controllable surfaces and the completely different structure, the control developed for this system has not been considered useful for the DeltaStream project.

Mbabazi (2010) focuses on the modelling and control of tidal turbine. The device is equipped with a permanent magnet synchronous generator (PMSG). The presence of a control system is required in order to extract the maximum amount of power at any tidal current speed. The author argues that for any tidal speed there is a rotor speed which generate the maximum energy, as shown in Figure 2.10.

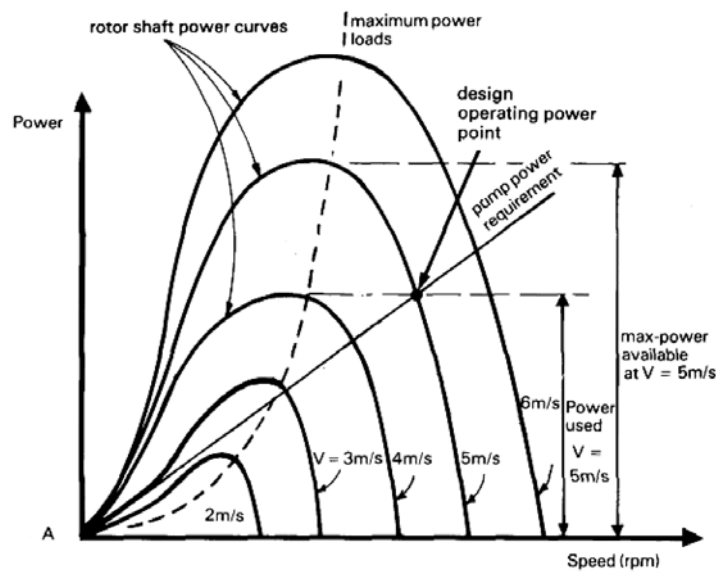


Figure 2.10 Maximum Power Curve - [19]

Hence, if the controller modifies the rotational speed of the rotor following the change in tidal speed, it is possible to optimise, at any instant, the power extraction. In order to achieve this goal the model uses pulse width modulation (PWM) and power electronics to adapt the generator parameters. Another reason to install a controller is to protect the turbine from over power, load and torque. The implemented control system does not include active control surface and the rotor windings currents are chosen as controllable variables [22]. Although the results are encouraging, the utilisation of advanced power electronics has a great economic impact in the system. In fact, when the maximisation of the power extraction is the main topic of the analysis the economic impact of the control system gains even more importance. On the other side, when a load reduction analysis is considered the costs are less relevant because the damage of the whole device would result in an higher economic impact.

As has been analysed in the previous paragraphs there are different ways to implement a control system: from passive strategy to active control surface or controlling the generator characteristics and parameters. The following section focuses on the DeltaStream project, giving a complete description of the turbine and analysing the control strategy which has been chosen.

2.3 The DeltaStream Project

The DeltaStream unit consists of three open rotor turbines located at the vertices of a triangular shaped base. Because the device is not anchored to the seabed, the total axial force which affects the structure must be lower than the frictional forces in order to avoid any motion. Hence, the design requirement is translated into a maximum power-to-thrust ratio [23]. To fulfil this requisite different options have been considered.

As noted above the most effective control strategy is the dynamic blade pitch control. With this approach the power output would be maximised, improving also the quality of the energy extracted, and the overall loads applied on the tower would be substantially reduced. However, there are some issues related to this technology. First of all, the installation of a pitch mechanism would increase the vulnerability of the device reducing its reliability; moreover, the presence of this control system would imply the existence of moving interfaces which are a serious threat for the insulation of the whole structure. For these reasons, this concept has been judged too risky and it has been abandoned [24].

If an active control system is too complex for the turbine, a complete passive control strategy is not efficient enough. The stall controlled turbines, as has been seen, present limitations both with regards to the quality of the power extracted and the reduction of the loads on the structure. Moreover, the stall phenomena produce turbulence which generate vibration and transient loads which affect the blades of the rotor. Due to these drawbacks and because the different working fluid of the tidal turbines implies an amplification of the effects of the turbulence, this strategy has also not been considered a sensible choice.

The control strategy developed for the DeltaStream tidal turbine is unique in its genre. It is a middle way between an active and a passive control system. The blade shape has been specifically designed with the purpose of obtaining a reduction in thrust without having resort to stalling. The thrust reduction beyond rated flow, above 2.7 m/s, is achieved through the speeding up of the rotor, Figure 2.11.

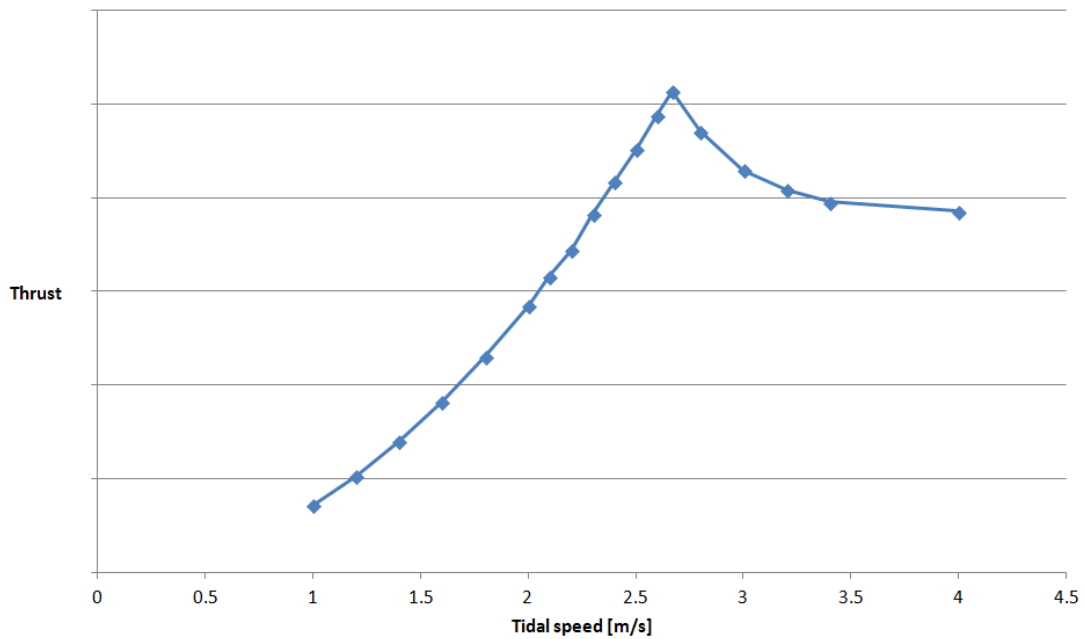


Figure 2.11 DeltaStream Thrust vs. Tides Speed (Courtesy of Tidal Energy Limited)

As it is clear from the pictures above, the thrust generated by the interaction between the tidal current and the turbine blades decreases as the tidal speed increases. The analysis of the process which brought to the creation of this particular blade is fully detailed in [23].

Although the reduction of the axial load is a fundamental requirement, the improvement of the power output quality is no less important. Hence, an analysis of the remaining active control strategies has been carried out with the aim of coupling the effects of two controllers. Because the dynamic pitch controller has already been rejected, the only remaining controllable variable are the yaw of the machine and the torque of the generator.

As it is observed in [25], in wind turbines the yaw control it is commonly used to rotate the nacelle with the purpose of minimize the misalignment between the flow current and the rotor plane. Moreover, when the speed of the wind is too high the turbine is turned to reduce the airflow through the rotor and so limit the loads on the structure and the power extraction. Even if the installation of a yaw control system has been evaluated, it has not been reputed a reliable solution

because of the possible high transient loads generated during the movement of the nacelle. However, a yaw mechanism is installed to position the rotor plane parallel to the flow when the turbine is not in use. Moreover, to keep the rotor in the "parked mode", the turbine shafts are provided with brakes [24].

After all these considerations, it is clear that the only available variable for the control of the DeltaStream device is the generator torque. Above, it was mentioned the particular design of the rotor blades. Because of that, as the rotational speed of the rotor increases, the thrust produced by the turbine decreases. The power can remain constant or decrease depending on the rotational speed and eventually it can reach the point of minimum energy extraction or freewheel condition. While this behaviour can help the structure regarding the applied forces, it is not acceptable from the power generation point of view. So the generator torque must be modified in order to control the rotational speed of the rotor [24].

2.4 Techniques to control the generator torque

As is detailed in [8], each turbine of the DeltaStream system is equipped with an induction generator. Thanks to the flexibility of induction machines and to the presence of electronic converters, which decouple the rotational speed from the grid frequency, it is possible to operate at variable speed the tidal turbine increasing the efficiency of the device [26]; an explanation of the working theory of an induction generator will be presented in the next chapter. Up to now, it is important to know that induction machines can work both as motor and as generator, depending on the speed of the rotor. If the rotational speed is higher than the synchronous speed the machine is behaving as a generator; on the other hand when the rotor speed is lower than the synchronous speed the device is acting as a motor.

The parameter that allows to easily find out which is the behaviour of the machine is the "*machine slip*". It is defined as:

$$s = \frac{\omega_s - \omega_g}{\omega_s} \quad (2-1)$$

Where ω_s is the synchronous speed, which is the angular velocity of the rotating magnetic field, and ω_g is the electrical rotational velocity of the rotor, given by:

$$\omega_g = \omega_r \frac{p}{2} \quad (2-2)$$

Where p is the number of poles and ω_r is the actual rotor speed. Hence, if s is positive the machine is performing as a motor, if it is negative as a generator [27].

In order to understand how it is possible to control the torque of an induction machine it is interesting to take in consideration the "*steady-state torque-speed characteristics*" or "*torque characteristics for short*", given by:

$$T_g = -\frac{3 U_s^2}{2 \omega_s} \frac{R_r/s}{(R_r/s)^2 + (\omega_s L_{lr})^2} \quad (2-3)$$

Where, as before, ω_s and s are the grid angular frequency and the slip, R_r and L_{lr} are the resistance and leakage inductance of the rotor windings and U_s is the feed voltage of the generator. These, along the number of poles are the variables which can be used to control the generator torque and the generator slip [26].

There are two different control strategies:

- Scalar Control
- Vector Control

Kohlrusz and Fodor (2011) present a comparison between scalar and vector control strategies of induction machine. The authors argue that in order to change the speed there are three variables which can be modified: the number of pole pairs, the magnitude or the frequency of the feed voltage. The scalar control technique implies the variation of two parameters at the same time. An

example is the *"Volt/Hertz constant method"*, which allows to control the system acting on the feed voltage frequency and on the supplied voltage magnitude. The scalar control is convenient because it is a simple, not expensive and well-implementable method. However, because it gives slow reaction to transients, its application is not suitable for dynamic systems. On the other side, there are different types of vector control techniques, as *"direct torque control"* (DTC), *"direct self-control"* and *"field oriented control"* (FOC). The latter implies the control of the currents, represented by phasors in a complex coordinate system. The vector control is an high performance method and it permits fast responses to transients; hence, it can be installed on dynamic systems. The main drawbacks are the high complexity and the price of the circuit [28].

Because the tidal turbine control is a recent subject, not many studies have been published up to now. Hence, the next paragraphs will analyse some wind turbine case studies in order to better understand the different strategies.

Arbi et al. (2009), describe a new control strategy for a variable speed wind turbine equipped with a doubly fed induction generator (DFIG). The DFIG stator is directly connected to the grid, while on the rotor side a back-to-back converter provides the voltage and frequency control. The new method is called *"direct virtual torque control"* (DVTC) and it is derived from the usual DTC, by replacing the generator torque with a virtual torque. The control of this variable is achieved through the control of the generator rotor flux. The authors argue that this new technique provides different advantages. First, only the feedback on the rotor voltage is required. Moreover, the control is simple because of the absence of PI regulators. Second, it is possible to achieve the grid connection softly at any rotational speed resulting in safe operation condition for both grid and generator [29].

Rao and Laxmi (2012) focus on the description of a DTC of a DFIG installed on a wind turbine device affected by voltage dips. The principal objective of the control strategy analysed is to remove the necessity of the crowbar protection when voltage dips take place. The author argue that when a wind turbine is affected by a voltage dip, three main problems will arise. Firstly, a voltage dip

implies difficulties for the control of the system. In fact, this perturbation acts on the stator windings which are not directly controlled in a DFIG; usually, in this device the stator is directly linked to the three phase grid and the rotor is provided by two PWM converters. Secondly, due to the variation of the stator flux, the rotor voltage has to increase in order to keep on controlling the device. Thirdly, because rotor voltages and currents have increased also the power delivered to the converter will increase. This implies a consequent increment of the DC bus voltage that can lead to a failure. The authors explain that the rotor of a DFIG can be controlled using many different techniques: a scalar control where the effects of flux and torque are coupled, a vector control where torque and flux have decoupling effect and a sensor-less vector control, which means that no speed sensor are installed on the device. The technique used in the paper is a direct torque control method coupled with a rotor flux generation strategy and it has been developed in order to maintain the device linked to the grid producing energy from the wind and avoiding the problems previously mentioned. The results of the study show that the strategy implemented permits to not activate the crowbar protection when low depth voltage dips occur. However, the presence of the protection is still require in order to ensure the reliability of the machine even under high depth voltage dips [30].

Lei et al. (2006) present the modelling of a wind turbine system again equipped with a DFIG. The control system proposed by the author in this paper consists of two parts: an electrical control of the power converter and a mechanical control of the blade pitch angle. The voltage of the rotor circuit is the controlled variable used with the purpose of simulating the power converter. The control strategy relies on the idea that for a given wind speed there is only one rotational speed at which the turbine can achieve the objective of maximum power tracking (MPT). Hence, below the rated power, the wind turbine uses the variable speed modality in order to maximise the extraction of energy; however, as the wind speed increases also the rotational speed goes up and eventually the rotor velocity will reach its limit; at that instant the pitch control will act to reduce the aerodynamic loads [31].

Mahi et al.(2007) analyse once again a wind turbine system fitted with a doubly fed induction generator. The control method implemented by the authors is a direct torque control technique coupled with a multivariable strategy. The objective of the presented control system is to improve the quality of the electrical energy extracted and increase the strength of the turbine against the different perturbations. The author argue that the advantages of the DTC strategy respect to the typical FOC are the simpler structure and the lower parameter dependence. The results showed a good performance of the system [32].

Poitiers et al. (2001) focus on the control of electrical power generated by a wind energy conversion system and interchanged between the generator stator and the power network. The objective of the analysis is achieved by controlling independently the torque and the reactive power vectors using Integral-Proportional and RST controllers. The variables which affect the active and reactive power are the rotor currents. The comparison of the results obtained has shown that the performance of the two controllers are equivalent. However, the RST controller is more effective than the PI when the speed is rapidly changed [33].

Abdolghani et al. (2012) describe a DTC method for wind turbine equipped with a permanent magnet synchronous generator (PMSG). The proposed topology is composed of a variable speed turbine, a PMSG and a current source converter (CSC) which links the generator to the grid. The generator speed is variable in order to obtain the maximum power available from the wind flow. Regarding the control strategy, there are two control methods applied on the generator, and they depends on the wind speed. The maximum power point tracking (MPPT) method is applied until the wind velocity is lower than the nominal. As soon as the wind speed exceeds the nominal value, the torque limit is applied as reference parameter. Hence, as the wind velocity rises up the generator torque decreases and the currents remain constant [34].

Chen and Spooner (2001) analyse the problem of grid connection and power quality of direct-drive variable-speed wind turbines equipped with permanent-

magnet generators. They explain that there are strict conditions which have to be satisfied in order to connect the system to the grid. The main problems are related to voltage fluctuation and harmonic distortion. Hence, the objectives of the developed control system are to maximise the power output and minimising the problems above mentioned. The control is executed by the power electronics converter, because both generator and rectifier are not controllable. The results confirm that, using a proper power electronics interface, it is possible to fulfil the requirements [35].

As the literature survey has illustrated, there are many techniques to control the torque of an induction generator. The next section will describe the control strategy which has been investigated for the DeltaStream and the results obtained up to now.

2.5 DeltaStream Project control system

M.Cecchi (2012) carried out an investigation of the possible control systems available for the DeltaStream project. A complete model of the DeltaStream tidal turbine has been developed in MATLAB/SIMULINK environment with the purpose of simulating the behaviour of the complete system. The model consists of an hydrodynamic subsystem, which includes a steady-state BEM model and represents the tidal turbine rotor; an electrical subsystem, which is composed of a steady-state generator; a control subsystem which is modelled in order to fulfil the energy and loads requirements of the project.

The author argues that the first fundamental step required to develop a control technique is the choice of the reference signal. Two options have been considered as possible reference variables: the generator torque and the rotational speed. Results have shown that choosing the rotational speed permits to achieve higher stability and faster convergence. From the rotational speed it is possible to derive the required generator slip which gives the optimal power generation and loads reduction. The desired slip as function of the tides speed is shown in Figure 2.12.

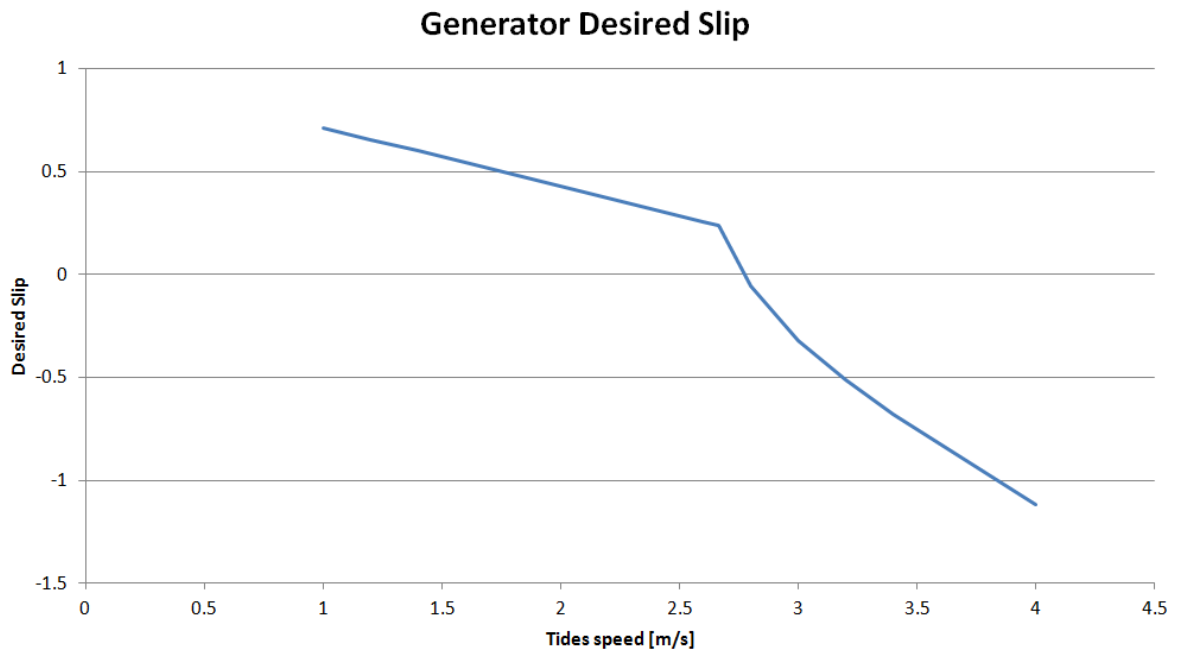


Figure 2.12 Desired Generator Slip - [24]

The second step is the development of the controller. The first method examined is an algebraic direct action controller based on the constant voltage-to-frequency ratio assumption. The control variables are the feed voltage and feed frequency. The idea of this method is that once the rotational speed of the generator rotor and the desired electromagnetic torque are known it is possible to calculate the required voltage and frequency using the assumption of constant voltage-to-frequency ratio previously mentioned. Although this strategy is the simplest possible, the results of the simulations have shown that the actual slip of the generator (green line) does not converge to the desired slip (blue line), as it is illustrated in Figure 2.13. Hence, the necessity of a closed loop strategy has been highlighted [24].

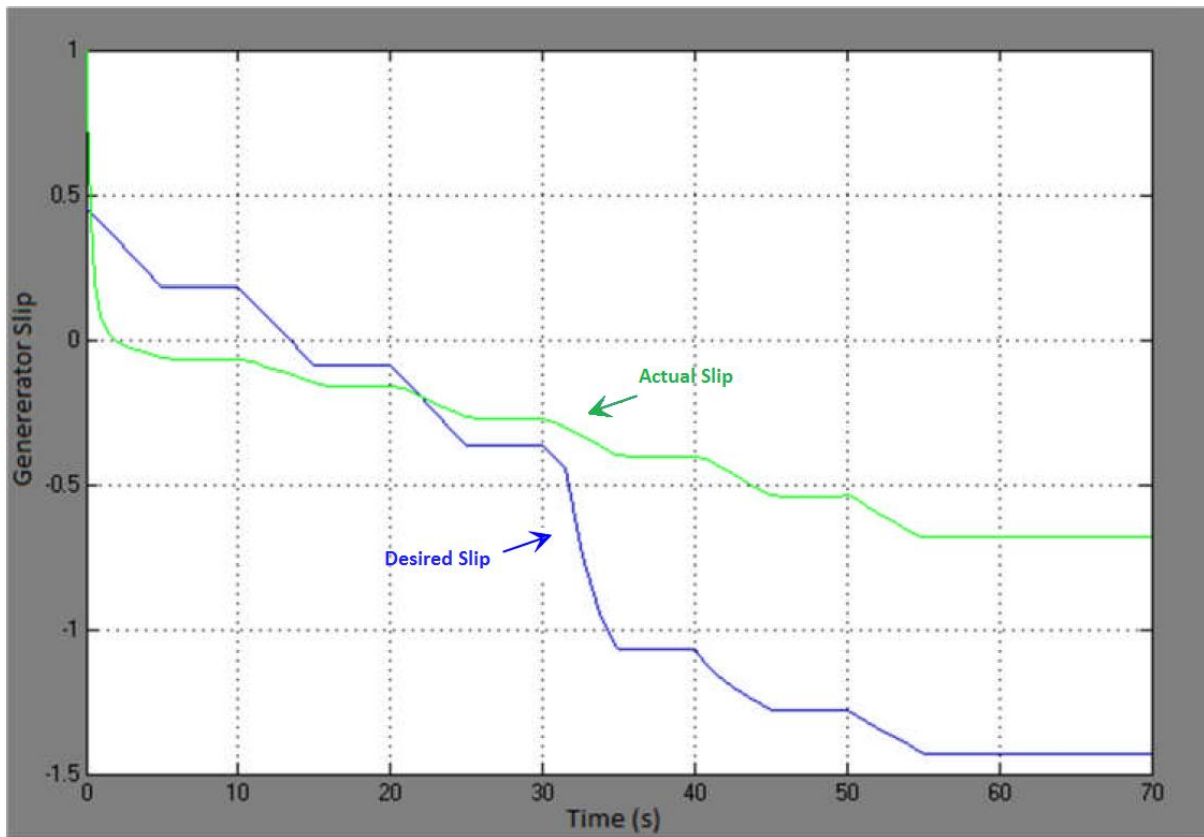


Figure 2.13 Desired Slip vs. Actual Slip - [24]

So, in the second strategy implemented it has been considered the possibility of using a feedback signal and create a dynamic control system. A PID controller has been developed in order to run simulations. As Rocco (2001) explains, PID controllers have many advantages: simplicity of construction, high efficiency on a variety of industrial processes, low cost and high reliability as standardised, ease of calibration and possibility of automatic calibration through simple tests [36].

The description of the strategy used to control the system is described in the next paragraphs. In order to explain the control loop and the logic path of the signals, it is interesting to observe Figure 2.14 which represents the complete model.

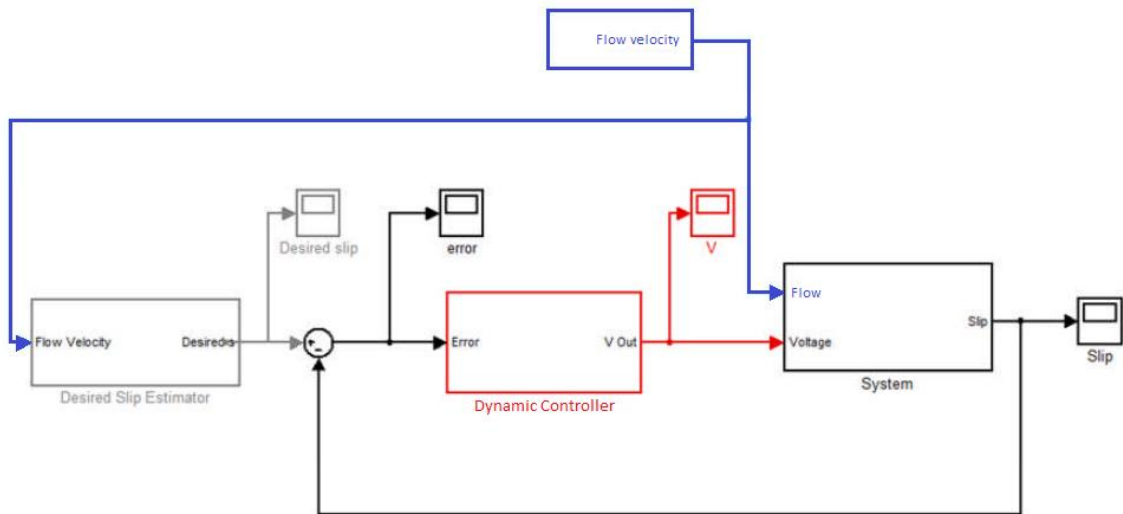


Figure 2.14 Complete DeltaStream System Model - [24]

Thanks to the presence of speed sensors, it is possible to measure the velocity of the tides. When the water current speed has been evaluated, the signal containing this information is sent to the Desired Slip Estimator (DSE) block and to the System block. The DSE block contains a look-up-table which calculates the desired slip relative to the velocity input signal. At the same time, the System block simulates the behaviour of the complete system and generate as output the actual generator slip. This output signal is then compared to the desired generator slip, and the error between the two measurements enters in the Dynamic Controller block where the PID controller has been implemented. The output of the control system is the generator voltage required for the convergence of the actual generator slip to the desired generator slip [24].

Many simulations have been run with the aim of testing the effectiveness of the PID control developed. The results have shown a good response of the device affected by the different current conditions, as illustrated in Figure 2.15 and Figure 2.16.

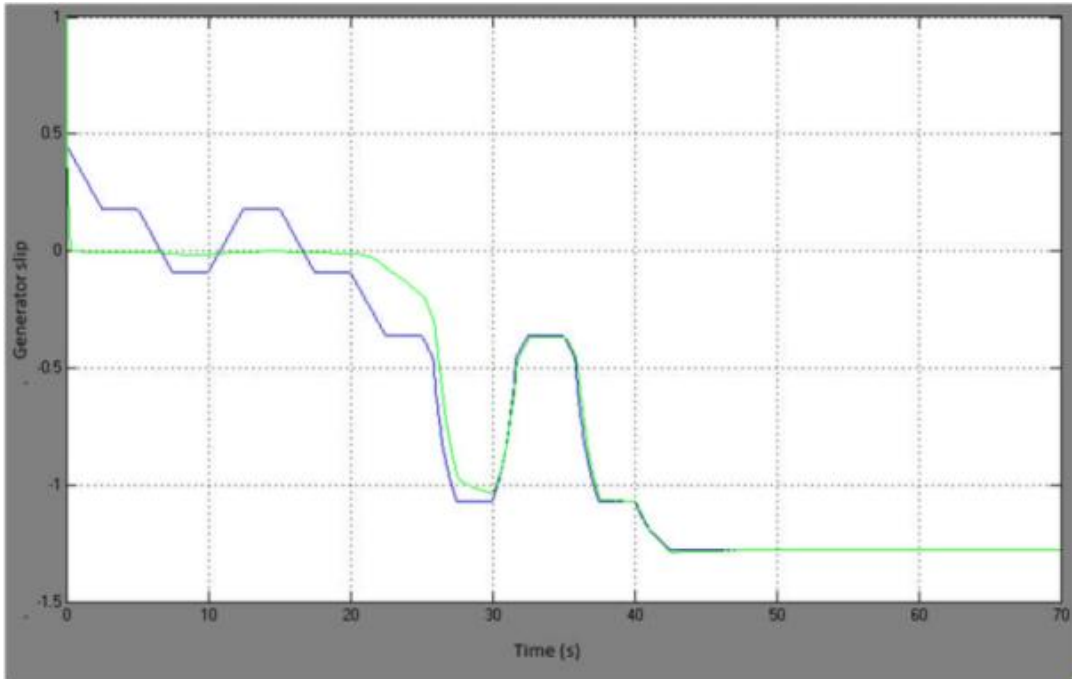


Figure 2.15 Large scale turbulence desired and real slip comparison PID torque controller - [24]

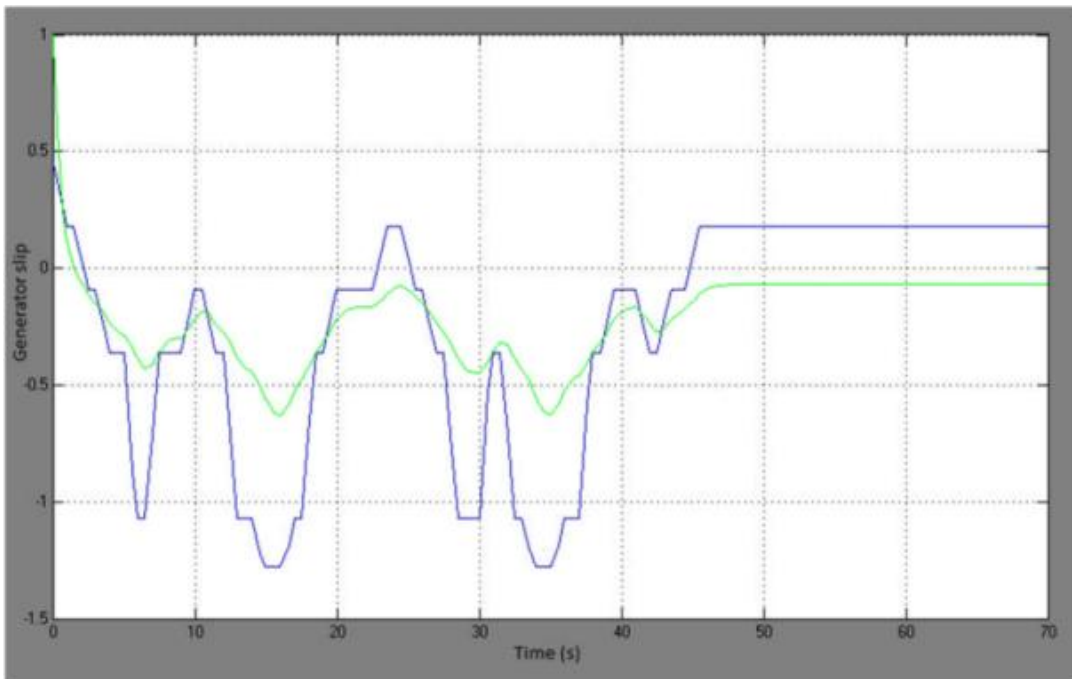


Figure 2.16 Small scale turbulence desired, slip comparison PID controller - [24]

Along with the PID controller a dynamic pitch control system has been evaluated. Although the results have pointed out that this method would give the best control, the installation of a pitch control system has been considered not effective on the DeltaStream tidal turbine. Hence, the dynamic pitch controller is not considered as an available option for the control of the device [24].

2.6 Aim and Objectives of the work

The previous sections described the problem related to the control of a tidal turbine and the importance of this subsystem. Hence, the aim of the thesis is to develop a control system able to reduce the axial loads applied to the structure and to improve the quality of the power output, that means extract the maximum amount of energy when the power is lower than the rated value and extract a constant amount of energy when the power could exceed the rated value.

To fulfil the aim of the thesis, different objectives have to be accomplished:

- Implementation of a BEM model (MATLAB).
- Development of a dynamic induction generator (MATLAB).
- Generation of a controller (MATLAB).
- Coupling of the entire system with time-space dependent distributions of velocity (MATLAB).

3 Methodology

A detailed model of each part of the device is required in order to simulate the realistic behaviour of the DeltaStream tidal turbine. The next sections focus on the procedures and methodology used to implement the different subsystems which are part of the entire tidal turbine model.

It is important to note that the model has been developed in MATLAB environment. However, a SIMULINK version of the complete model will be shown with the purpose of clarifying the logical path of the signals.

Section 3.1 describes the modelling and the validation of the hydrodynamic subsystem. Section 3.2 briefly analyses the gearbox subsystem. Section 3.3 includes a detailed analysis of the modelling and validation of the electrical subsystem. Section 3.4 explains the controller and the control strategy adopted. Section 3.5 gives information about the different flow fields which have been used to affect the turbine in order to analyse the behaviour of the complete system. Finally, Section 3.6 describes the complete model explaining the path followed by the signal during a simulation.

3.1 Hydrodynamic subsystem

The hydrodynamic subsystem of a tidal energy conversion system represents the rotor of the turbine. It has the purpose of converting the kinetic energy of the water current into mechanical power. The conversion takes place thanks to the interaction between the water flow and the rotor blades. For sake of simplicity in this analysis vibration and aeroelastic modes of the blades have not been considered.

With the classical blade element momentum model (BEM) it is possible to evaluate the steady loads, torque and thus power produced when the turbine is affected by variable wind speed. Moreover, different blades pitch and rotor speed configuration can be used in order to establish the optimal design [25]. The BEM model used for this project takes in consideration the real geometry of

the rotor, including the chord distribution and the twist angle at each section of the blade.

Although an unsteady BEM model could better represent the behaviour of the turbine, its implementation has not been considered because it exceeded the purpose of the thesis. The next paragraphs analyse the procedure used to build the steady BEM model.

The first step consists in representing the incoming flow as a stream tube and to divide it in N annular sections of height dr , as shown in Figure 3.1.

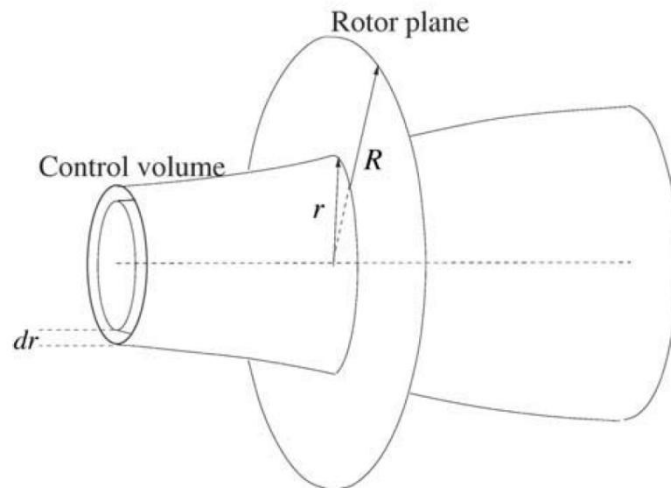


Figure 3.1 Stream tube divided in annular sections - [25]

Three main assumptions are considered in the BEM model:

- The boundary of the annular sections are stream lines; hence, the flow cannot pass from an annulus to another.
- There is no radial dependency between the elements.
- The rotor has an infinite number of blades; therefore, in each annular section the force produced by the blade on the flow is constant.

Obviously, the rotor represented in the model has not an infinite number of blades. Hence, a correction factor, called "*Prandtl's tip loss factor*", will be introduced with the intention of solving this problem [25].

As second step, it is important to note that the velocity seen by any element of each blade is different from the velocity V_0 of the flow, where this velocity is the speed of the flow far upstream of the rotor. In order to evaluate the loads produced, another velocity has to be considered. It is called "*relative velocity*" and it is given by the combination of the tangential velocity and the axial velocity, as shown in Figure 3.2.

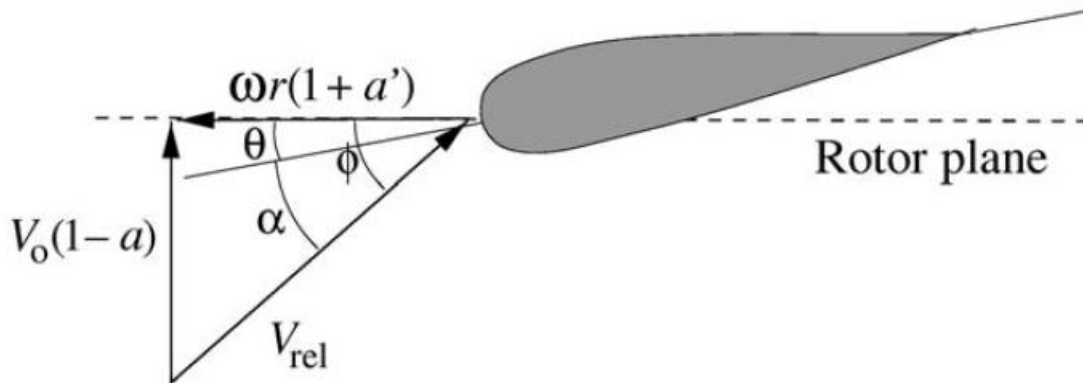


Figure 3.2 Relative Velocity - [25]

Where, $V_0(1 - a)$ is the axial velocity, $\omega r(1 + a')$ is the tangential velocity, ϕ is the angle between the relative velocity and the rotor plane, θ is the local pitch angle and α is the angle of attack, which is calculated as follow:

$$\alpha = \phi - \theta \quad (3-1)$$

In the picture above, there are other two parameters that worth to mention a and a' . They are called respectively "*axial induction factor*" and "*tangential induction factor*". The presence of these factors is needed in order to calculate the real velocities seen by the rotors [25].

Once the relative velocity has been determined, it is possible to calculate the lift and the drag forces applying the following formula:

$$L = \frac{1}{2} \rho V_{rel}^2 c C_l \quad (3-2)$$

$$D = \frac{1}{2} \rho V_{rel}^2 c C_d \quad (3-3)$$

Where ρ is the density of the water, V_{rel} is the relative velocity, c is the chord, C_l and C_d are respectively the lift coefficient and the drag coefficient which can be found in tables from the literature.

Although lift and drag are really interesting parameters, the axial force, which produces thrust, and the tangential force which generates momentum are more important. Hence, applying simple trigonometric transformation it is possible to calculate the normal and tangential forces, as it is illustrated in Figure 3.3.

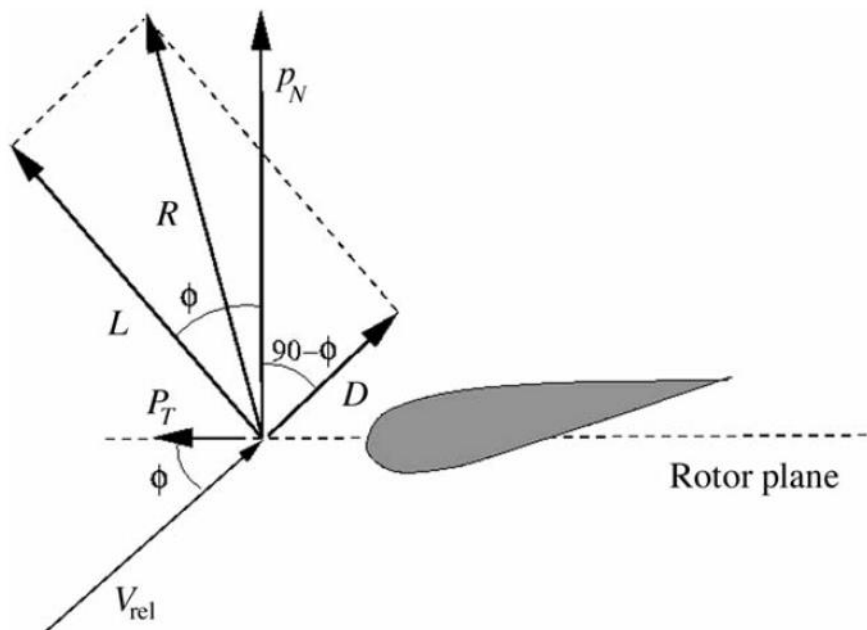


Figure 3.3 Local loads - [25]

Where R is the resultant of the sum between lift and drag, p_N and p_T are respectively the axial and the tangential forces. The formula giving the axial and tangential components are:

$$p_N = L \cos \varphi + D \sin \varphi \quad (3-4)$$

and

$$p_T = D \sin \varphi - L \cos \varphi \quad (3-5)$$

After these considerations it is possible to calculate the thrust and torque of each section using the following formula:

$$dT = B p_N dr \quad (3-6)$$

and

$$dM = r B p_T dr \quad (3-7)$$

Where B is the number of blades, dr is the height of the annular section and r is the radial position of the control volume.

Although this is the formulation related to the BEM model, there is a further step which must be taken into account. In order to start all the calculation it is required to know which are the induction factors. Hence, because it is not easy to calculate analytically the values of the induction factors, an iterative process is needed in order to establish them. So, at the first step the induction factors are set equal to zero and a first cycle is carried out. Once all the calculations have been done, using the following expression the new values of the induction factors are computed.

$$a = \frac{1}{\frac{4(\sin \varphi)^2}{\sigma C_n} + 1} \quad (3-8)$$

$$a' = \frac{1}{\frac{4 \sin \varphi \cos \varphi}{\sigma C_t} - 1} \quad (3-9)$$

Where C_n and C_t are coefficients obtained dividing p_N and p_T by $\frac{1}{2}\rho V_{rel}^2 c$ and σ is the solidity of the blade and it is defined as:

$$\sigma(r) = \frac{c(r)B}{2\pi r} \quad (3-10)$$

Where $c(r)$ is the local chord. If the difference between the old and the new induction factor satisfy the required accuracy the iterative process can stop. On the other side, if the error is too high the process start again using the new values for the axial and tangential induction factors [25].

As it has been announced at the beginning of the section, a correction factor must be taken into account in order to correct the infinite number of blade hypothesis. In fact, the vortex system in the wake depends on the number of rotor blades. This parameter is called "*Prandtl's tip loss factor*" and it is applied to the induction factors as follow:

$$a = \frac{1}{\frac{4F(\sin \varphi)^2}{\sigma C_n} + 1} \quad (3-11)$$

$$a' = \frac{1}{\frac{4F \sin \varphi \cos \varphi}{\sigma C_t} - 1} \quad (3-12)$$

Where F is the "*loss factor*" [25].

3.1.1 Validation of the model

As this project is the natural continuation of [24] the BEM model used is the same. The model has been developed completely in MATLAB environment. The validation process consisted of two steps. A first validation of the code has been done against a wind turbine case study. Afterwards, the validation has been carried out against a tidal turbine case study. The decision of starting with a wind turbine comparison is due to the fact that the convergence of the method for a tidal turbine system is more problematic. In fact, because of the lower velocity of the fluid the calculation of the induction factors is more complicated [24]. Buckland et al. (2010) describe a BEM optimisation which should be used if more accurate results are required.

The wind turbine case study here considered is the Nordtank 500/41 installed at Risø National Laboratories. The information available regarding the structure of the Nordtank 500/41 turbine is shown in Table 3.1.

Nordtank 500/41 Characteristics

Cut-in Wind Speed	4 m/s
Cut-out Wind Speed	25 m/s
Radius	20.5 m
Number of Blades	3
Swept Area	1320 m ²
Blades Type	LM 19.1
Length	19.04 m
Weight	1960 kg
Profile	NACA 63-4xx & NACA FFA-W3
Blade Tip Angle	-0.2° ± 0.2°
Max root Chord	1.65 m
Rotational Speed	27.1 rpm

Table 3.1 Nordtank 500/41 Characteristics

The results of the validations are shown in Figure 3.4 and Figure 3.5.

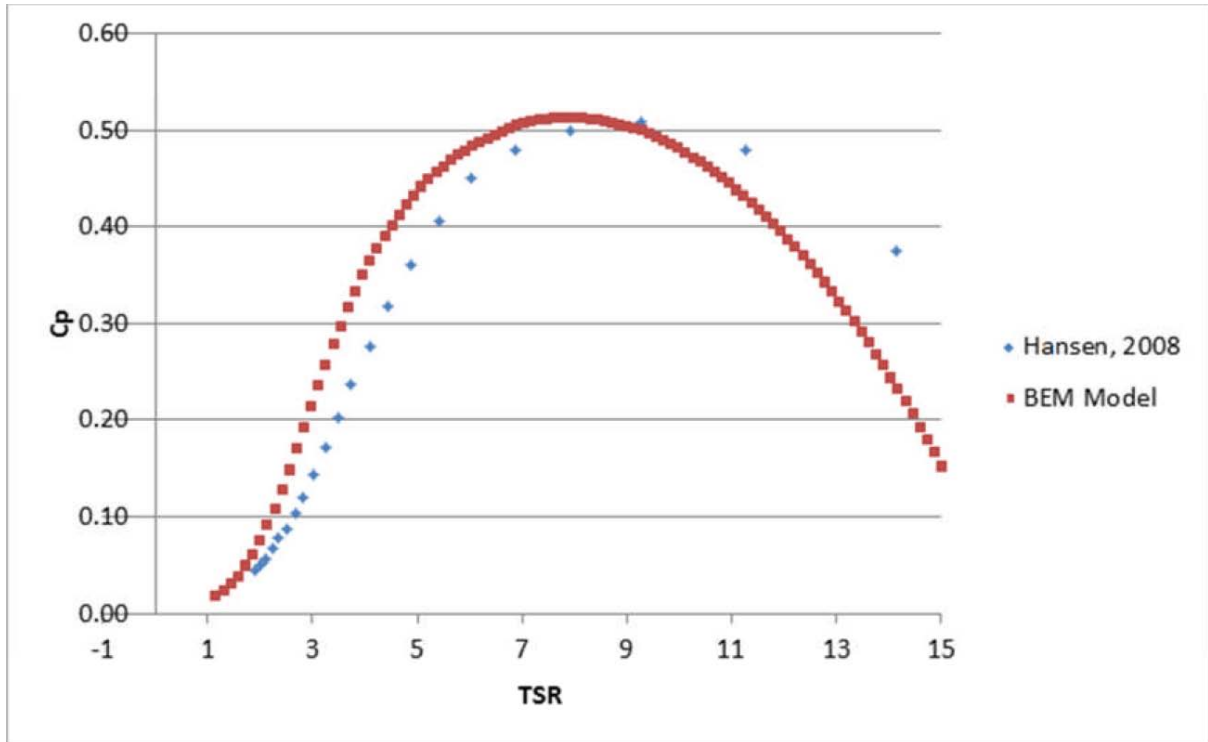


Figure 3.4 Wind turbine case, C_p comparison - [24]

Figure 3.4 shows the comparison between the results published by Hansen (2008) and the results calculated using the BEM model implemented. Cecchi (2012) argues that, although the C_p comparison presents an error around the 10%, the BEM can be considered accurate enough. In fact, no information was given regarding the blades pitch angle, the flow speed and the airfoil used. Hence, the assumptions made to replace this lack of information (5° pitch angle, 13 m/s flow speed, NACA 0012 airfoil) imply a mismatch in the results.

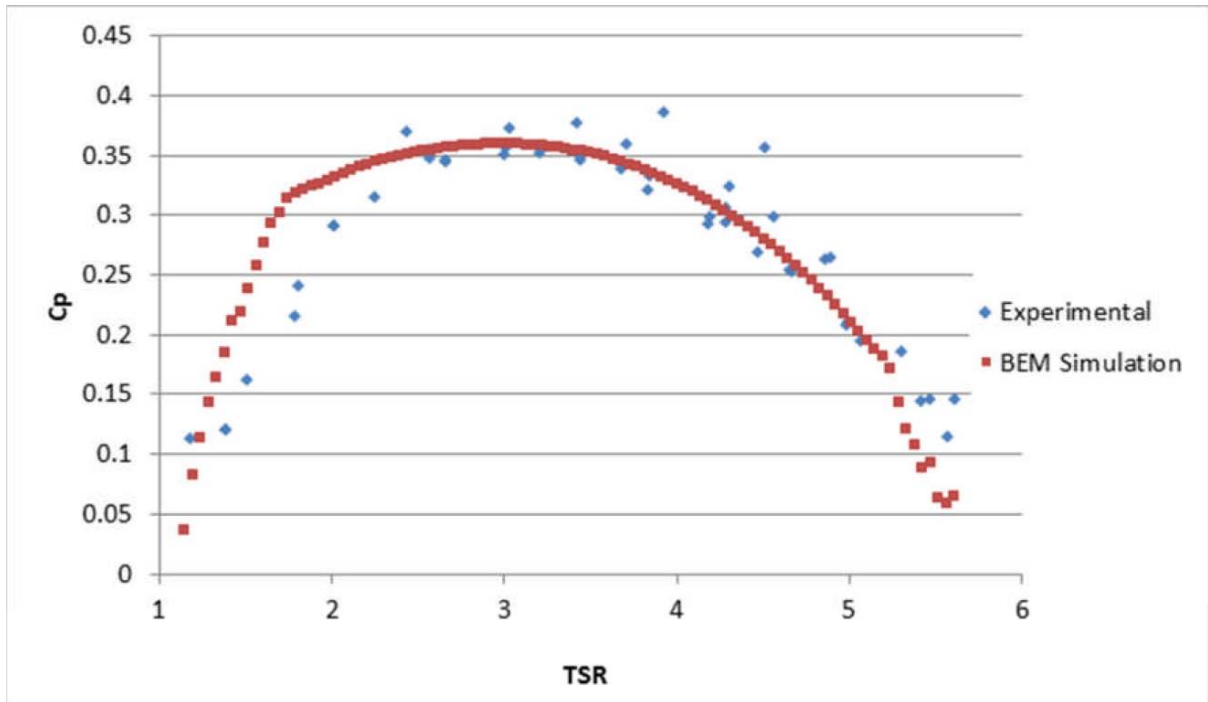


Figure 3.5 Tidal turbine case, C_p comparison - [24]

For the tidal turbine case study, the device considered is a scaled turbine unit, with a diameter of 800 mm, tested in a water tunnel. Figure 3.5 illustrates the comparison between the C_p calculated with the BEM code and the experimental data. As it is clear, the results show a good agreement, in particular for a tip-speed ratio (TSR) higher than 2, where the error is about 2-3% [24].

3.2 Gearbox subsystem

An important subsystem of the tidal turbine is the gearbox. Its function is to link the rotor shaft to the generator shaft, in order to obtain the required velocity and loads. In the model developed in MATLAB the generator is represented just by a 1:72 ratio, which means that the velocity of the rotor shaft is 72 times lower than the velocity of the generator and that the torque produced by the turbine is 72 times higher than the loads applied on the generator. Despite this simple representation, the gearbox is one of the most expensive elements of an energy conversion turbine [37]. Moreover, it is also one of the major causes of failure in wind turbines [38]. For the similarity between wind and tidal turbines it must be considered a critical component also for the DeltaStream device. Figure 3.6 illustrates a generalized gearbox system.

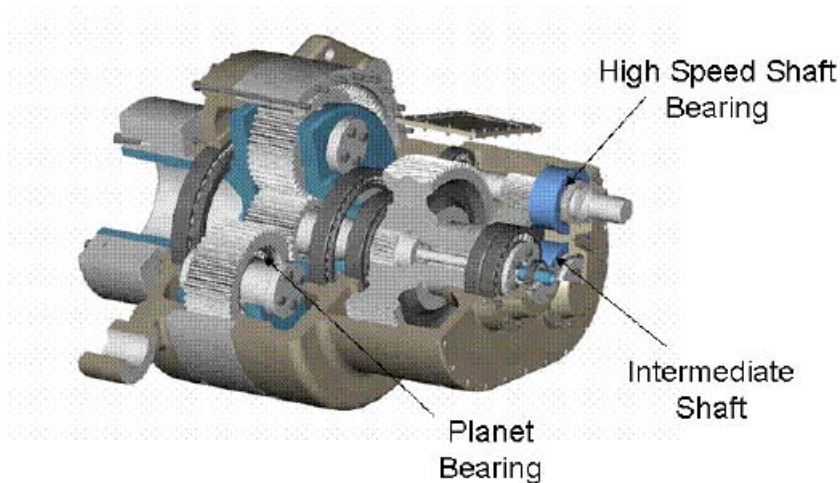


Figure 3.6 Generalized gearbox system - [37]

Before proceeding with the other subsystems, it is interesting to briefly describe the problems related to the gearbox which make this component so critical.

As McNiff et al (1991) pointed out, torque loads applied to a wind turbine gearbox are caused by the interaction of the effects produced by the wind acting on the rotor, the braking system of the turbine and the electrical generator. Because the magnitude of the total applied load is quite unpredictable, the gearbox requirements are difficult to estimate. Hence, a great number of gearbox systems were built underestimating the real stress which the device was going to encounter. Additionally, the gearbox is usually placed at the top of the tower, plunged in a vibrating environment which increases even more the variability of the loads. Moreover, the peak transient loads due to the start up, emergency stop or generator speed variation can be higher than the peak load experimented during the steady operation. Although these forces affect the device for a short period of time, they can significantly reduce the lifetime of the gearbox, leading to unexpected failure [38].

3.3 Electrical Subsystem

As it is illustrated in [8] an induction generator is placed at the corner of each tower of the DeltaStream turbine. The role of this machine is to convert the mechanical energy of the shaft into electrical power.

Before describing the model implemented in MATLAB it is worth to briefly describe the working theory of an induction generator and what are the most common types of induction generator used in the energy conversion sector.

3.3.1 Working theory

The induction machines derive this name from their principle of action. When the stator is supplied by a three-phase current, a rotating magnetic field B_s is generated and it affects the rotor. According to the *Lenz's law*, this interaction induces in the rotor an electromotive force which can be calculated as follows:

$$emf = -\frac{d\phi_B}{dt} \quad (3-13)$$

Where emf is the electromotive force, and $d\phi_B$ is the change in magnetic flux. The minus represents the fact that the induced electromotive force acts against the change in magnetic flux.

This electromotive force circulates a current which produces a magnetic field B_r mechanically linked to the rotor. Through the interaction between the primary magnetic field (stator-side) and the secondary magnetic field (rotor-side) the machine produces torque. As the relative velocity between the two magnetic fields decreases, also the electromotive force and the induced rotor current drop. Eventually, when the rotor reaches the synchronous angular velocity the electromotive force generated is zero and there is no more torque production [39].

This description applies to a generic induction machine; no attention has been paid to the behaviour of the device either as generator or as motor. As it has been briefly explained in Section 2.4, an important factor used to assess if the machine is working as a motor or as a generator is the "*generator slip*", which is defined by the following formula:

$$s = \frac{\omega_s - \omega_g}{\omega_s}$$

Where ω_s is the synchronous speed and ω_g is the electrical rotational velocity of the rotor, given by:

$$\omega_g = \omega_r \frac{p}{2}$$

Where p is the number of poles and ω_r is the actual rotor speed. If the slip is positive the machine is behaving as a motor; in fact, the rotor magnetic field is following the stator magnetic field. On the other side, when the slip is negative the device starts to work as a generator sending power back to the electrical grid [39].

3.3.2 Types of Induction Generator

The tidal turbine considered in this study is a variable speed turbine. This characteristic has consequences on the design of the electrical subsystem of the machine. Variable speed induction generator are a common choice in both wind and tidal turbines. There are three possible configuration for the generator:

- Squirrel cage induction generator (SCIG)
- Doubly-fed induction generator (DFIG)
- Permanent magnet generator (PMG)

Among these choices, a very attractive solution is represented by the squirrel cage induction machines. The principal advantages of this technology are the robustness, the low cost and the absence of high maintenance requirements [40]. On the other side, the attractiveness of the DFIG derives primarily from its ability to handle high speed variation around the synchronous speed; moreover, using a DFIG it is possible to control the reactive power and reduce the converter rating [41,42]. The newest technology is represented by the PMG generator. The benefits of this component are the more compact design and an easier fulfilment of the latest grid connection requirements [43].

3.3.3 Dynamic SCIG choice and modelling

In [24] the author developed a steady-state induction generator. The torque-speed characteristic of this device is given by the following formula:

$$T_g = -\frac{3 U_s^2}{2 \omega_s} \frac{R_r/s}{(R_r/s)^2 + (\omega_s L_{lr})^2}$$

Where ω_s and s are the grid angular frequency and the slip, R_r and L_{lr} are the resistance and leakage inductance of the rotor windings and U_s is the feed

voltage of the generator [26]. In order to improve the accuracy of the results obtained in his work, the author recommended the development of a dynamic induction generator. Hence, in this thesis a dynamic squirrel cage induction generator has been implemented in MATLAB environment.

Unfortunately, it has not been possible to obtain data regarding the real generator of the system. Hence the choice of using a squirrel cage induction generator has been considered to be advantageous for different reasons. First of all, because the device has to be mounted on a tidal turbine the operations of maintenance are really challenging. Hence, a machine which does not require an high level of maintenance has been judged to be an optimal solution. Moreover, the generator is robust and with this configuration it is also possible to reduce the development costs. However, this can be considered the worst scenario and future works could take into account to implement a DFIG in order to increase the precision of the control system; in fact, the doubly fed induction generator has one more degree of freedom which can be used to improve the quality of the controller.

The SCIG has been implemented following the guidelines by Ozpineci and Tolbert (2003). Because the induction machine has been represented in the d-q reference system (Figure 3.7) also the three phase voltages must be transformed into the d-q reference system. Hence, the following conversions have been applied.

$$\begin{bmatrix} v_{qs}^s \\ v_{ds}^s \end{bmatrix} = \begin{bmatrix} 1 & 0 & 0 \\ 0 & -\frac{1}{\sqrt{3}} & -\frac{1}{\sqrt{3}} \end{bmatrix} \begin{bmatrix} v_a \\ v_b \\ v_c \end{bmatrix} \quad (3-14)$$

Where v_a, v_b, v_c are the voltages in the three-phase voltages, v_{qs}^s and v_{ds}^s are the voltages in the two-phase stationary frame.

$$\begin{bmatrix} v_{qs} \\ v_{ds} \end{bmatrix} = \begin{bmatrix} v_{qs}^s \cos \theta_e - v_{ds}^s \sin \theta_e \\ v_{qs}^s \sin \theta_e + v_{ds}^s \cos \theta_e \end{bmatrix} \quad (3-15)$$

Where v_{qs} and v_{ds} are the two-phase synchronously rotating frame and θ_e is the electric angle calculated by the integration of the three-phase input frequency.

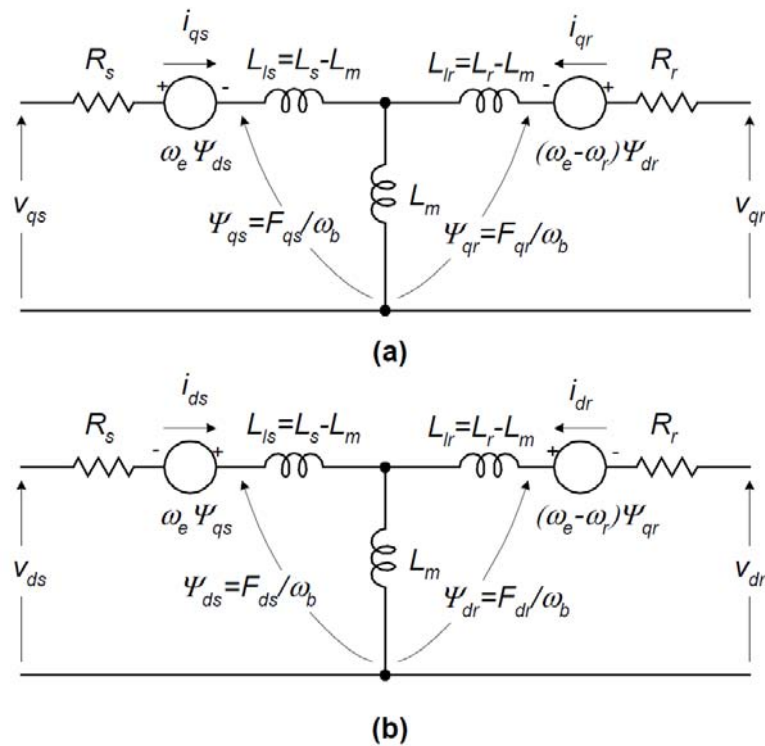


Figure 3.7 d-q equivalent circuit of an induction machine - [44]

The second step has been to implement the entire model in MATLAB. According with the Ozpineci and Tolbert paper, the Krause's model is one of the most popular choice. Hence, the modelling equation in flux linkage form are:

$$\frac{dF_{qs}}{dt} = \omega_b \left[v_{qs} - \frac{\omega_e}{\omega_b} F_{ds} + \frac{R_s}{x_{ls}} (F_{mq} + F_{qs}) \right] \quad (3-16)$$

$$\frac{dF_{ds}}{dt} = \omega_b \left[v_{ds} + \frac{\omega_e}{\omega_b} F_{qs} + \frac{R_s}{x_{ls}} (F_{md} + F_{ds}) \right] \quad (3-17)$$

$$\frac{dF_{qr}}{dt} = \omega_b \left[v_{qr} - \frac{(\omega_e - \omega_g)}{\omega_b} F_{dr} + \frac{R_r}{x_{lr}} (F_{mq} - F_{qr}) \right] \quad (3-18)$$

$$\frac{dF_{dr}}{dt} = \omega_b \left[v_{dr} + \frac{(\omega_e - \omega_g)}{\omega_b} F_{qr} + \frac{R_r}{x_{lr}} (F_{md} - F_{dr}) \right] \quad (3-19)$$

Where F_{ij} ($i = q$ or d and $j = s$ or r) are the flux linkages, F_{mq} and F_{md} are the magnetizing flux linkages, R_s and R_r are the stator and rotor resistances, x_{ls} and x_{lr} are the stator and rotor leakage reactance, v_{qs} and v_{ds} are the stator d-q voltages, v_{qr} and v_{dr} are the rotor d-q voltages, ω_e is the stator feed frequency, ω_g is the electrical rotational velocity of the rotor (as it has been defined in Section 2.4) and ω_b is the base frequency which is related to the stability of the system. Moreover:

$$F_{mq} = x_{ml}^* \left[\frac{F_{qs}}{x_{ls}} + \frac{F_{qr}}{x_{lr}} \right] \quad (3-20)$$

$$F_{md} = x_{ml}^* \left[\frac{F_{ds}}{x_{ls}} + \frac{F_{dr}}{x_{lr}} \right] \quad (3-21)$$

$$i_{qs} = \frac{1}{x_{ls}} [F_{qs} - F_{mq}] \quad (3-22)$$

$$i_{ds} = \frac{1}{x_{ls}} [F_{ds} - F_{md}] \quad (3-23)$$

$$i_{qr} = \frac{1}{x_{lr}} [F_{qr} - F_{mq}] \quad (3-24)$$

$$i_{dr} = \frac{1}{x_{lr}} [F_{dr} - F_{md}] \quad (3-25)$$

$$T_e = \frac{3}{2} \left(\frac{p}{2} \right) \frac{1}{\omega_b} (F_{ds} i_{qs} - F_{qs} i_{ds}) \quad (3-26)$$

$$T_e - T_l = J \left(\frac{2}{p} \right) \frac{d\omega_g}{dt} \quad (3-27)$$

Where $x_{ml}^* = 1 / \left(\frac{1}{x_m} + \frac{1}{x_{ls}} + \frac{1}{x_{lr}} \right)$ and x_m is the magnetizing impedance, i_{qs} and i_{ds} are the stator d-q currents, i_{qr} and i_{dr} are the rotor d-q currents, T_e is the electrical output torque, T_l is the load torque, p is the number of poles and J is the moment of inertia.

Taking into account all these relations, it is now possible to describe the induction machine model using a set of five differential equations. By rearranging the previous formulas the differential equation system becomes:

$$\frac{dF_{qs}}{dt} = \omega_b \left[v_{qs} - \frac{\omega_e}{\omega_b} F_{ds} + \frac{R_s}{x_{ls}} \left(\frac{x_{ml}^*}{x_{lr}} F_{qr} + \left(\frac{x_{ml}^*}{x_{ls}} - 1 \right) F_{qs} \right) \right] \quad (3-28)$$

$$\frac{dF_{ds}}{dt} = \omega_b \left[v_{ds} + \frac{\omega_e}{\omega_b} F_{qs} + \frac{R_s}{x_{ls}} \left(\frac{x_{ml}^*}{x_{lr}} F_{dr} + \left(\frac{x_{ml}^*}{x_{ls}} - 1 \right) F_{ds} \right) \right] \quad (3-29)$$

$$\frac{dF_{qr}}{dt} = \omega_b \left[-\frac{(\omega_e - \omega_g)}{\omega_b} F_{dr} + \frac{R_r}{x_{lr}} \left(\frac{x_{ml}^*}{x_{ls}} F_{qs} + \left(\frac{x_{ml}^*}{x_{lr}} - 1 \right) F_{qr} \right) \right] \quad (3-30)$$

$$\frac{dF_{dr}}{dt} = \omega_b \left[\frac{(\omega_e - \omega_g)}{\omega_b} F_{qr} + \frac{R_r}{x_{lr}} \left(\frac{x_{ml}^*}{x_{ls}} F_{ds} + \left(\frac{x_{ml}^*}{x_{lr}} - 1 \right) F_{dr} \right) \right] \quad (3-31)$$

$$\frac{d\omega_g}{dt} = \left(\frac{p}{2J} \right) (T_e - T_l) \quad (3-32)$$

It is interesting to note that the voltages v_{qr} and v_{dr} have been set equal to zero in order to simulate a squirrel cage induction generator. The input of all these equations are the feed voltages v_{qs} and v_{ds} , the electrical angular velocity of the stator ω_e , the characteristics of the generator and the base frequency ω_b . On the other side, the output are the currents i_{ij} , the electrical torque T_e produced by the generator and the rotor electrical speed ω_g .

3.3.4 Validation of the generator model

As for the BEM model, also the generator model has been validated. First of all, the program which permits to convert the three-phase voltages into the two-phase synchronously rotating frame has been simulated. The results are shown in Figure 3.8.

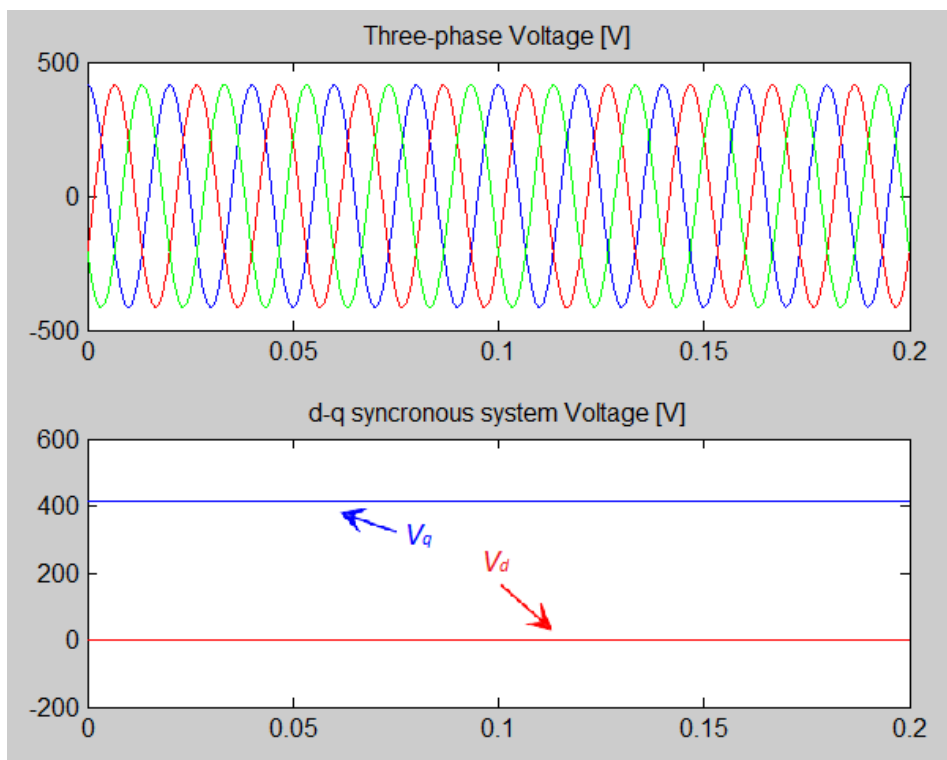


Figure 3.8 Voltages d-q transformation

As it is possible to see, the transformation from the three-phase system to the two-phase synchronously rotating frame works perfectly. It is worth noting that the voltages v_{qs} and v_{ds} are constant because, for control purpose, the phase of the generator voltage has been chosen equal to the phase of the grid voltage.

Once the efficacy of the reference system transformation has been confirmed, the second step has been to make a comparison between the results of the MATLAB simulation and the data available from the Ozpineci and Tolbert (2003) paper in order to evaluate the accuracy of the model. It has been chosen to implement the generator model using the parameters given in [44] and shown in Table 3.2.

SCIG Parameters

Stator Resistance	$R_s = 0.19 \Omega$
Rotor Resistance	$R_r = 0.39 \Omega$
Stator Inductance	$L_{ls} = 0.21 \cdot 10^{-3} \text{ H}$
Rotor Inductance	$L_{lr} = 0.6 \cdot 10^{-3} \text{ H}$
Magnetizing Inductance	$L_m = 4 \cdot 10^{-3} \text{ H}$
Feed Frequency	$f = 100 \text{ Hz}$
Number of Poles	4
Inertia	$J = 0.0226 \text{ Kg}\cdot\text{m}^2$
Feed Voltage	$V = 220 \text{ V}$

Table 3.2 SCIG parameters - [44]

The results of the comparison are illustrated in the following picture. In the charts are presented the three-phase stator currents, the applied torque T_l and the electrical torque T_e , the synchronous speed ω_e and the electrical angular velocity of the rotor ω_g . Figure 3.9 is available in [44] while Figure 3.10 shows the results obtained by the implemented generator code. As it is possible to see, the data show a good match. It is interesting to note that after the transient of about 0.1 seconds, the device becomes stable and produces the required torque, which in this case is set equal to zero.

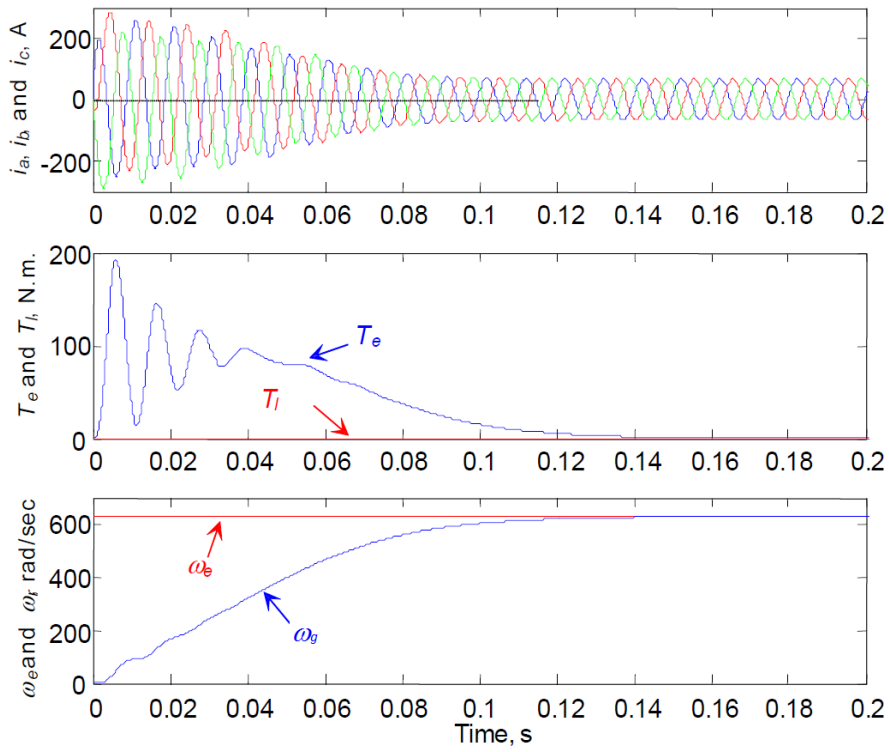


Figure 3.9 Generator experimental data - [44]

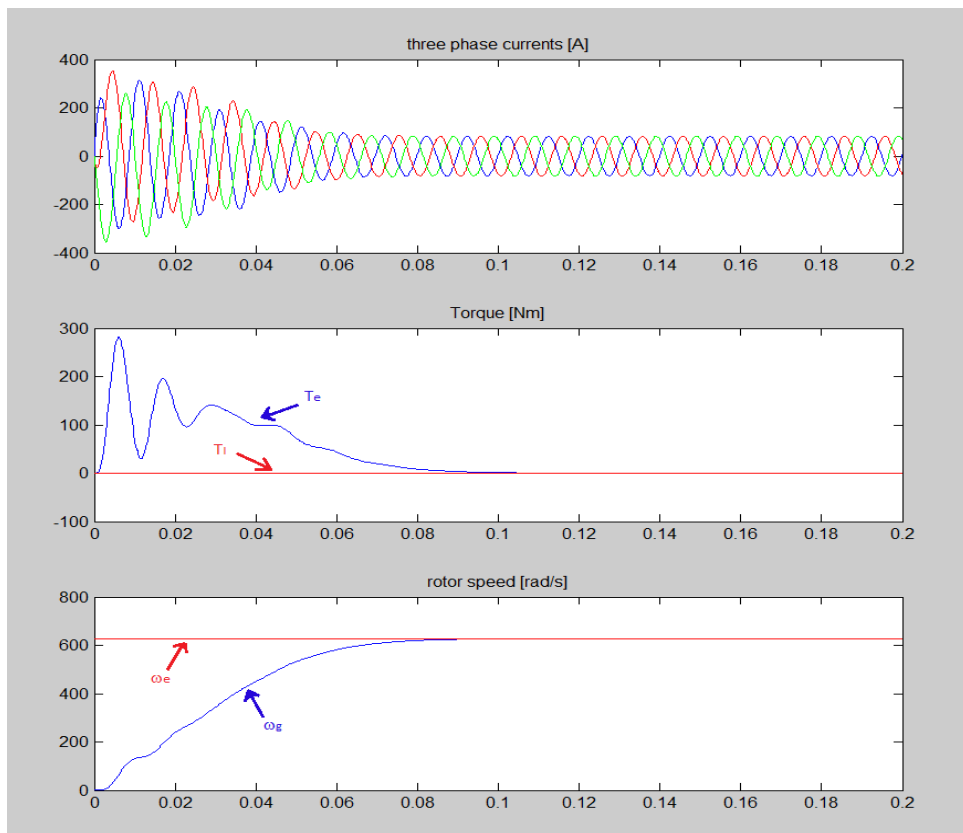


Figure 3.10 Generator simulation data

Although the model is working, for this comparison no load was applied to the machine. Hence, because the final objective is to couple this SCIG generator to the whole tidal turbine, it has been required to check that the device is able to tolerate also an higher load applied. The model has been slightly modified using the generator parameters available from [24] and different simulations have been run giving good results. An example is given in Figure 3.11.

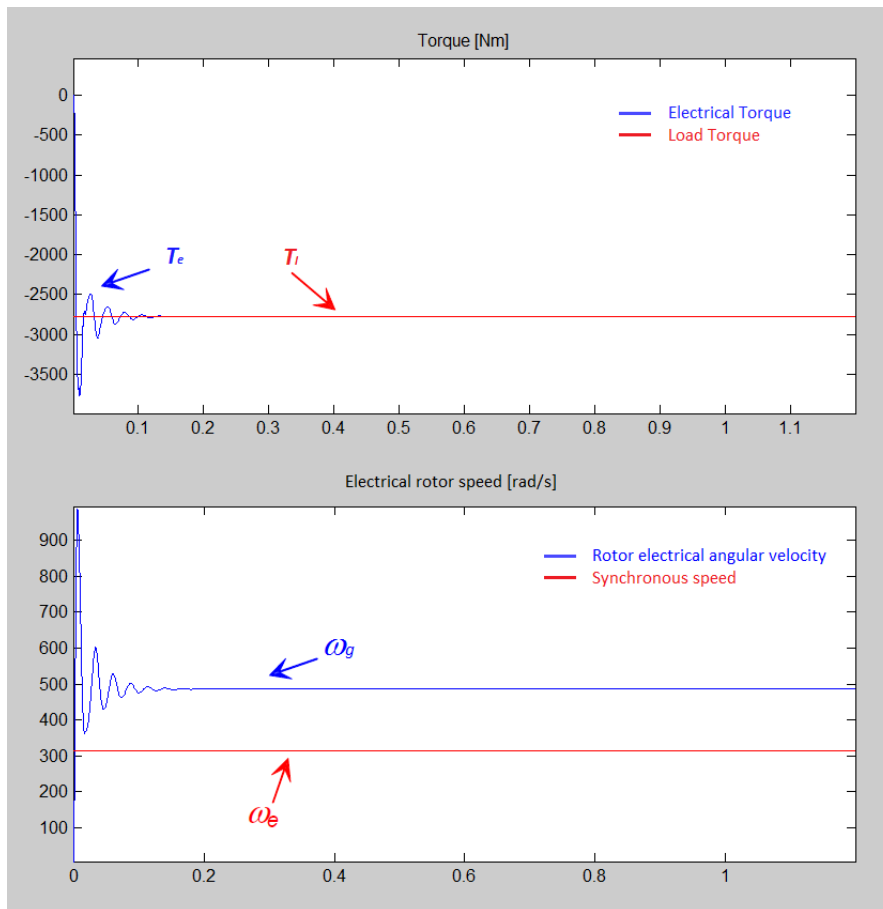


Figure 3.11 Simulation of the generator with a torque applied

There are a couple of points which are worthy of note. First of all, it is interesting to see that the theory has been respected by the simulation. In fact, as it has been said in the previous paragraph, if the induction device is behaving as a generator the rotor speed is higher than the synchronous speed and so the slip

is negative. Secondly, it is important to clarify that the torque applied to the model is considered negative in order to make the machine work as a generator. Indeed, this model could be used as a motor, just applying a positive torque load.

3.4 Controller and Control Strategy

As it has been explained in the previous chapters the requirements imposed to the DeltaStream project have two different natures. Firstly, the reduction of the loads generated by the interaction between the structure and the water current. Secondly, the improvement of the power output quality. To fulfil these requisites it has been decided to follow the work of [24] and implement a feedback control using a PID controller.

3.4.1 PID controller

A standard PID controller produces a control action which depends on the error obtained by the comparison between the desired and the simulated value of the reference parameter, as illustrated in equation 38.

$$u(t) = K_p e(t) + K_I \int_0^t e(\tau) d\tau + K_D \frac{de(t)}{dt} \quad (3-33)$$

Where $e(t)$ is the error, $u(t)$ is the control action, K_p , K_I , and K_D are respectively the proportional, integrative and derivative gains. The proportional factor K_p is typically the main drive in the control loop and it reduces a substantial part of the error. However, in order to minimize the final error it is necessary to implement also the integrative part of the controller, which is related to K_I . The derivative term, which involves the use of the derivative gain K_D , is used when the output changes rapidly. However, it has no effect on the final error [36,45].

From the general PID control law it is possible to implement other different options, as for example:

- P, using only the proportional factor.
- PI, considering the proportional and integrative parameters.
- PD, applying the proportional and derivative actions.

The results of the simulations have shown that a PI configuration was enough to achieve a good control of the system. Hence, this type of controller has been implemented. The following images illustrate the different behaviour of the device, in particular the generator slip, in the case of P and PI controllers. It is possible to see how the theory regarding the action of the different gains (proportional and integrative) , which has been explained some paragraphs before, is respected by the results. In fact, the proportional control alone managed to reduce the error, Figure 3.12. However, in order to minimise it, an integrative factor has to be added, Figure 3.13.

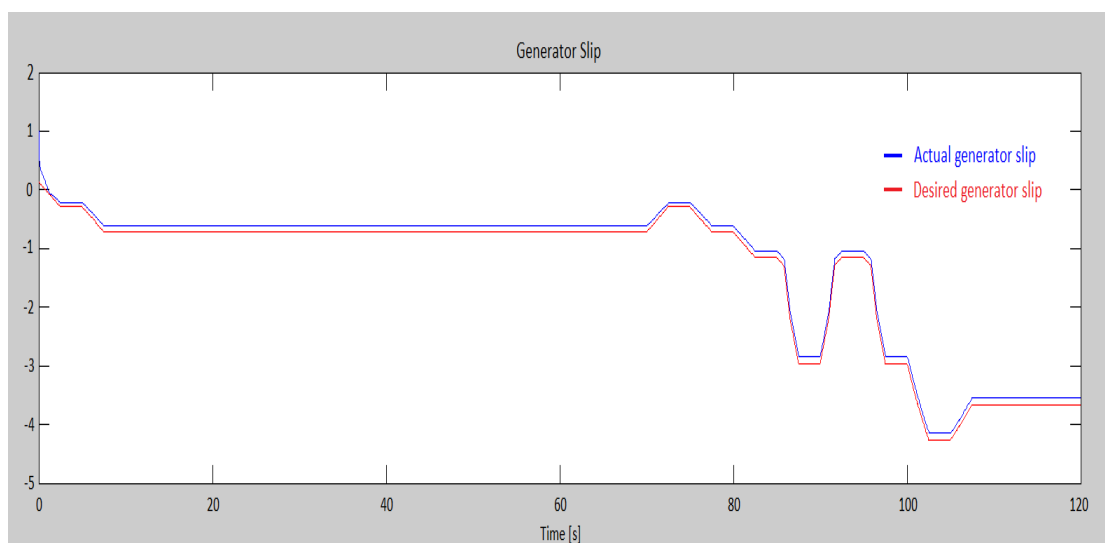


Figure 3.12 Generator slip using a P control

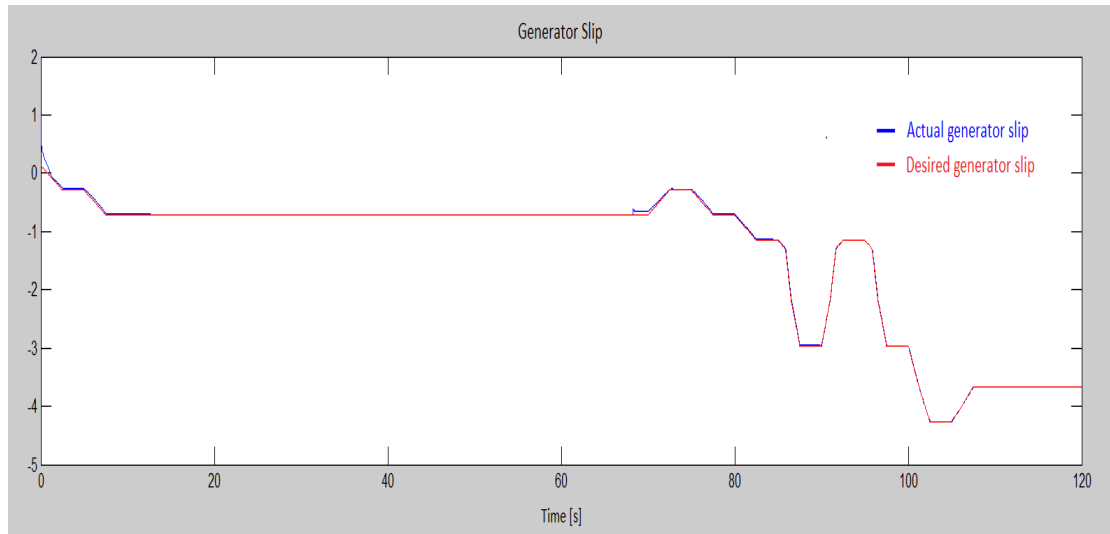


Figure 3.13 Generator slip using a PI control

3.4.2 Control strategy

In order to create a control system it is necessary to define the variables which have to be measured and the parameters which have to be modified to control the behaviour of the whole system. The control strategy implemented in this project is described in the following paragraph.

Because of the particular design of the rotor blades, to any tide velocity corresponds a rotor speed which maximises the quality of the power output and maintains acceptable the axial loads applied to the structure. Hence, the basic idea of the strategy is to measure at any instant the velocity of the water flow and evaluate, from the current experimental data given by TEL (Figure 3.14), which one is the optimum rotational speed of the rotor. Once the desired angular velocity is known, it is possible to calculate the desired generator slip, which becomes the reference value.

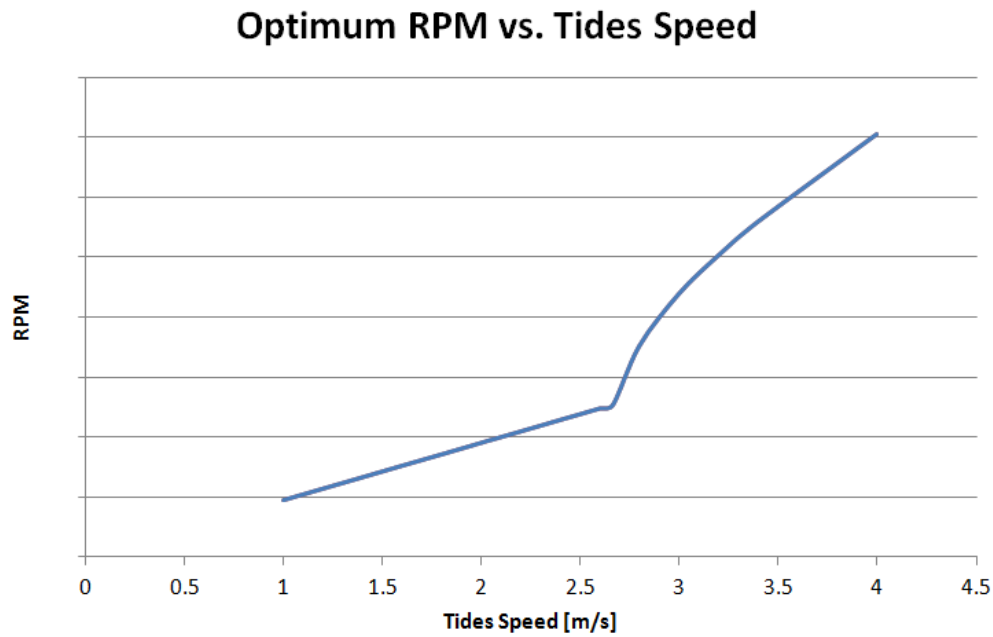


Figure 3.14 Optimum RPM vs. Tides Speed (Courtesy of Tidal Energy Limited)

This parameter is then compared to the actual generator slip. The difference between these two values represents the error which is the input of the PI controller. As it has been explained in Chapter 2, the control method thought for the DeltaStream project implies the variation of the generator torque, in order to obtain the desired slip. Hence, the parameter which has been chosen as control variable is the feed voltage of the SCIG. At any instant, the controller modifies the feed voltage with the aim of reaching the correct generator slip to respect the requisites imposed to the system. A SIMULINK representation of the logical path here described is given in Figure 2.14.

Although the results are promising, this procedure presents some limitations which will be pointed out in Chapter 4.

3.5 Flow field distributions

A fundamental step that must be realized to obtain an accurate simulation of the behaviour of a tidal turbine is the representation of the flow field which affects the system. It is important to note that the marine environment is characterised by lower current velocity compared to the wind. However, the denser working fluid and the level of turbulence produce high stresses on the structure.

In order to run the simulation, different types of flow distributions have been created. Initially, some flow fields uniform in space and variable in time have been considered. With this configuration, at any instant every part of each rotor blade is affected by the same flow velocity. Hence, the hydrodynamic model can be simplified and the loads and power output of the whole system become three times the values produced by a single blade. Three different time-dependent distributions of velocity, with a different level of unsteadiness, have been implemented and they are shown in Figure 3.17, Figure 3.16 and Figure 3.17.

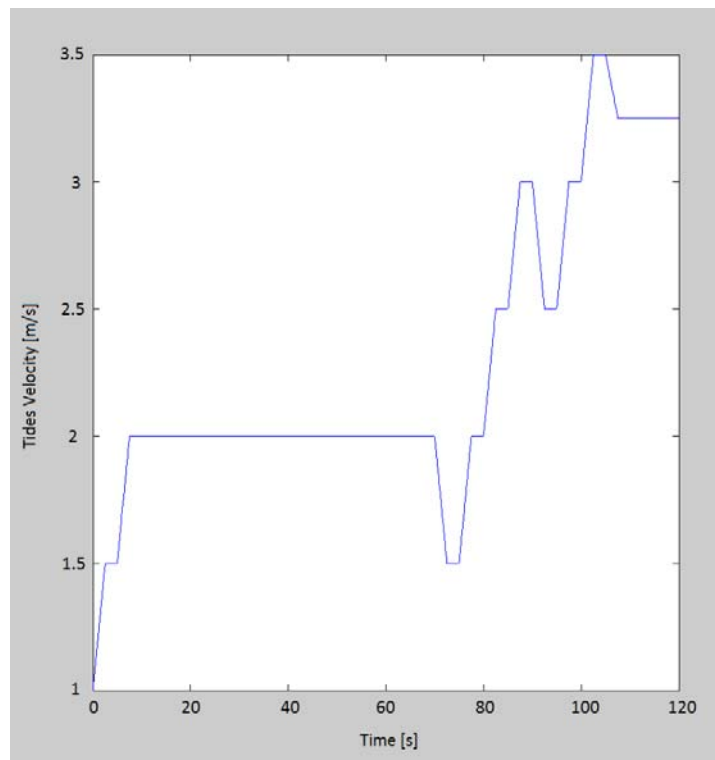


Figure 3.15 First time dependent velocity distributions

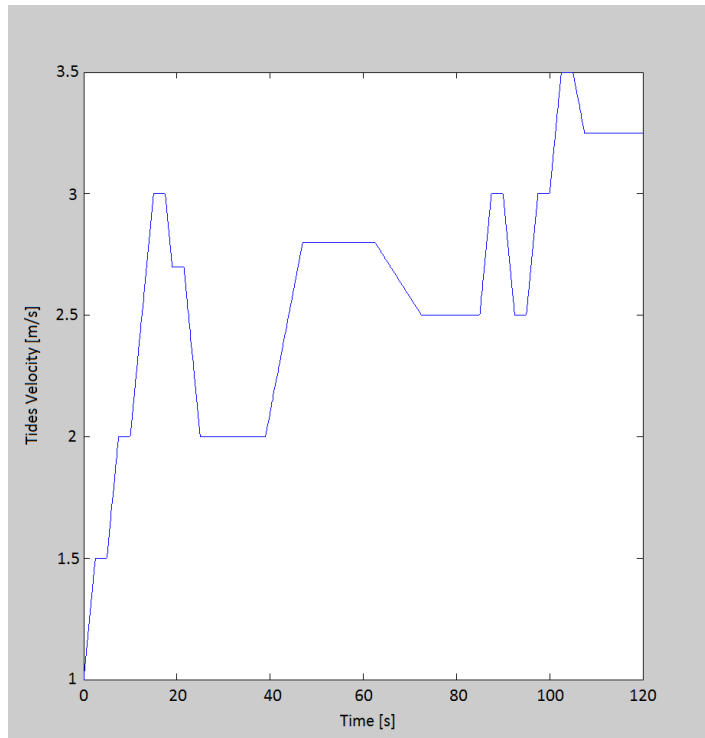


Figure 3.16 Second time dependent velocity distributions

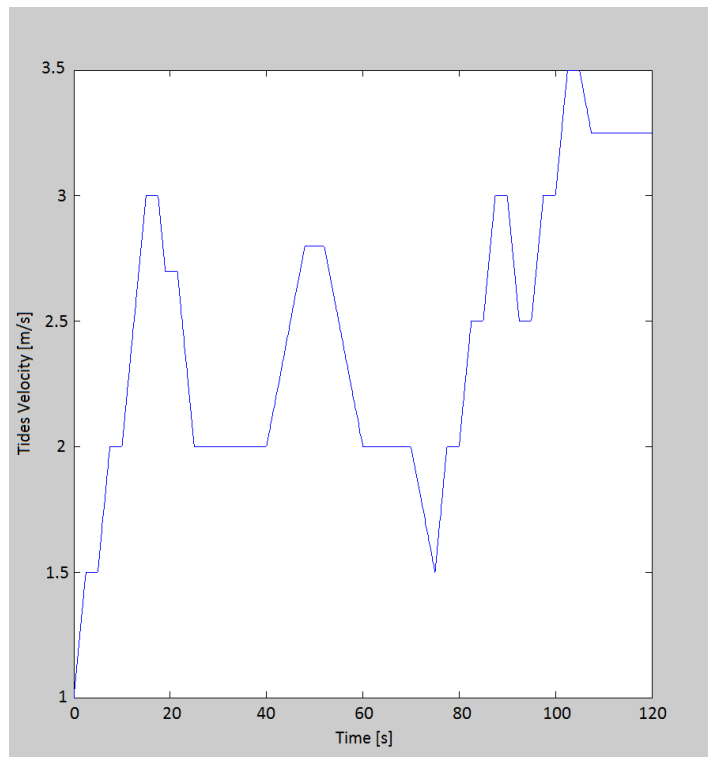


Figure 3.17 Third time dependent velocity distributions

Although this representation is good for a preliminary evaluation of the device, it is not accurate enough to represent the real inflow conditions to the tidal turbine. In order to obtain a higher degree of precision, it is necessary to employ a time-space dependent turbulent flow field. This distribution has been created by M. Corsar as part of his PhD research and an example is shown in Figure 3.18.

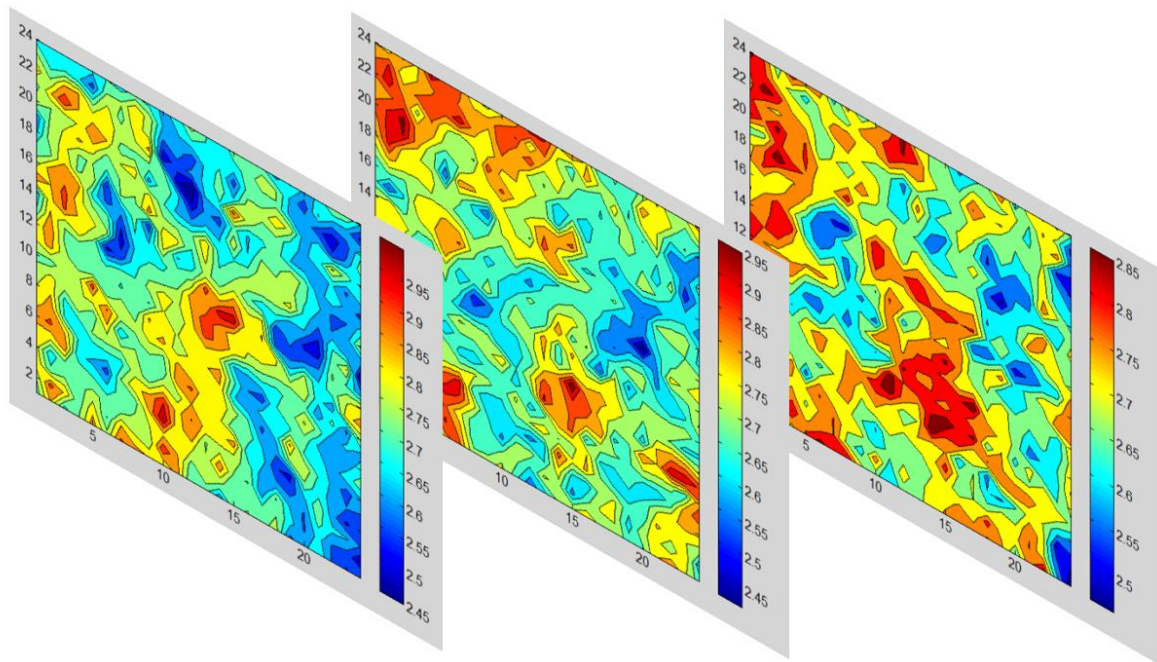


Figure 3.18 Time-space dependent turbulent flow field - [46]

A flow field of this genre implies that a different velocity is applied at any node of the blades.

However, an unsteady BEM model would be required to produce noteworthy results which exceeds the aim of this thesis. Therefore, at this stage another simplification has been made. The MATLAB code has been modified in order to assess at any instant the real velocity distribution on the three different blades. Thereafter, the mean velocity applied on the three blades is calculated and given as input to the BEM model. Although with this simplification the model

developed does not increase dramatically its accuracy, this change represents an improvement because a more realistic flow field is applied to the system, as it is shown in Figure 3.19. Hence, the analysis carried out using this model is more significant.

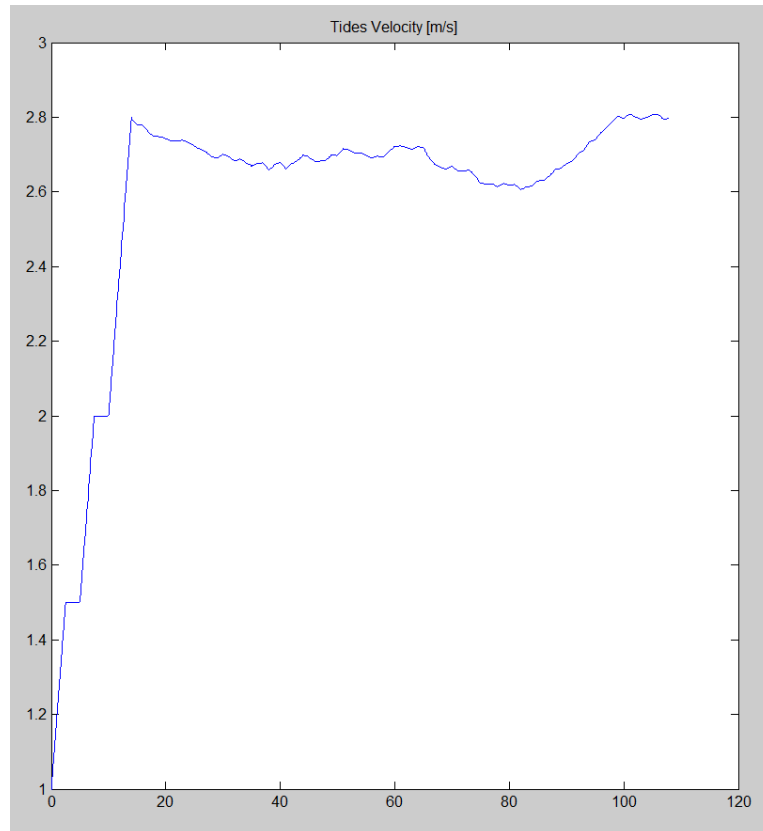


Figure 3.19 Velocity distribution obtained by the time-space dependent flow field

3.6 Complete system

To conclude the methodology, it is interesting to show a flow chart representative of the complete system (Figure 3.20) and describe the logical path followed by the information inside the MATLAB code that has been developed.

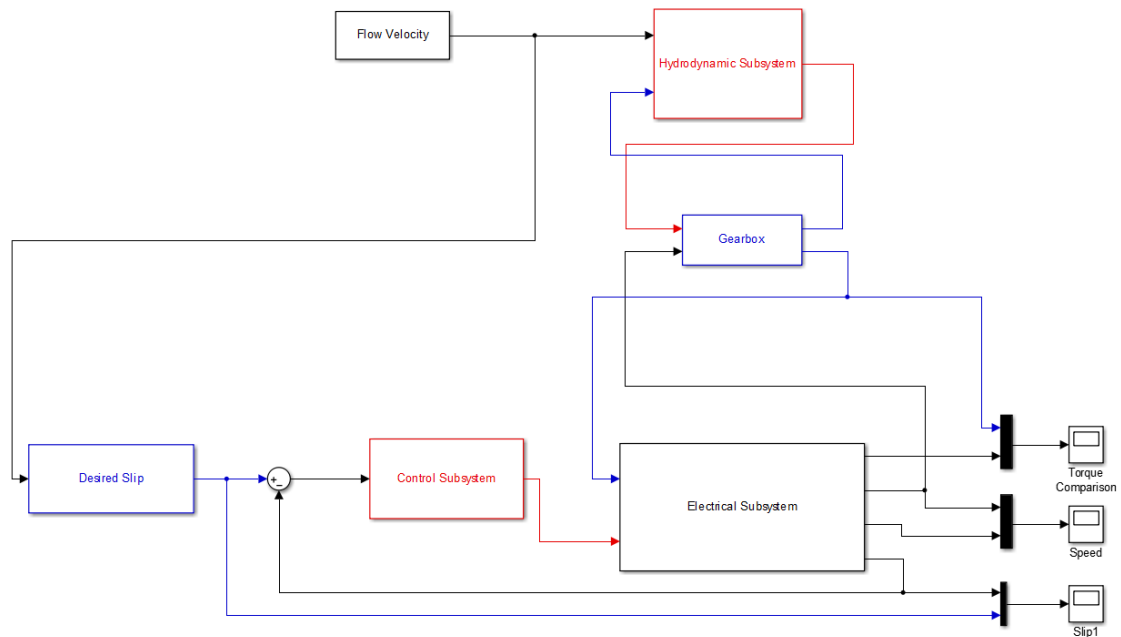


Figure 3.20 Complete system

The initial input to the model is the distribution of velocity. If it is a time-space dependent flow field the program evaluates the velocities at any node of the three blades and then calculates the mean speed which affects the turbine rotor. The mean velocity is the input of the "desired slip" block. In this block, the program estimates the optimal generator slip which permits to maximise the power extraction and minimise the axial loads. Meanwhile, the mean speed value is also the input of the hydrodynamic subsystem which evaluates the load applied to the structure and the power extracted. The information obtained from the hydrodynamic subsystem passes through the "gearbox" block and then becomes the input of the electrical subsystem which calculates the actual generator slip. This value is then compared to the desired generator slip. The difference between these two parameters becomes the error which is the input of the controller. Using the error, the "control" block acts on the electrical torque modifying the input voltage in order to produce the required slip.

4 Results

This chapter focuses on the results obtained from the simulations of the complete implemented model. It is subdivided in three sections. Section 4.1 illustrates the results obtained measuring at any instant the incoming flow velocity. Although this solution shows the best results, it is not feasible. Hence, a sensitivity analysis is carried out in Section 4.2 in order to assess the behaviour of the turbine when is affected by the real flow field while it is controlled using a mean velocity value as input. Finally, a possible solution to decrease the error is pointed up.

4.1 Instantaneous control

This section analyses the response of the tidal turbine affected by two different distributions of velocity and controlled with the PI controller. In order to assess the effectiveness of the control a comparison between the desired and the actual generator slip will be illustrated. Additionally, the power output and axial force produced will be evaluated, since they are considered the most critical parameters for the structure.

4.1.1 First case study

For the first case study it has been used a distribution of velocity which is time dependent while it is uniform in space. An high degree of flow unsteadiness has been added in order to observe the reaction of the turbine when it is subjected to hard environmental conditions. The time history of the speed which has been given as input to the model is shown in Figure 4.1.

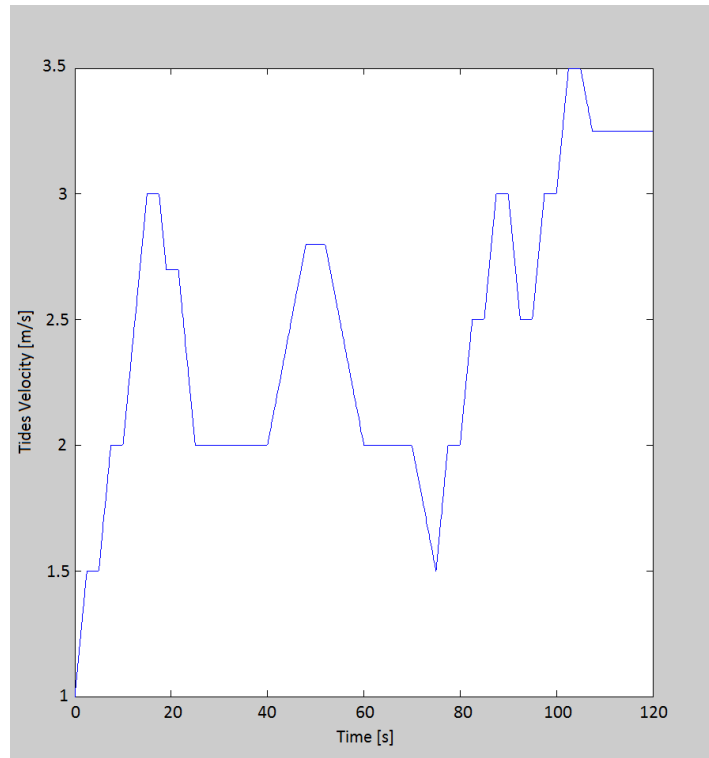


Figure 4.1 First case study - Distribution of velocity

In order to assess the effectiveness of the implemented control against this transient flow field it is necessary to evaluate the reaction of the turbine. Hence, Figure 4.2 and Figure 4.3 illustrate the comparison between the desired and the actual generator slip and the rotor RPM variation.

As it is clear from Figure 4.2 the control works well and permits to achieve an optimum match between the two slips. It is interesting to note that, when the current speed increases over about 2.7 m/s, the rotor speed rises up significantly. This is due to the fact that, once the flow velocity exceeds that value, the power output should be kept constant and the thrust should be reduced. Hence, because of the particular blade design, an increase in rotational speed means a reduction in torque and axial force generation, which permits to satisfy both the requirements previous mentioned.

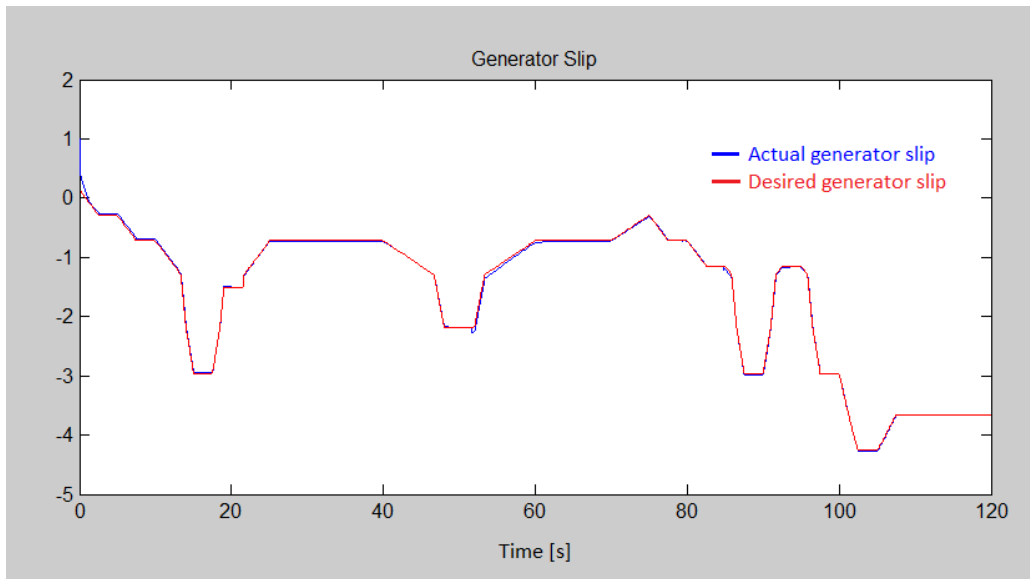


Figure 4.2 First case study - Generator slip comparison

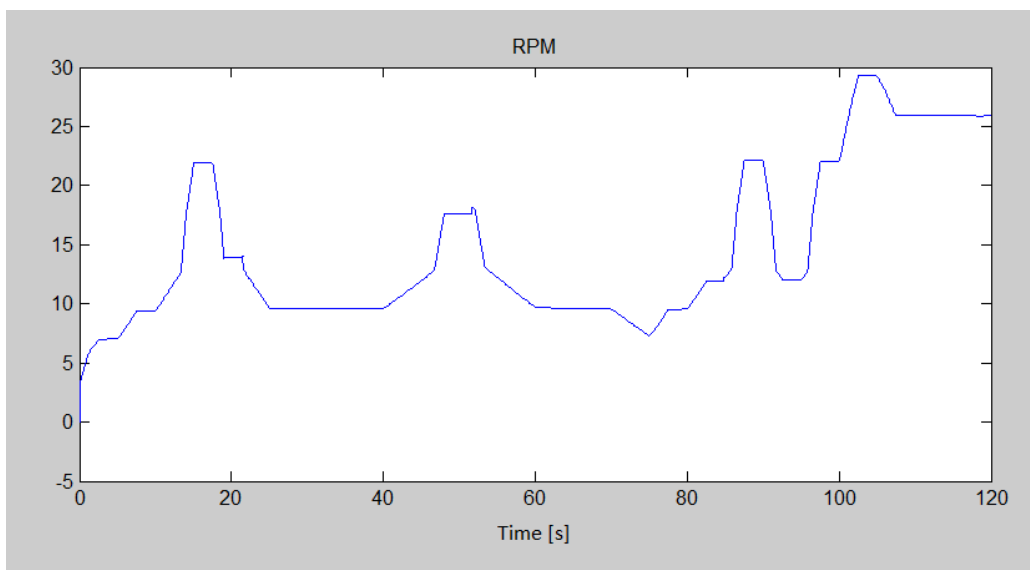


Figure 4.3 First case study - RPM

Although the error between the desired and actual generator slip is low, all the other parameters must be analysed in order to evaluate the real effectiveness of the control. Hence, the next step is to analyse the curve which describes the power output, as illustrated in Figure 4.4.

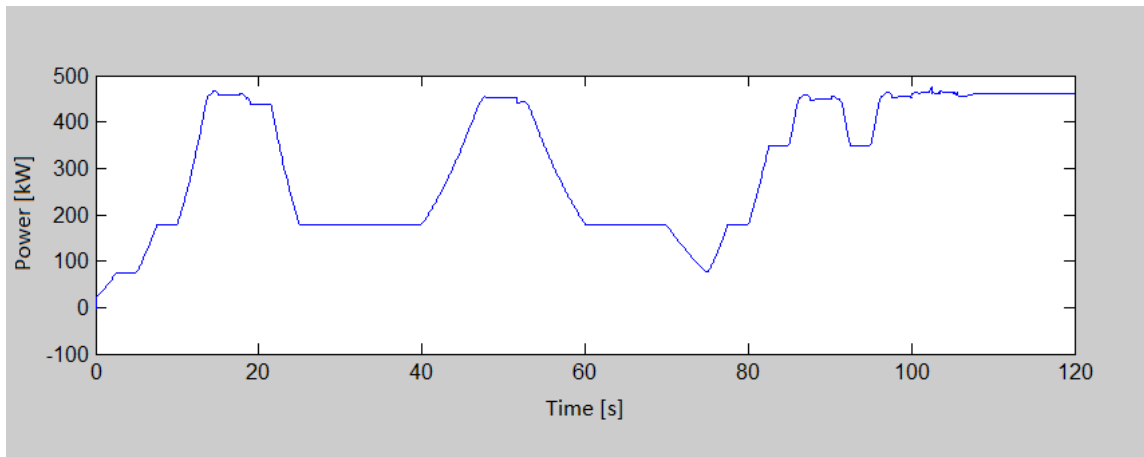


Figure 4.4 First case study - Power production

As it is possible to see, the control maximises the power extraction while the velocity of the incoming flow is lower than about 2.7 m/s. Once the velocity exceeds this value, as for example at seconds 18, 50 and 100 the power output is maintained nearly constant. Hence, the aim of increasing the power output quality is fulfilled.

The second parameter to check in order to assess the efficacy of the control is the axial force generation. If the turbine is well controlled, once the flow velocity surpasses the rated value the thrust should decrease in order to avoid the movement of the gravity-based structure. The data obtained from the simulation are shown in Figure 4.5.

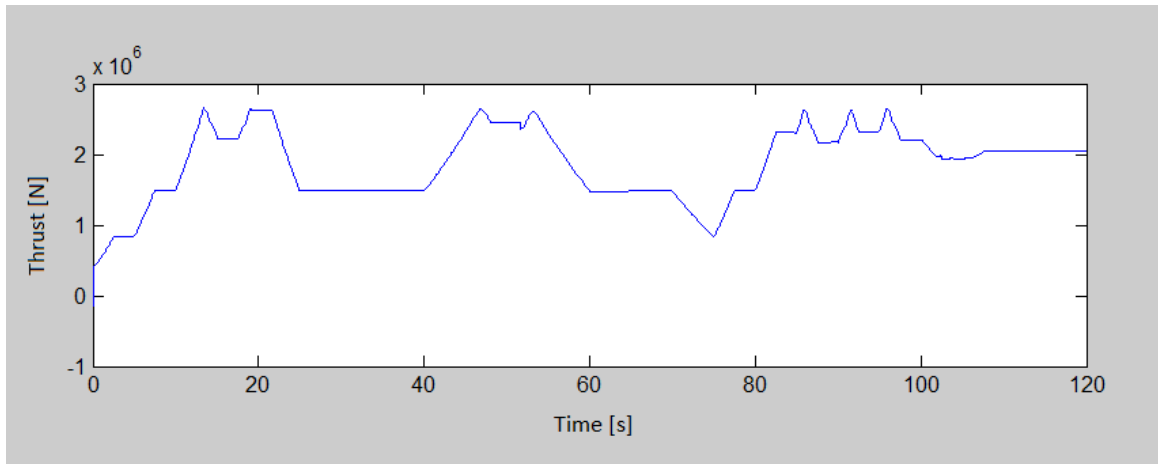


Figure 4.5 First case study - Axial force generation

The chart shows that the control manages to limit the value of the axial force under the maximum permitted even when the current speed exceeds the value of about 2.7 m/s. However, this implies the generation of peaks which can be dangerous for the structure in terms of fatigue. This drawback is due to the control strategy adopted. In fact, once the upper speed limit is reached the controller increases the rotational speed of the rotor in order to reduce the axial loads applied to the structure.

4.1.2 Second case study

As it has been clarified, the first case study was characterised by the use of a test time dependent distribution of velocity. However, the principal scope of this project is to simulate the behaviour of the tidal turbine in the most realistic way possible. Hence, a step further has been made.

Section 3.5 introduced the work of Corsar (2013). As part of his PhD research, the author implemented a MATLAB code which produces as output a distribution of velocity which is dependent on time and it is not uniform in space. Figure 4.6 shows turbulent velocity distributions for the same plane taken at three different instances in time.

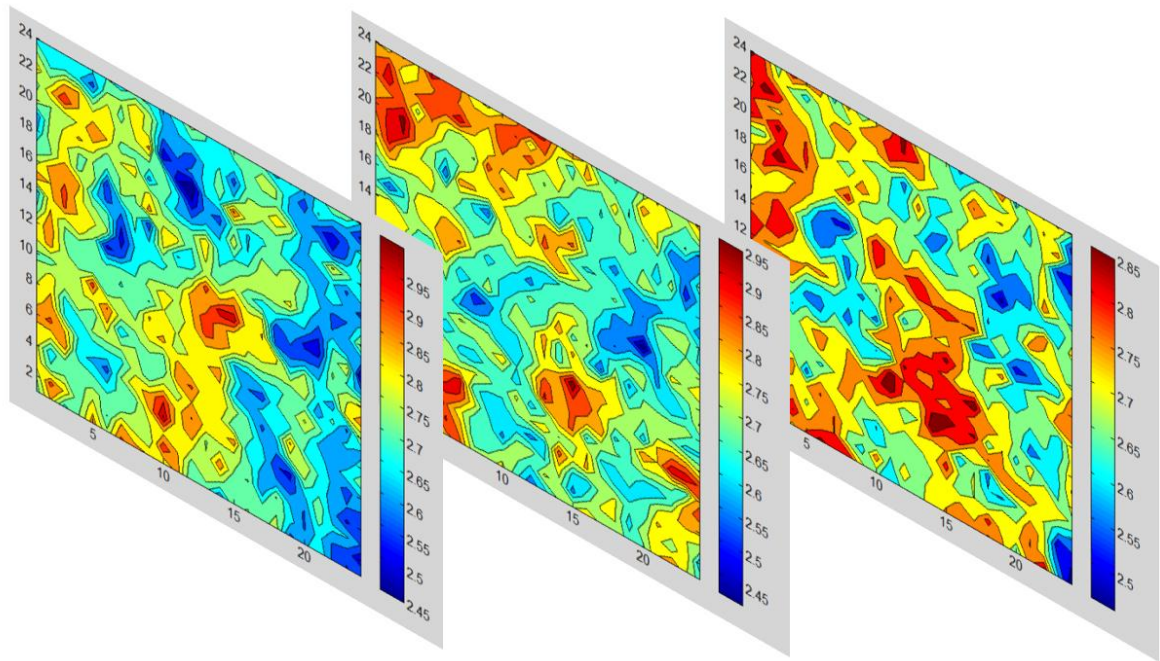


Figure 4.6 Second case study - Time-space dependent distribution of velocity - [46]

In this case, the turbine will be positioned in the centre of the picture and any node of each blade will be affected by a different flow speed. Although the best solution to evaluate accurately the behaviour of the device would be to couple the complete model with an unsteady BEM, this has been considered beyond the purpose of the thesis. Hence, it has been decided to simplify the situation. The MATLAB code has been modified in order to evaluate at any instant the velocities affecting the turbine blades. Afterwards, using the instantaneous distribution just estimated, the program calculates the total mean velocity and produce a time dependent flow field which becomes the input of the steady BEM model. The accuracy of the model does not increase radically; however, thanks to this modification it is possible to produce a more realistic trends of the incoming current speed.

The distribution of velocity obtained is illustrated in Figure 4.7.

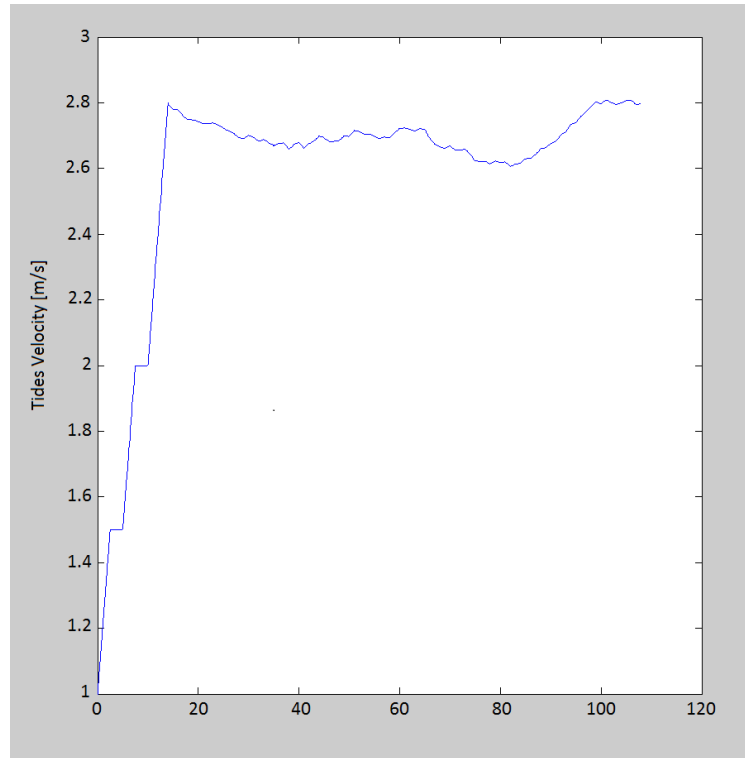


Figure 4.7 Second case study - Distribution of velocity

The first 14 seconds ramp is made just with the purpose of permitting the model to adapt to the velocity of about 2.8 m/s. Hence, the real flow field is from 14 seconds to the end. The chart shows a high level of turbulence which can affect the performance of the turbine.

Before analysing in detail the power and axial force productions of the turbine when affected by this new incoming flow field, it has been decided to run some simulations modifying the generator inertia and studying the response of the device.

Figure 4.8 shows the results of this preliminary assessment.

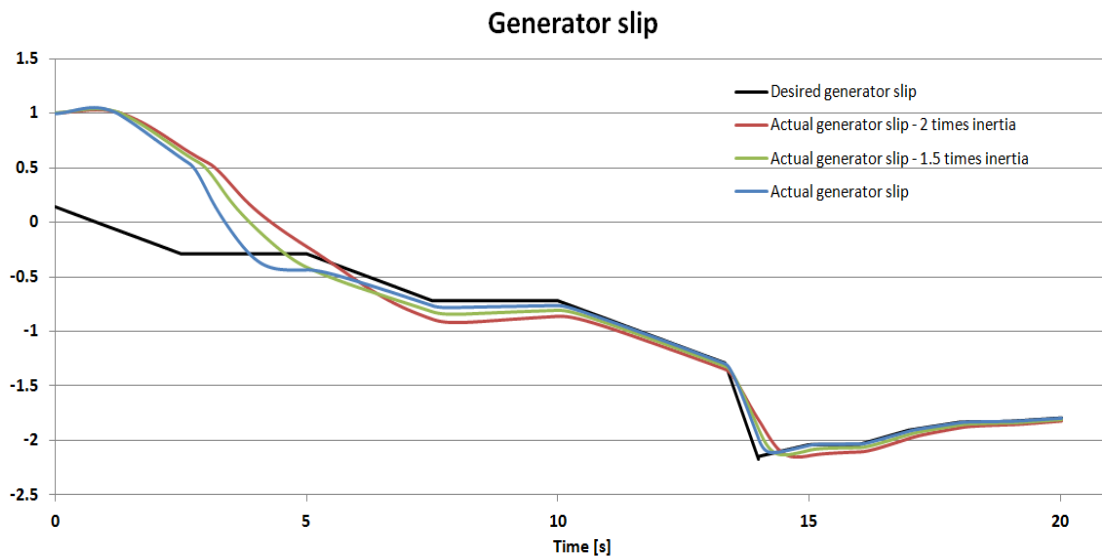


Figure 4.8 Second case study - Turbine response to generator inertia variation

As it is possible to see, the chart illustrates that the reaction of the turbine changes with the variation in generator inertia, which in this case has been modified from the actual to a 50% and 100% higher value. It is interesting to observe that as soon as the generator inertia increases the time required by the device to react and settle becomes higher. Indeed, a more massive generator rotor needs more time to change its state either if it is accelerating or if it needs to reduce its speed.

Once the inertia effects have been assessed, the next step is to analyse the response of the turbine in order to verify the effectiveness of the controller implemented. To fulfil this objective the case with the actual generator inertia has been considered.

Figure 4.9 and Figure 4.10 highlight the comparison between the desired and actual slip of the induction generator and the variation of the turbine rotor RPM.

As it is possible to observe, the model reacts well to the incoming flow field and the error between the ideal and real slip is kept at a minimum. Although the results show a good behaviour of the device, it is important to note that, in order to follow the variation in current speed the RPM of the turbine has to change

continuously and this is possible only measuring at any instant the flow speed. Even though this measurement is feasible during a computer simulation, in the reality there are not instruments able to dependably measure at any instant the exact flow current velocity. Hence, this is a limitation of the "instantaneous control" here implemented. A potential solution to this problem will be described in the next section.

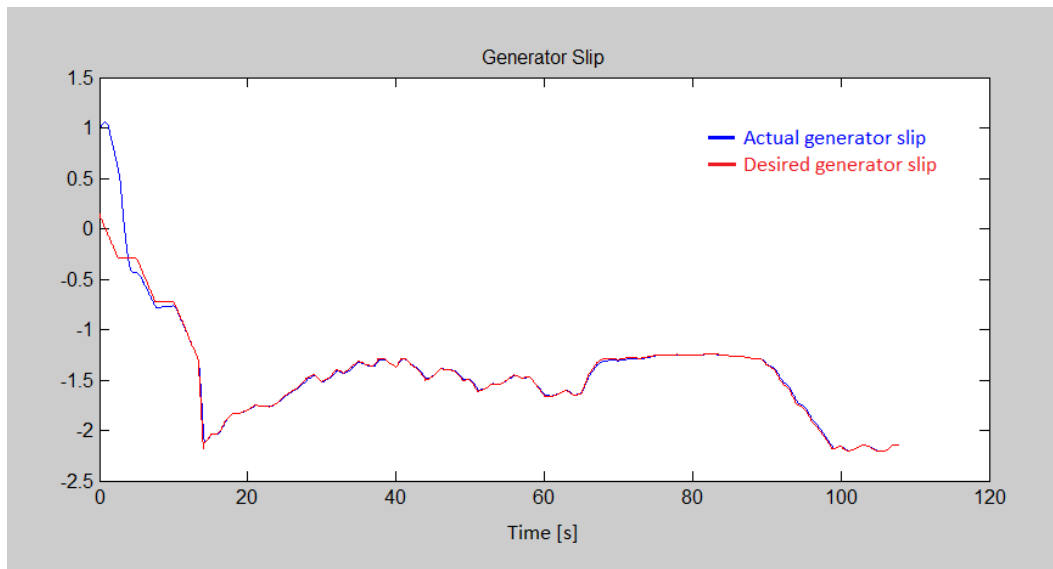


Figure 4.9 Second case study - Generator slip comparison

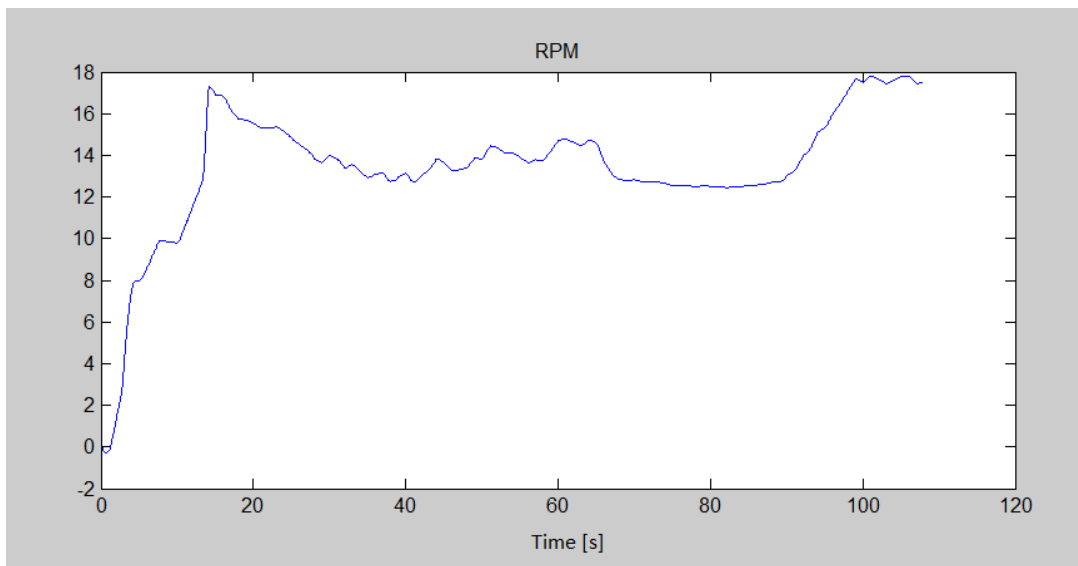


Figure 4.10 Second case study - RPM

Temporarily omitting this problem, it is anyway interesting to examine the power production (Figure 4.11) and the thrust generation (Figure 4.12).

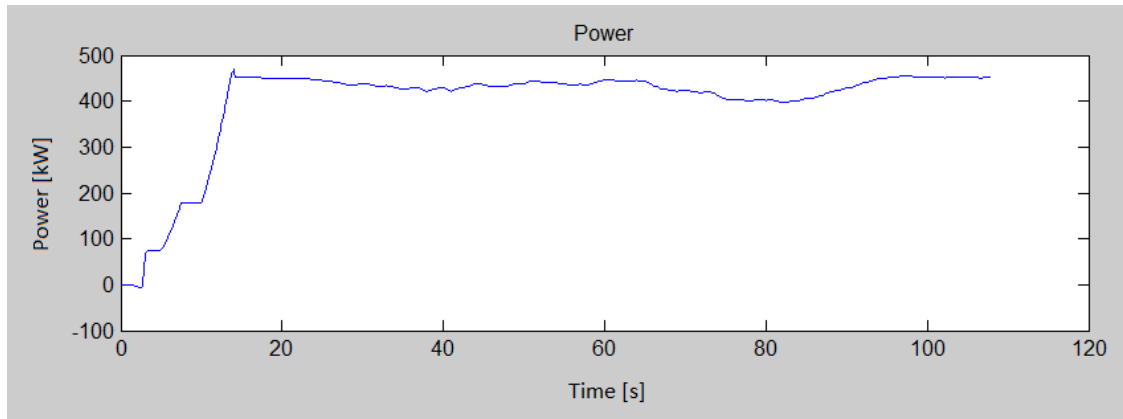


Figure 4.11 Second case study - Power production

The chart shows that the PI controller fulfils the requirement of increasing the quality of the power extracted limiting the energy output once the velocity of the water exceeds the rated value.

The last parameter which must be checked is the axial force applied to the structure.

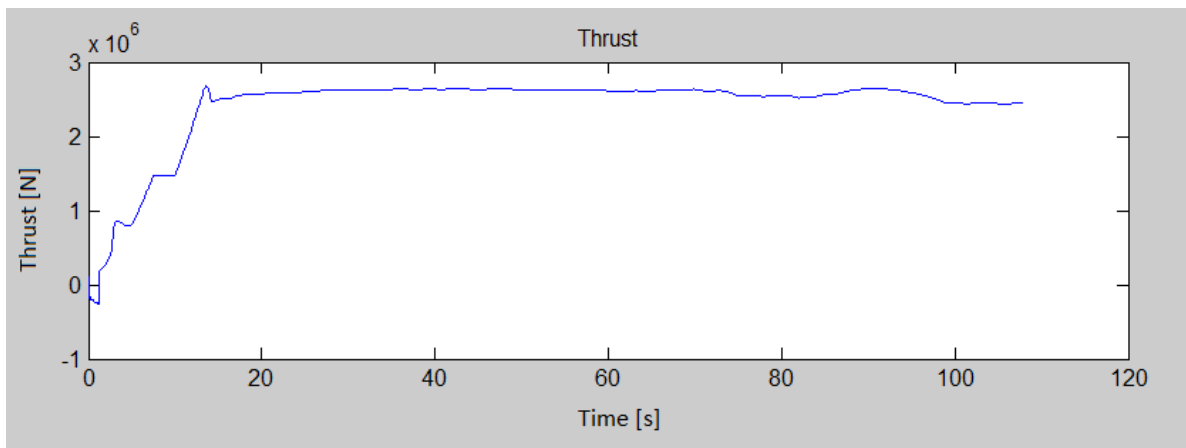


Figure 4.12 Second case study - Axial force generation

Again, the control system manages to avoid the increasing in thrust when the velocity passes the value of about 2.7 m/s. Moreover, it is worth to note that with this distribution of velocity, more realistic than the previous one, there are less peaks and so less problem related to fatigue stress.

4.2 Sensitivity analysis

As it has been mentioned in Section 4.1.2, the instantaneous measurement of the incoming velocity is not feasible with the instruments available. Hence, the control proposed in the above section cannot be implemented in the reality. So, what are the existing solutions? Using the current instrumentation and technology available and exploiting the astronomic nature of the phenomena which cause currents and tides it is possible to predict the mean velocity affecting the rotor turbine with high accuracy.

Therefore, the idea is to control the turbine imposing to the controller an incoming flow speed which is the mean value of the real distribution of velocity. Obviously, because the tidal turbine will be affected by the real water speed distribution, the device will optimise the power output and the reduction of axial force only when the mean velocity is equal or slightly different to the real one. Hence, a sensitivity analysis is required in order to understand which is the variation in power generation and thrust production when the flow speed is different from the one used to control the device.

Section 4.2.1 presents the analysis of the results obtained by the simulation of the model controlled using the velocity calculated as the mean value of the distribution from 14 to 108 seconds. This is due to the fact that the first 14 seconds are not considered for the analysis because they are required just to stabilise the model. Section 4.2.2 illustrates an attempt of reducing the error detected with the sensitivity analysis.

4.2.1 First case study

The flow field shown in Section 4.1.2 has been chosen to carry out the sensitivity analysis. As it has been said, the control is based on the mean value of the velocities from 14 to 108 seconds. In order to run the simulation, the MATLAB code has been modified. It has been decided to use the real velocity as input of the BEM model. On the other side, the mean velocity has been given as input of the control, as it is illustrated in Figure 4.13.

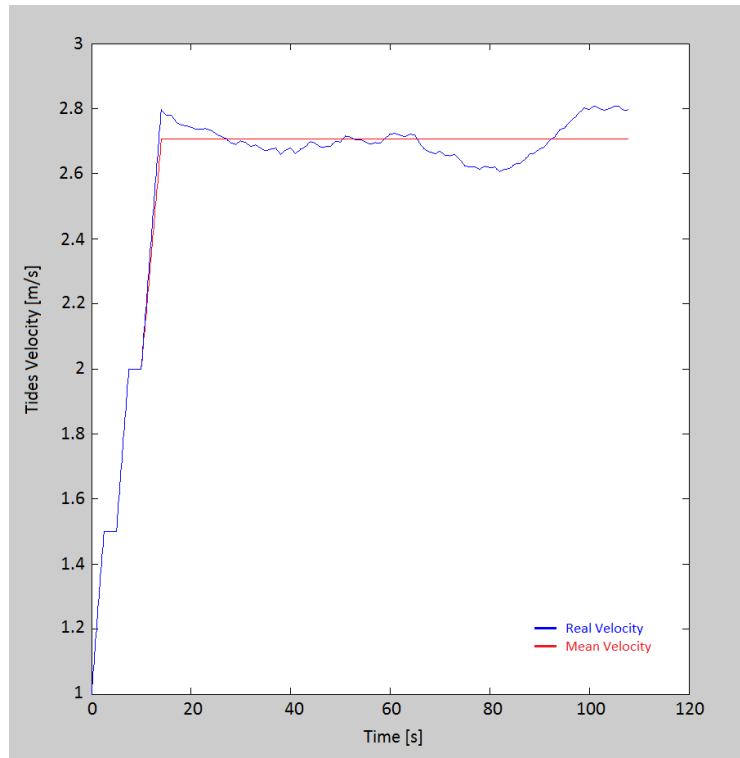


Figure 4.13 Sensitivity analysis - Real and mean velocity distributions

To assess the behaviour of the turbine, a comparison has been made between the principal parameters, power extraction and thrust. The results obtained using the instantaneous controller and the new, more feasible, control strategy have been matched and the error has been calculated.

Figure 4.14 illustrates the power generation curves achieved with the two methods.

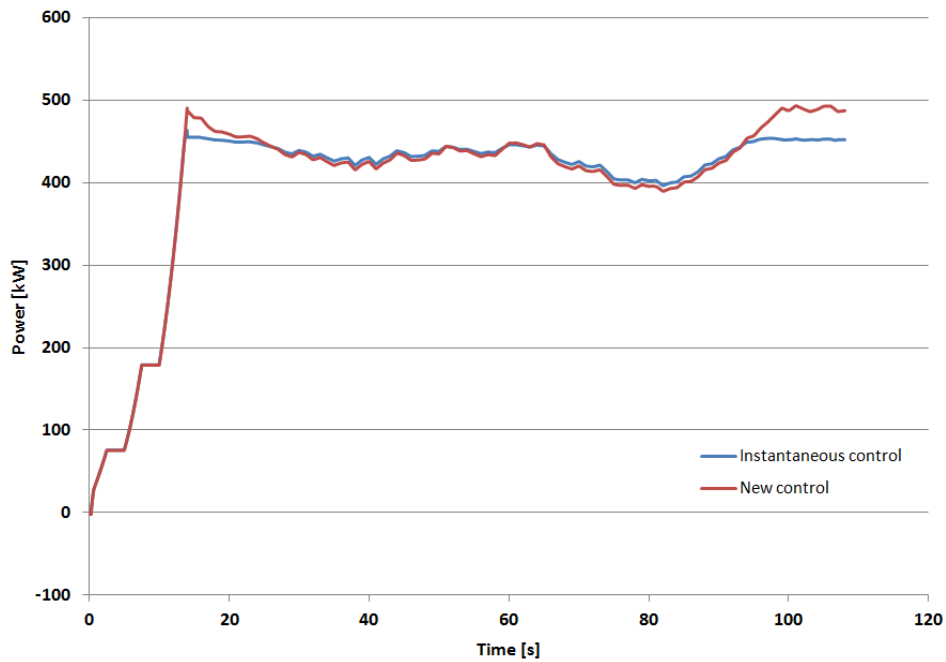


Figure 4.14 Sensitivity analysis - Power production comparison

As it is possible to observe, when the real speed is equal or lower than the mean speed, the power output is pretty similar. However, once the real velocity exceeds the mean value the power generation increase dramatically and the device is no more able to optimise the energy production.

Figure 4.15 illustrates a comparison between the velocities discrepancy and the power extraction difference, in order to better understand which is the relation between this two parameters.

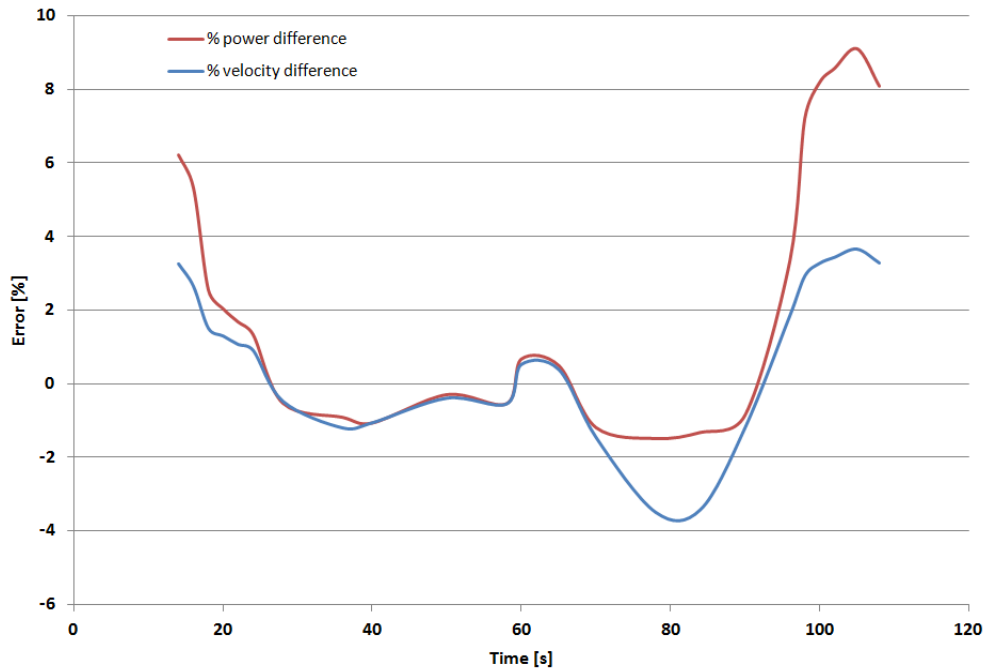


Figure 4.15 Sensitivity analysis - Velocity and Power output errors

It is now possible to quantify the power generation difference in terms of percentage error. As has been mentioned before, when the real velocity is lower than the mean value or slightly different, the error in power extraction is limited to the 1%. However, once the real velocity exceeds the mean value the power output increases dramatically. For example, at second 15 to an error of 3% in flow velocity corresponds an error of about 6% in power output. Another example is about second 105. Here the velocity difference is about the 4% and the power extracted by the tidal turbine controlled using the new method is about the 9% higher respect to the turbine controlled at any instant.

The second fundamental parameter to confront is the axial force production. As it has been done for the power, Figure 4.16 illustrates the thrust generation obtained with the two control strategies.

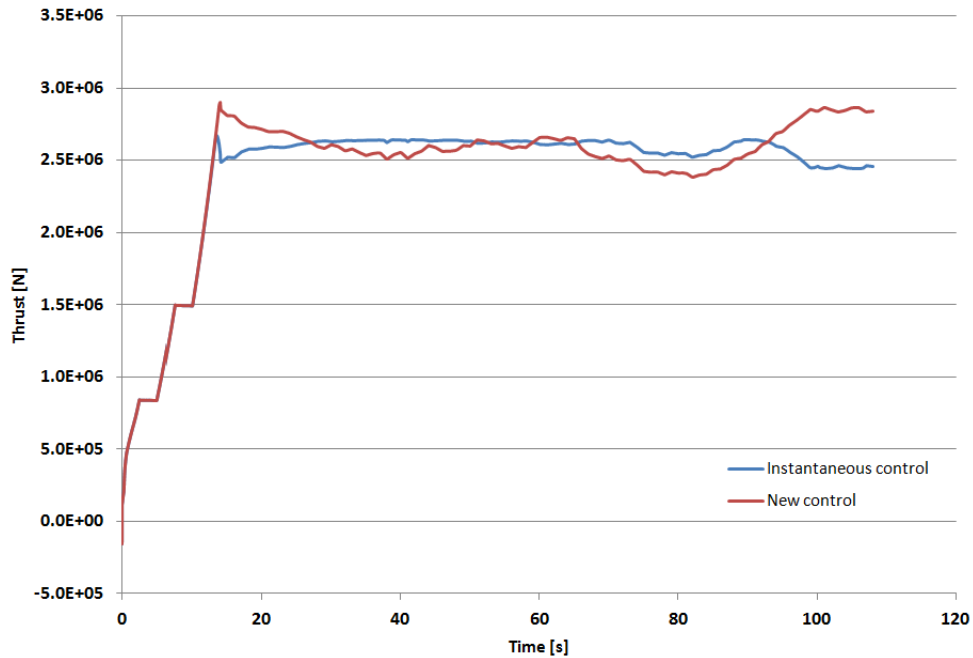


Figure 4.16 Sensitivity analysis - Axial force generation comparison

It is possible to observe that the discrepancy between the thrust productions is higher than the power extractions. In fact, when the real speed is lower than the mean value the thrust produced is lower but once the real velocity exceeds the limit the thrust increases significantly.

Again, Figure 4.17 shows a comparison between the velocity difference and the axial thrust generated using the two control methods.

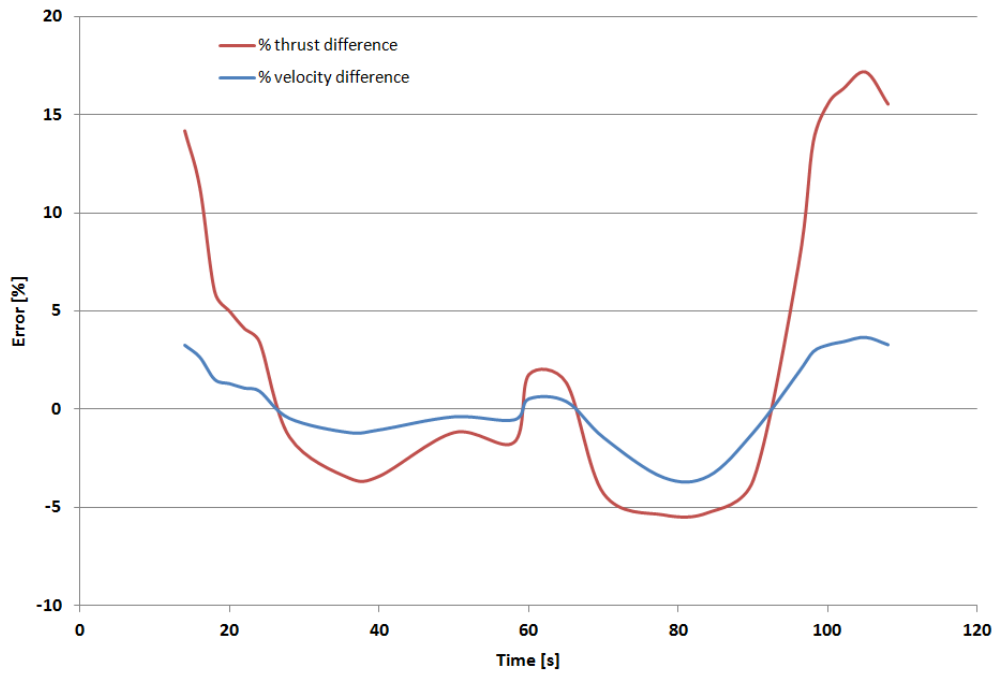


Figure 4.17 Sensitivity analysis - Velocity and thrust generation errors

This chart gives the possibility of quantifying the variation in axial force with respect to the velocity difference. It is worth to note that the turbine reacts well when the real velocity is lower than the mean value calculated. In fact, in that case the new control reduces the axial loads more than the instantaneous control strategy. However, once the velocity grows, the controller is no more able to limit the thrust generation which increases considerably. This behaviour is evident at second 15 and 100, where to a 4% error in velocity corresponds an increment of about 15% in thrust generation. Hence, this parameter is much more sensitive to the flow speed difference than the power extraction, which for the same velocity discrepancies produces an error about the 7% lower.

The sensitivity analysis has pointed out the limits of the new control strategy. The use of the mean velocity implies a situation of over power production and over thrust, which is more significant since the DeltaStream structure is gravity stabilized. Hence, something must be done in order to reduce the error between the two methods. A possible solution is given in the following section.

4.2.2 Proposed strategy improvement

The objective of this section is to show an improvement on the control strategy implemented. An idea is to subdivide the time history in pieces and calculate for each part the mean velocity, instead of using an unique mean value for the entire time. In this way it is possible to obtain a higher degree of precision regard the speed evaluation and so a better control. The next paragraph illustrates the case study carried out in order to validate this hypothesis.

The distribution of velocity has been split into four parts and for each one the mean value has been detected. Thereafter, the four mean speed values obtained have been linked together with a ramp in order to not have sudden step which can be source of problems. The trend achieved is shown in Figure 4.18.

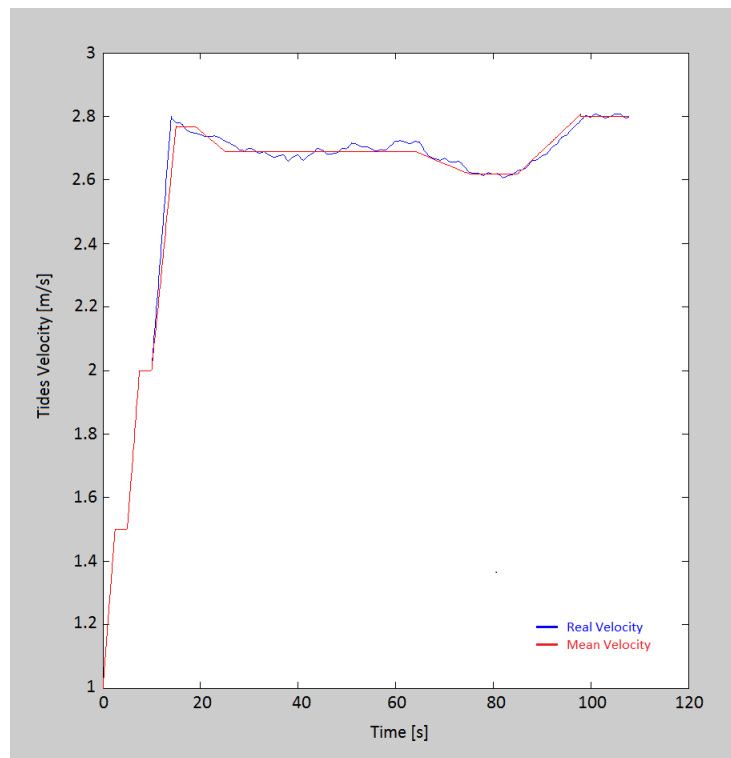


Figure 4.18 Sensitivity analysis - Real and new mean velocity distributions

From a starting point of view the discrepancy between real and mean velocity has been reduced; shorter are the steps better is the representation. Obviously, when the time steps tend to zero the control strategy becomes the one explained in Section 4.1.

The usual parameter, power output and thrust generation, have been analysed in order to evaluate the effectiveness of the new control method. Figure 4.19 illustrates the power produced using the last method and the instantaneous control.

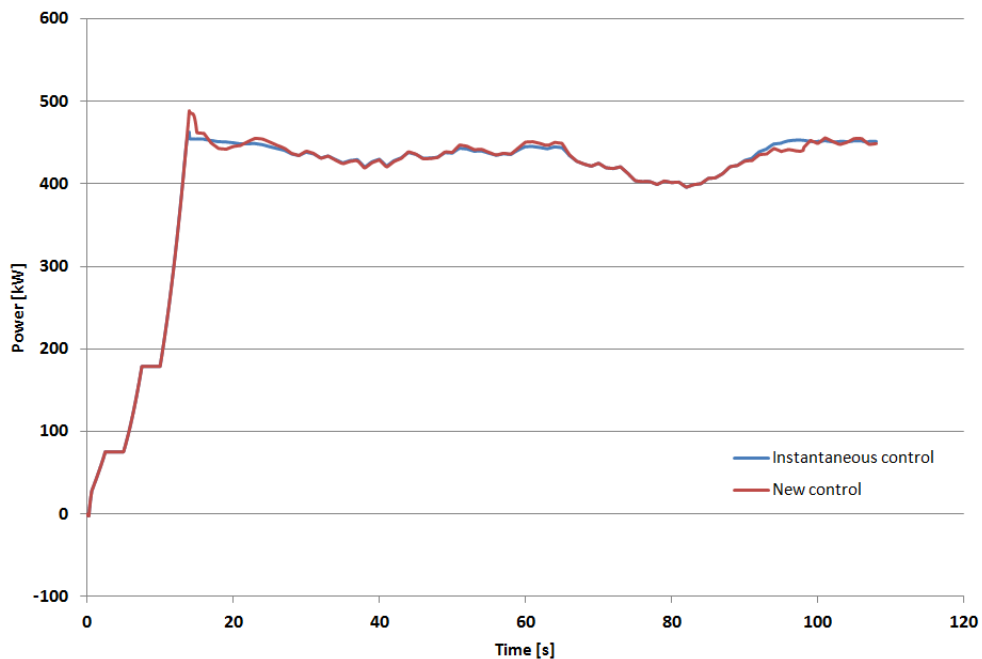


Figure 4.19 Sensitivity analysis - New power production comparison

As it is clear from the chart the power output error with the new control strategy has been drastically diminished, avoiding great over production of power and maintaining an acceptable level of maximisation of the energy extraction. The reduced discrepancy between the first type of control and this last attempt is shown in Figure 4.20.

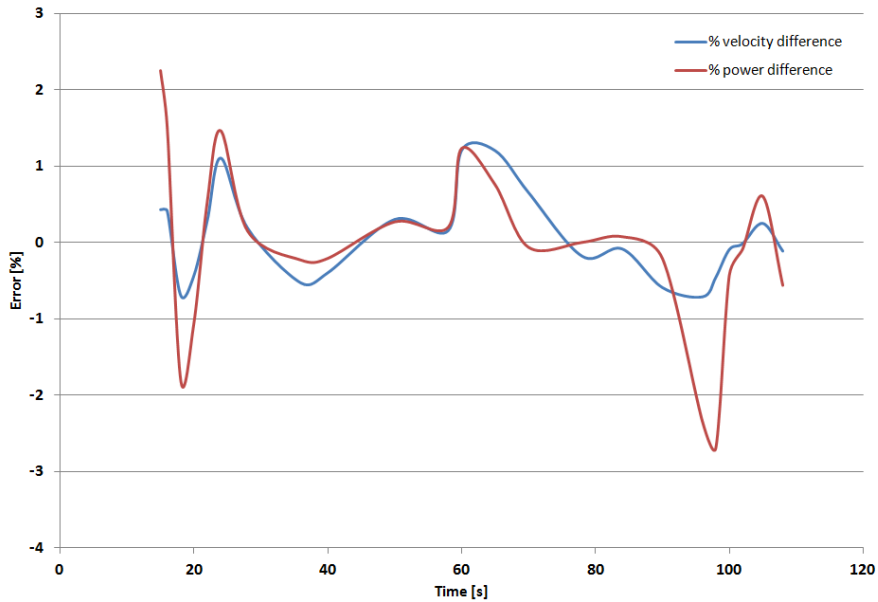


Figure 4.20 Sensitivity analysis - New velocity and power output errors

The chart illustrates that maintaining the velocity error about the 1% it is possible to respect the power generation requirements with a maximum error of about 2.5%.

Although the device reacts well regarding the power output, it has been shown in the previous analysis that the most sensitive parameter to the water speed variation is the thrust. Hence, to conclude this study it is necessary to assess if there is a reduction of the axial loads applied to the structure. The comparison between the thrust produced using the last method and the instantaneous one is given in Figure 4.21.

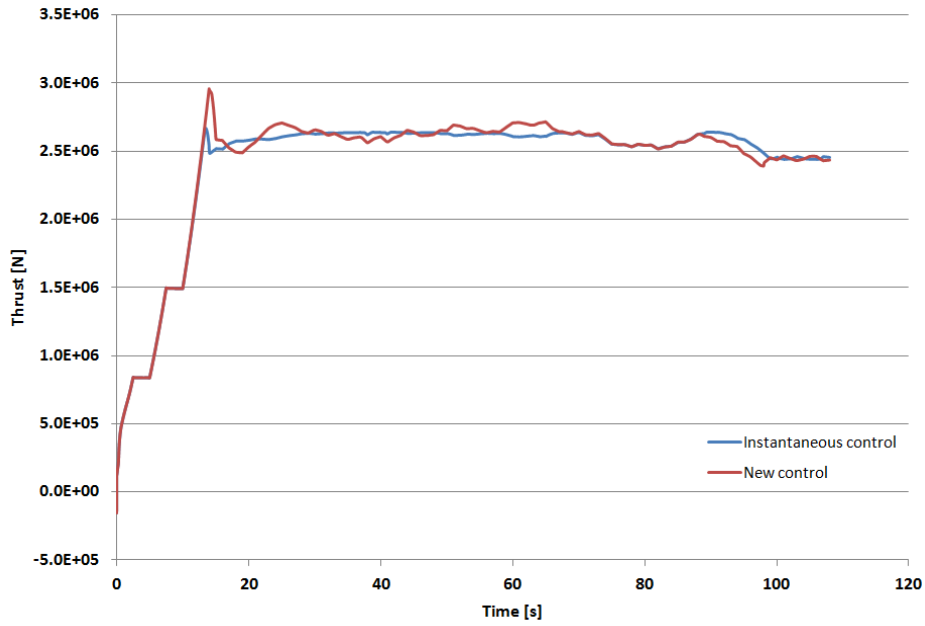


Figure 4.21 Sensitivity analysis - New axial force generation comparison

Once again, the thrust chart shows an higher degree of difference between the two methods used to simulate the turbine. Anyway, to better understand the real discrepancy it is necessary to analyse the chart of the error, illustrated in Figure 4.22.

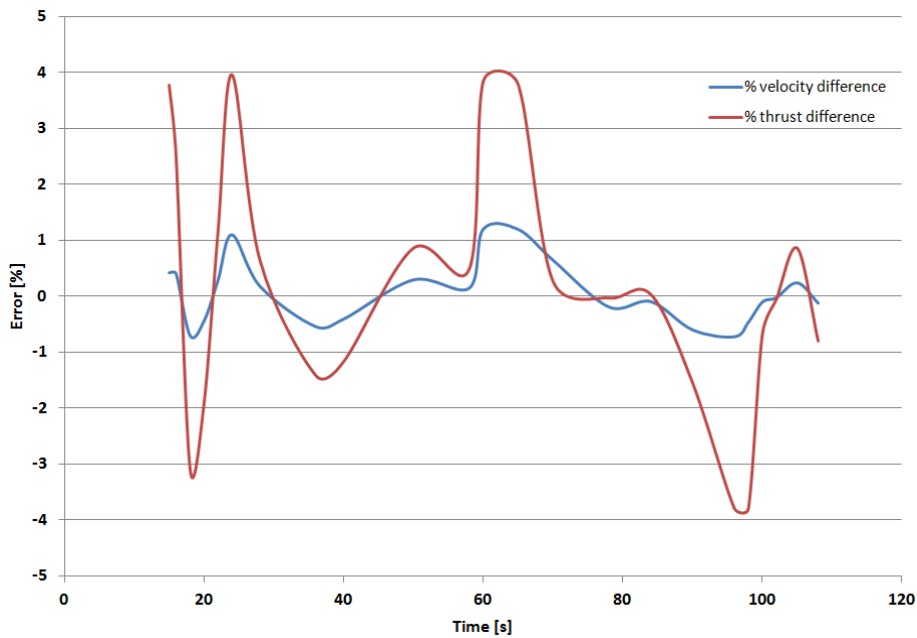


Figure 4.22 Sensitivity analysis - New velocity and thrust generation errors

This graph shows that with the last control implemented, the error on the axial force production is limited under about the 4%. This is a great improvement from the previous stage, where the error reached peaks of about 15% as it is described in Figure 4.17.

Finally, from the analysis carried out in this chapter it is possible to conclude that, using the mean velocity as parameter to control the turbine does not permit to obtain the optimum response, but it allows to reach a reasonable degree of accuracy. Moreover, reducing the time step in which the mean speed value is calculated implies an increment of power output quality and lower axial loads applied to the structure.

5 Summary

This thesis has analysed the development of a control system for a tidal turbine. As explained in Section 2.6, the aim of the project is the creation of a control able to reduce the axial loads applied to the structure and to increase the quality of the power output, that means extract the maximum amount of power until the energy reaches the rated value and generate a constant power output when the turbine could produce an higher amount of energy. The thesis has been structured as follow.

Chapter 1 gave an introduction of the tides as renewable resource, the tidal turbine working theory and an overview of the challenges related to this innovative technology. Moreover, the main characteristics of the DeltaStream project have been introduced and the reasons which imply the installation of a control system have been briefly illustrates.

Chapter 2 presented a literature review about the control system available for wind turbine technology. Passive and active controllers have been explained and then analysed in order to understand which of them could be an appealing choice for the DeltaStream tidal turbine device. An overview of the tidal turbine projects has been done and the technique which has been chosen for the DeltaStream project has been illustrated. The possibility of controlling the turbine modifying the torque of the generator has been analysed. Finally, the work of Cecchi (2012) has been introduced as a starting point for this thesis.

Chapter 3 focused on the methodology used to represent the entire turbine. The different subsystems and the procedure used to implement them have been analysed. The chapter includes details on the BEM theory used to represent the hydrodynamic subsystem, the electrical subsystem which consists of a dynamic induction generator, the gearbox, the PI control strategy and the distribution of velocity which have been used to simulate the environmental condition affecting the turbine.

Chapter 4 illustrated the results obtained by the simulations of the turbine controlled using two different control strategies. A sensitivity analysis has been

carried out in order to observe the relation between the different parameters and to assess the effectiveness of the control implemented.

5.1 Conclusions

As it has been illustrated in Section 2.6 this thesis project had some objectives which have been achieved in order to extract the results:

- The BEM model has been implemented and validated.
- A dynamic induction generator has been developed in MATLAB environment, as suggested by Cecchi (2012), in order to obtain more realistic results from the simulations.
- A PI controller, acting on the voltage of the generator, has been created in order to fulfil the requirements of the device regarding the power output quality and the reduction of the axial loads.
- Different flow fields have been generated in order to test the turbine in different working situation.
- Finally, all the subsystems have been coupled in order to implement the entire model and run simulations to study the behaviour of the complete tidal turbine device.

The results of the simulations shown in Section 4.1 have pointed out that a control strategy which implies the measurement of the incoming velocity at any instant would be the best option. However, this kind of control cannot be implemented in the reality for different reasons; first of all, it is possible to know with a certain accuracy only the average value of the incoming flow speed thanks to the predictability of the marine current resource; secondly, as for the wind turbine, in order to measure the flow with an higher degree of precision an anemometer should be installed somewhere upstream the rotor turbine. However, this is not feasible because the marine environment is totally different from the atmospheric ambient. In fact, there are many more debris and objects

which are moved by the tides and which can easily hit and damage the anemometer, decreasing the reliability of this device.

Relying on the possibility of knowing the mean velocity, Section 4.2 analysed the response of the turbine when controlled with this new strategy. The sensitivity analysis has pointed out that the axial force is much more sensitive to the difference between the real and mean velocity than the power output. The analysis has shown that knowing the mean velocity of short periods of time permits the control system to maintain the power extraction error under 2.5% and the axial force error under 4%, which are acceptable values at this stage.

5.2 Future work recommendations

Regarding the future work on the control system for tidal turbines there are some major recommendations.

First of all, the time-space dependent distribution of velocity, implemented by Corsar (2013), should be employed. To achieve this goal, an unsteady BEM model should be implemented in order to take into account the real speed distribution that affects each blade of the rotor obtaining much more accurate and realistic results about the loads applied on the structure and the power output quality.

Secondly, as far as the generator modelling is concerned, in this thesis it has been developed a dynamic squirrel cage induction generator. Although the SCIG is a good starting point, the development of a doubly-fed induction generator is highly recommended. In fact, a DFIG implies more degrees of freedom and permits to achieve a better design of the controller.

Thirdly, but no less important, another control strategy should be investigated. As it has been shown in Chapter 4, the best control would be achieved measuring and knowing at any instant the velocity of the flow that is affecting the structure. It has been pointed out that this is not feasible and that the mean velocity value can be used. The sensitivity analysis has shown that it is possible to reduce the discrepancy between the instantaneous control and the "mean value" strategy, reducing the time period in which the mean velocity is

calculated. Although it seems possible to obtain acceptable results using this method, there is an alternative. The new control strategy should take into account to measure the torque and the power output of the turbine at any instant and generate a desired generator slip curve for the control system relying on these quantities. This could improve significantly the effectiveness of the controller leading to the results obtained with the instantaneous controller.

REFERENCES

- [1] AEA Energy & Environment, 2006. *"Review and Analysis of Ocean Energy Systems Development and Supporting Policies."* [online PDF] Available at: <http://mhk.pnnl.gov/wiki/images/0/0e/Review_and_Analysis_of_Ocean_Energy_Systems_Development.pdf> [Accessed 10.05.2013].
- [2] de Laleu, V. 2009. *"La Rance Tidal Power Plant. 40-Year Operation Feedback - Lessons Learnt."* [online PDF] Available at: <<http://www.british-hydro.org/downloads/La%20Rance-BHA-Oct%202009.pdf>> [Accessed 10.05.2013].
- [3] Ben Elghali, S.E. et al., 2007. *"Marine Tidal Current Electric Power Generation Technology: State of the Art and Current Status."* [online PDF] Available at: <<http://ieeexplore.ieee.org/stamp/stamp.jsp?tp=&arnumber=4270855>> [Accessed 10.05.2013].
- [4] Tidal Energy Ltd, 2012. *"Tidal Stream Energy Demonstration Array. Environmental Scoping Report."* [online PDF] Available at: <<http://www.marineenergypembrokeshire.co.uk/wp-content/uploads/2012/10/TEL-St-Davids-Head-Scoping-Report-Aug12.pdf>> [Accessed 10.05.2013].
- [5] Fraenkel, P. 2004. *"Windmills Below The Sea. A Commercial Reality Soon?"* [online PDF] Available at: <<http://www.sciencedirect.com/science/article/pii/S1471084604001118>> [Accessed 10.05.2013].
- [6] Stewart, R. 2008. *"Introduction to Physical Oceanography."* [online PDF] Available at: <http://oceanworld.tamu.edu/resources/ocng_textbook/PDF_files/book.pdf> [Accessed 10.05.2013].
- [7] Tidal Energy Ltd, 2013. *"Deltastream. The Core Design Principles and Intellectual Property."* [online PDF] Available at: <http://www.tidalenergyLtd.com/cms/wp-content/uploads/downloads/2013/02/DeltaStream_The_core_design_principles_and_IP_Feb13.pdf> [Accessed 10.05.2013].

- [8] Tidal Energy Ltd, 2012. "*DeltaStream Tidal Energy Solution.*" [online PDF] Available at: <http://www.tidalenergyltd.com/cms/wpcontent/uploads/downloads/2012/10/DeltaStream_White_Paper_Aug12.pdf> [Accessed 10.05.2013].
- [9] Lackner, M. 2009. " Wind Turbine Control Systems: Current Status and Future Developments." [online PDF] Available at: <<http://web.mit.edu/windenergy/windweek/Presentations/P9%20-%20Lackner.pdf>> [Accessed 5 February 2013].
- [10] Hau, E. 2006. "Wind Turbines. Fundamentals, Technologies, Application, Economics." 2nd ed. Springer. [online PDF] Available at: <<https://extranet.cranfield.ac.uk/book/10.1007/3-540-292845/page/,DanaInfo=link.springer.com+1>> [Accessed 5 February 2013].
- [11] Bard, J. 2009. " Control of Marine Current Turbines and Wave Energy Converters" [online PDF] Available at: < http://www.iwes.fraunhofer.de/en/highlights20112012/highlights20102011/control_of_marinecurrentturbinesandwaveenergyconverters.html> [Accessed 5 February 2013].
- [12] Les Energies des Mers, 2008. "*L'énergie Hydrolienne.*" [Image online] Available at: <<http://tpe.energiesdelamer.free.fr/hydrolienne.html>> [Accessed 23 February 2013].
- [13] Mattarolo, G. et al. , 2006. " Control and Operation of Variable Speed Marine Current Turbines. Results from a Project funded by the German Ministry for the Environment" [online PDF] Available at: < <http://192.107.92.31/test/owemes/31.pdf>> [Accessed 5 February 2013].
- [14] Keysan, O. et al. , 2011. " Direct Drive Permanent Magnet Generator. Design for a Tidal Current Turbine(SeaGen)." [online PDF] Available at: <<http://ieeexplore.ieee.org/stamp/stamp.jsp?tp=&arnumber=5994850>> [Accessed 5 February 2013].
- [15] Power-Technology.com, 2012. "*Strangford Lough Tidal Turbine, United Kingdom.*" [Image online] Available at: <<http://www.power-technology.com/projects/strangford-lough/>> [Accessed 23 February 2013].

[16] Houde, J. 2012. "Cost-Benefit Analysis of Tidal Energy Generation in Nova Scotia: a Scenario for a Tidal Farm With 300MW of Installed Capacity in the Minas Passage in 2020. " [online PDF] Available at: <<http://dalspace.library.dal.ca/bitstream/handle/10222/14578/Houde%2c%20Julie%2c%20MDE%2c%20ECON%2c%20April%202012.pdf?sequence=3>> [Accessed 6 June 2013].

[17] Cornelius, T. et Smith, M. 2009. "Presentation to Offshore Engineering Society Tidal Stream Energy." [online PDF] Available at: <<http://www.atlantiresourcescorporation.com/download/OES%20Presentation%20London%20Oct%202009.pdf>> [Accessed 5 February 2013].

[18] Greenfudge.org, 2013. "*World's Largest Tidal Power Turbine to Be Deployed in Scotland.*" [Image online] Available at: <<http://www.greenfudge.org/2010/08/13/worlds-largest-tidal-power-turbine-to-be-deployed-in-scotland/>> [Accessed 23 February 2013].

[19] Ben Elghali, S.E. et al. , 2010. "Modelling and Control of a Marine Current Turbine Driven Doubly-Fed Induction Generator." [online PDF] Available at:<http://hal.archives-ouvertes.fr/docs/00/52/52/11/PDF/IET_RPG_2010_BEN_ELGHALI.pdf> [Accessed 5 February 2013].

[20] Luo, Y. et al. , 2002. "Integrated Control System for First Tidal Flow Electricity Generating Ship of China." [online PDF] Available at:<<http://link.springer.com/content/pdf/10.1007%2FBF02921416.pdf>> [Accessed 5 February 2013].

[21] VanZwieten, J. et al. , 2006. "Design of a Prototype Ocean Current Turbine. Part I: Mathematical Modelling and Dynamics Simulations." [online PDF] Available at:<<http://202.114.89.60/resource/pdf/2473.pdf>> [Accessed 8 March 2013].

[22] Mbabazi, S. 2010. " Modelling and Control of a Variablespeed Subsea Tidal Turbine Equipped with Permanent Magnet Synchronous Generator." [online PDF] Available at:<http://e-futures.group.shef.ac.uk/publications/pdf/55_Shonan%20Mbabazi.pdf> [Accessed 8 March 2013].

- [23] Freeman, C. et al. , 2009. "Design of a Gravity Stabilised Fixed Pitch Tidal Turbine of 400kW." [online PDF] Available at:<[http://www.see.ed.ac.uk/~shs/Wave%20Energy/EWTEC%202009/EWTEC%202009%20\(D\)/papers/138.pdf](http://www.see.ed.ac.uk/~shs/Wave%20Energy/EWTEC%202009/EWTEC%202009%20(D)/papers/138.pdf)> [Accessed 8 March 2013].
- [24] Cecchi, M.A. 2012. "Investigation of a Control System for a Tidal Turbine." [Unpublished MSc thesis], Cranfield University.
- [25] Hansen, M. 2008. "Aerodynamics of Wind Turbines." 2nd ed. EARTHSCAN. [online PDF] Available at: <https://extranet.cranfield.ac.uk/web/portal/browse/,DanalInfo=www.knovel.com+display?_EXT_KNOVEL_DISPLAY_bookid=2277> [Accessed 5 February 2013].
- [26] Bianchi, D. et al., 2007. "Wind Turbine Control System." Springer. [online PDF] Available at: <<https://extranet.cranfield.ac.uk/content/pdf/,DanalInfo=link.springer.com+10.1007%2F1-84628-493-7.pdf>> [Accessed 5 February 2013].
- [27] Warnes, L. 2003. "Electronic and Electrical Engineering. Principles and Practice." 3rd edition Basingstoke: Palgrave Macmillan. p.602
- [28] Kohlrusz, G. et Fodor, D. 2011. "Comparison of Scalar and Vector Control Strategies of Induction Motors." [online PDF] Available at: <http://konyvtar.uni-pannon.hu/hjic/HJIC39_265_270.pdf> [Accessed 8 March 2013].
- [29] Arbi, J. et al., 2009. "Direct Virtual Torque Control of Doubly Fed Induction Generator Grid Connection." [online PDF] Available at: < <http://ieeexplore.ieee.org/stamp/stamp.jsp?tp=&arnumber=4895343>> [Accessed 8 March 2013].
- [30] Rao, Y. et Laxmi, J. 2012. "Direct Torque Control of Doubly Fed Induction Generator Based Wind Turbine under Voltage Dips." [online PDF] Available at: <<http://www.e-ijaet.org/media/0001/75I8-IJAET0805911-DIRECT-TORQUE-CONTROL.pdf>> [Accessed 12 June 2013].
- [31] Lei, Y. et al., 2006. "Modelling of the Wind Turbine with a Doubly Fed Induction Generator for Grid Integration Studies." [online PDF] Available at: <<http://ieeexplore.ieee.org/stamp/stamp.jsp?tp=&arnumber=1597345>> [Accessed 8 March 2013].

[32] Mahi, Z. et al., 2007. " Direct Torque Control of a Doubly-Fed Induction Generator of a Variable Speed Wind Turbine Power Regulation." [online PDF] Available at: < http://proceedings.ewea.org/ewec2007/allfiles2/522_Ewec2007_fullpaper.pdf> [Accessed 8 March 2013].

[33] Poitiers, F. et al., 2001. " Control of a Doubly-Fed Induction Generator for Wind Energy Conversion Systems." [online PDF] Available at: <http://itee.uq.edu.au/~aupec/aupec01/026_%20POITIERS%20_AUPEC01%20paper%20revised.pdf> [Accessed 8 March 2013].

[34] Abdolghani, N. et al., 2012. "A Direct Torque Control Method for CSC Based PMSG Wind Energy Conversion Systems." [online PDF] Available at: <<http://www.icrepq.com/icrepq'12/448-abdolghani.pdf>> [Accessed 10 June 2013].

[35] Chen, Z. et Spooner, E. 2001. "Grid Power Quality with Variable Speed Wind Turbine." [online PDF] Available at: <<http://ieeexplore.ieee.org/stamp/stamp.jsp?arnumber=00921466>> [Accessed 10 April 2013].

[36] Rocco, P. 2001. "Dispense di Controllo Automatico per l'Ingegneria Aerospaziale." Politecnico di Milano. [online PDF] Available at: <<http://home.deib.polimi.it/rocco/leonardo/dispensa.pdf>> [Accessed 5 June 2013].

[37] Musial, W. et al., 2007. "*Improving Wind Turbine Gearbox Reliability.*" [online PDF] Available at:<http://www.townoflenox.com/Public_Documents/LenoxMA_Wind/NREL%20Gearbox%20Reliability%20Collaborative%20Description.pdf> [Accessed 10 June 2013].

[38] McNiff, P. et al., 1991. "*Variation in Gear Fatigue Life for Different Wind Turbine Braking Strategies.*" [online PDF] Available at:<<http://www.osti.gov/bridge/servlets/purl/5828926>> [Accessed 10 June 2013].

[39] Hughes, E. 1977. "*Electrical Technology.*" 5th edition London and New York: Longman. p.710

[40] Molinas, M. et al., 2005. "*Cage Induction Generators for Wind Turbines with Power Electronics Converters in the Light of the New Grid Codes.*" [online PDF] Available at: <<http://ieeexplore.ieee.org/stamp/stamp.jsp?tp=&arnumber=1665880>> [Accessed 13 April 2013].

[41] Boghos, H. 2007. "*Analysis, Modelling and Control of Doubly Fed Induction Generators for Wind Turbines.*" [online PDF] Available at: <<http://www.damascusuniversity.edu.sy/mag/eng/images/stories/boghosE.pdf>> [Accessed 13 April 2013].

[42] Abbey, C. 2004. "*A Doubly-Fed Induction Generator and Energy Storage System for Wind Power Applications.*" [online PDF] Available at: <http://digitool.library.mcgill.ca/webclient/StreamGate?folder_id=0&dvs=1374318563417~459> [Accessed 20 June 2013].

[43] De Vries, E. 2011. "*Wind Tech: Electrical Generators - Doubly-Fed Induction v Permanent Magnet.*" [online archive] Available at:<<http://www.windpowermonthly.com/article/1076824/wind-tech-electrical-generators---doubly-fed-induction-v-permanent-magnet>> [Accessed 25 June 2013].

[44] Ozpineci, B. et Tolbert, M. 2003. "*Simulink Implementation of Induction Machine Model - A Modular Approach.*" [online PDF] Available at: <<http://memberfiles.freewebs.com/15/83/80738315/documents/induction%20motor%20modeling.pdf>> [Accessed 13 April 2013].

[45] eCircuit Center, 2002. "*PID Controller.*" [online archive] Available at: <<http://www.ecircuitcenter.com/Circuits/pid1/pid1.htm>> [Accessed 25 June 2013].

[46] Corsar, M. 2013. Private communication.